ON THE ESTIMATION OF RETURN PERIODS FROM SHORT SEA LEVEL RECORDS

By

Dona Suvineetha Swarna Ranasinghe

SUBMITTED IN PARTIAL FULFILLMENT OF THE
REQUIREMENTS FOR THE DEGREE OF
DOCTOR OF PHILOSOPHY
AT
DALHOUSIE UNIVERSITY
HALIFAX, NOVA SCOTIA
SEPTEMBER 1993

ISBN 0-315-93732-7

Name Dona Suvineetha Swarna Ranasinghe

Dissertation Abstracts International is arranged by broad, general subject categories. Please select the one subject which most nearly describes the content of your dissertation. Enter the corresponding four-digit code in the spaces provided.

STATISTICS | 0463 | U·M·I

SUBJECT TERM | SUBJECT CODE

Subject Categories

THE HUMANITIES AND SOCIAL SCIENCES

COMMUNICATIONS AND THE ARTS
Architecture 0729
Art History 0377
Cinema 0900
Dance 0378
Fine Arts 0357
Information Science 0723
Journalism 0391
Library Science 0399
Mass Communications 0708
Music 0413
Speech Communication 0459
Theater 0465

EDUCATION
General 0515
Administration 0514
Adult and Continuing 0516
Agricultural 0517
Art 0273
Bilingual and Multicultural 0282
Business 0688
Community College 0275
Curriculum and Instruction 0727
Early Childhood 0518
Elementary 0524
Finance 0277
Guidance and Counseling 0519
Health 0680
Higher 0745
History of 0520
Home Economics 0278
Industrial 0521
Language and Literature 0279
Mathematics 0280
Music 0522
Philosophy of 0998
Physical 0523
Psychology 0525
Reading 0535
Religious 0527
Sciences 0714
Secondary 0533
Social Sciences 0534
Sociology of 0340
Special 0529
Teacher Training 0530
Technology 0710
Tests and Measurements 0288
Vocational 0747

LANGUAGE, LITERATURE AND LINGUISTICS
Language
General 0679
Ancient 0289
Linguistics 0290
Modern 0291
Literature
General 0401
Classical 0294
Comparative 0295
Medieval 0297
Modern 0298
African 0316
American 0591
Asian 0305
Canadian (English) 0352
Canadian (French) 0355
English 0593
Germanic 0311
Latin American 0312
Middle Eastern 0315
Romance 0313
Slavic and East European 0314

PHILOSOPHY, RELIGION AND THEOLOGY
Philosophy 0422
Religion
General 0318
Biblical Studies 0321
Clergy 0319
History of 0320
Philosophy of 0322
Theology 0469

SOCIAL SCIENCES
American Studies 0323
Anthropology
Archaeology 0324
Cultural 0326
Physical 0327
Business Administration
General 0310
Accounting 0272
Banking 0770
Management 0454
Marketing 0338
Canadian Studies 0385
Economics
General 0501
Agricultural 0503
Commerce-Business 0505
Finance 0508
History 0509
Labor 0510
Theory 0511
Folklore 0358
Geography 0366
Gerontology 0351
History
General 0578
Ancient 0579
Medieval 0581
Modern 0582
Black 0328
African 0331
Asia, Australia and Oceania 0332
Canadian 0334
European 0335
Latin American 0336
Middle Eastern 0333
United States 0337
History of Science 0585
Law 0398
Political Science
General 0615
International Law and Relations 0616
Public Administration 0617
Recreation 0814
Social Work 0452
Sociology
General 0626
Criminology and Penology 0627
Demography 0938
Ethnic and Racial Studies 0631
Individual and Family Studies 0628
Industrial and Labor Relations 0629
Public and Social Welfare 0630
Social Structure and Development 0700
Theory and Methods 0344
Transportation 0709
Urban and Regional Planning 0999
Women's Studies 0453

THE SCIENCES AND ENGINEERING

BIOLOGICAL SCIENCES
Agriculture
General 0473
Agronomy 0285
Animal Culture and Nutrition 0475
Animal Pathology 0476
Food Science and Technology 0359
Forestry and Wildlife 0478
Plant Culture 0479
Plant Pathology 0480
Plant Physiology 0817
Range Management 0777
Wood Technology 0746
Biology
General 0306
Anatomy 0287
Biostatistics 0308
Botany 0309
Cell 0379
Ecology 0329
Entomology 0353
Genetics 0369
Limnology 0793
Microbiology 0410
Molecular 0307
Neuroscience 0317
Oceanography 0416
Physiology 0433
Radiation 0821
Veterinary Science 0778
Zoology 0472
Biophysics
General 0786
Medical 0760

EARTH SCIENCES
Biogeochemistry 0425
Geochemistry 0996
Geodesy 0370
Geology 0372
Geophysics 0373
Hydrology 0388
Mineralogy 0411
Paleobotany 0345
Paleoecology 0426
Paleontology 0418
Paleozoology 0985
Palynology 0427
Physical Geography 0368
Physical Oceanography 0415

HEALTH AND ENVIRONMENTAL SCIENCES
Environmental Sciences 0768
Health Sciences
General 0566
Audiology 0300
Chemotherapy 0992
Dentistry 0567
Education 0350
Hospital Management 0769
Human Development 0758
Immunology 0982
Medicine and Surgery 0564
Mental Health 0347
Nursing 0569
Nutrition 0570
Obstetrics and Gynecology 0380
Occupational Health and Therapy 0354
Ophthalmology 0381
Pathology 0571
Pharmacology 0419
Pharmacy 0572
Physical Therapy 0382
Public Health 0573
Radiology 0574
Recreation 0575
Speech Pathology 0460
Toxicology 0383
Home Economics 0386

PHYSICAL SCIENCES

Pure Sciences
Chemistry
General 0485
Agricultural 0749
Analytical 0486
Biochemistry 0487
Inorganic 0488
Nuclear 0738
Organic 0490
Pharmaceutical 0491
Physical 0494
Polymer 0495
Radiation 0754
Mathematics 0405
Physics
General 0605
Acoustics 0986
Astronomy and Astrophysics 0606
Atmospheric Science 0608
Atomic 0748
Electronics and Electricity 0607
Elementary Particles and High Energy 0798
Fluid and Plasma 0759
Molecular 0609
Nuclear 0610
Optics 0752
Radiation 0756
Solid State 0611
Statistics 0463

Applied Sciences
Applied Mechanics 0346
Computer Science 0984

Engineering
General 0537
Aerospace 0538
Agricultural 0539
Automotive 0540
Biomedical 0541
Chemical 0542
Civil 0543
Electronics and Electrical 0544
Heat and Thermodynamics 0348
Hydraulic 0545
Industrial 0546
Marine 0547
Materials Science 0794
Mechanical 0548
Metallurgy 0743
Mining 0551
Nuclear 0552
Packaging 0549
Petroleum 0765
Sanitary and Municipal 0554
System Science 0790
Geotechnology 0428
Operations Research 0796
Plastics Technology 0795
Textile Technology 0994

PSYCHOLOGY
General 0621
Behavioral 0384
Clinical 0622
Developmental 0620
Experimental 0623
Industrial 0624
Personality 0625
Physiological 0989
Psychobiology 0349
Psychometrics 0632
Social 0451

To My Loving Parents

and

To Prof. Lise Manchester.

Contents

List of Tables

List of Figures

Abstract

Techniques for obtaining return periods of extreme levels from short records are investigated focusing on processes which are partly stochastic and partly deterministic. The physical motivation for the problem comes from the need to estimate return periods for short sea level records which contain a deterministic component, in the form of a tide, and a nonstationary stochastic component associated with seasonally changing variance and autocorrelation. Nonstationarity was modeled by a periodic autoregressive state space model which allowed for the seasonality in the autocovariance structure of the surge process. State space representation was able to take the measurement error into account. This model was then used in the estimation of return periods using the exceedance probability method (Middleton and Thompson, 1986) and the revised joint probability method (Tawn, 1992). Extensions were made to the methods to allow for the nonstationarity of the surge process, which was defined in discrete time, and to allow for estimates of sampling variability of the return period estimates.

The 50-100 year return period estimates obtained using just one year of data using the techniques introduced in this thesis are in good agreement with standard estimates based on more than 50 years of data.

Acknowledgements

I would like to thank my supervisors, Prof. Bruce Smith and Prof. Keith Thompson, for their guidance, patience and generousity in helping me complete this thesis.

I would also like to thank my external examiner Prof. J. Tawn of Lancaster University for his comments and suggestions.

My foremost thanks also go to Prof. David Hamilton and to Prof. R. P. Gupta for reading this thesis and making valuable comments.

I like to acknowledge the Association of Universities and Colleges of Canada for providing me a scholarship to come to Canada to do my graduate studies.

I like to mention all the professors in the Department of Mathematics, Statistics division with a deep sense of gratitude, for their help in many ways in my graduate studies.

This thesis was proof read by Michael Dowd and many thanks to Michael.

I also like to thank my friend Barbara Lacy for constantly reminding me for several years that I have a thesis to be finished.

My final and foremost thanks are due to my ever loving husband Indra and my precious son Vinod for their kindness and patience.

Chapter 1

Introduction

An understanding of the frequency of extreme environmental events is required in order to minimize their potentially damaging economic and social effects. The study of extreme sea levels is one particularly important research area due to the risk of flooding of coastal communities. This is further exacerbated by the global warming trend and the associated potential for sea level rise. Accurate prediction of sea level would allow coastal infrastructure to be designed in such a way as to minimize the adverse consequences of extremely high or low sea levels.

The return period of sea levels is not a well defined concept. For a purely deterministic process, such as the tide, the return period can simply be defined as the time period in which the process reaches the level of concern starting from some time origin. However, due to the stochasticity of the surge, the definition of the return period of sea levels cannot be explicitly defined as an exact event but rather must be defined probabilistically. Different authors have defined return periods in several ways. However, the most widely used definition is due to Gumbel (1958) where the return period is defined as the reciprocal of the probability of exceedance.

Conventional methods for estimating return periods are based on analysis of the maximum level observed in each year, over a period of many years. The extremal analysis of Gumbel (1958) has proved to be of great use in estimating return periods of extreme sea levels, provided that fairly long records of data are available. Pugh and

Vassie (1980) suggested that at least twenty five years of hourly data are required by Gumbel's method to achieve suitable accuracy in the final return period estimates. Further complicating the issue is that the level of the sea at a given time and a particular location is dependent on many atmospheric and environmental conditions which are site specific. Therefore it is unlikely to have historical records for this length of time available at each coastal site.

Return period estimation using the Gumbel (1958) method requires an independent set of consecutive data points. However, hourly sea levels are serially correlated and as a result this technique cannot be applied directly to hourly sea level data. However, if a large record is available and blocked into appropriate time periods, (*e.g.* annual), the maximum within these blocks provides an approximately independent series of data for the Gumbel analysis.

Many authors have since designed schemes for achieving the required independent series. Smith (1984) considered the peak values over a prespecified threshold, to study the return period of wave heights. This peak over threshold method (POT) was originally introduced in the English Flood Studies Report (1975). In this method, a threshold level is selected, often arbitrarily, and the observed data are reduced to clusters above the threshold. The series consisting of maximum, or peak value, within each cluster provides an independent sequence for the Gumbel analysis. A key feature of this method is that the threshold level must be high enough to ensure that the resulting series of peak values is independent. This method requires a long record of data and the final return period estimates are often highly dependent on the arbitrarily chosen threshold.

Pugh and Vassie (1980) pioneered the estimation of return periods from short sea level records. Their joint probability method (JPM) was based on separating the sea level into tide and surge components. They considered the tide to be deterministic and able to be predicted for decades into the future. The surge was considered as stochastic. The tide and the surge distribution were recombined to obtain the instantaneous probability of sea level exceedance for a given level l, denoted by $\tilde{Q}_1(l)$.

Following Gumbel's definition, the return period in years was defined as $1/n\tilde{Q}_1(l)$, where n is the number of samples in one year. A correction factor was used to take care of the dependence between hourly sea levels. The correction factor was designed by Cartwright (1958) and takes care of 1-dependence. Note that for a stochastic process $\{\eta_i\}$, 1-dependence is defined such that, if $|i-j| > 1$ then η_i is independent from η_j.

The JPM introduced by Pugh and Vassie was an important breakthrough in the estimation of return periods of extreme sea levels. It provided ways of estimating the distribution of sea levels including unobserved levels, using the predictability of the tide and a surge model. One deficiency of the JPM approach is that the return period estimate depends on n, the number of samples per year and thus the sampling interval.

Motivated by Pugh and Vassie's separation of sea level into a deterministic tidal component and a stochastic surge component, Middleton and Thompson (1986) introduced the exceedance probability method (EPM) as another solution to the unavailability of long records. They demonstrated their method for the Canadian ports of Halifax and Victoria and showed that their method works as effectively as other methods which use twenty five years of data. The tidal component was considered deterministic whereas the stochastic surge distribution was expressed by a compound Gaussian model. The return period was obtained by integrating forward in time until the expected number of exceedances equals to one. The integration interval was then defined as the return period. Note that this return period does not depend on the sampling interval or number of samples per year thereby eliminating the deficiency noted in the JPM. However, the use of the EPM was limited as the sampling variability of the return periods were not estimated.

Having recognized that 1-dependence is not valid for sea levels and that the JPM return period depends on the sampling interval, Tawn and Vassie (1989) extended the JPM by introducing an extremal index (Leadbetter 1983) to account for the serial dependence. Their revised JPM (RJPM) is also invariant with regards to the number of samples per year. Later in this thesis all these return period definitions will be investigated in detail.

The goal of this thesis is to design a new set of techniques to estimate return periods from short records, focusing attention on stochastic modeling of the surge component and deterministic modeling of the tidal component. Since the primary focus of this study is on sea level, the methods and techniques derived here will concentrate mainly on the nature and behavior of the sea level process. However, it will become clear that the techniques can easily be adapted to any other process of a similar nature, *i.e.* ones which are partly deterministic and partly stochastic. An example of such a process is wave-induced currents where the tidal component is deterministic.

The objective of this study is to design a scheme for estimating return periods from a short record of data. An attempt will be made to estimate decadal long return periods for sea level using a single year of data. Methods are developed to make inferences about the estimated return periods in the form of standard errors and confidence intervals. The estimates are validated by comparing them with the estimates from conventional methods which use many years of data.

In this chapter, a brief description of the practical problem of estimation and inference of return periods is given. The application of conventional methods for obtaining return periods of sea level from short records are difficult due to the presence of nonstationarity and dependence in the data. These issues are discussed in detail in Section 1.1. The occurrence of a sea level exceeding a specific level can be considered as a sequence of events happening over time, or more specifically, as a point process of extreme events. The influence of the stochastic nature of the surge and the deterministic nature of the tide on these extreme events will be investigated in Section 1.2. For the purpose of estimation, many authors have defined return periods in different ways. These alternative definitions will be discussed in Section 1.3. Applications of the techniques and methods of estimating return periods will be investigated in Section 1.3. Finally, the contents of the thesis are briefly outlined in Section 1.4.

1.1 Sea level processes

Sea level varies irregularly in both space and time. As the concern of this study is mainly in the changes occurring over time, it is assumed hereafter that the location is fixed. Note that the results obtained using the observed sea level at a particular location are not directly applicable to the other locations, however, the techniques developed here can be readily adapted to sea level analysis for any location.

The level of the sea at a particular location is measured using an instrument called a sea level gauge. The mechanism is described by Pugh (1987). The instrument uses a pen attached to a float which moves with the the vertical movements of the sea level. The height of the float above the sea bed is recorded as the level of the sea at that particular instant. Thus, the sea level is recorded in a time series comprising the vertical movements of the sea at a particular location.

Any time series of sea level will have both tidal and nontidal components. In the last century, mainly as a result of instrument design and analysing techniques, identification of the physical factors governing the tides has made considerable progress. These developments have enabled scientists to identify and quantify the regular patterns in the motion of the sea due to planetary motions. These are collectively known as *tides*.

After removing the tide from the sea level, the remaining residual nontidal component is known as the *surge*. The surge results from the regular and predictable pattern of the tide being distorted by irregular factors such as the atmospheric forcing. Pugh (1987) noted that, hydrodynamically, the term surge implies a sudden movement of water which is quickly generated but soon dissipates. In statistical terms, the surge is characterized as a random or stochastic process.

Based on the discussion above, the observed sea level at time t, η_t, can be represented in the following form,

$$\eta_t = \mu_t + \eta_t^T + \eta_t^S.$$

Here, η_t^T is the deterministic part known as the tide, η_t^S is the stochastic part known as the surge and the part which does not change periodically (tide) or rapidly (surge) is categorized as the mean sea level μ_t.

1.1.1 Tide

Extensive studies on the estimation of the tidal component have been conducted by oceanographers. These studies focus on the character of the variations and physical factors controlling these motions and have enabled the tidal component of the sea level to be determined with a high degree of accuracy. There are now computer programs available for predicting hourly tidal heights, such as that of Foreman (1977). Relying on these estimates, this study considers the tidal component as deterministic and therefore able to be predicted decades into the future.

The two main tidal features of any sea level record are the amplitude, measured according to half of the height between successive high and low levels, and the period, the time between one high (or low) level and the next. Periodic oscillations due to tide are described mathematically as

$$\eta_t^T = \sum_{i=1}^{M} H_i \cos(\omega_i t - g_i)$$

where M is the number of tidal constituents, H_i is the amplitude of the *ith* constituent, ω_i is the angular frequency and g_i is the phase lag relative to some time origin. For Halifax tide the number of constituents (M) is 69. A sample of the tidal constituents obtained for Halifax is given in Table 1.1.

Of the total number of tidal constituents, three components often important for return period estimation are the semidiurnal tides, the spring-neap cycles and the nodal cycles. These are explained below for Halifax sea level; Pugh (1987) gives their patterns for other ports.

The Halifax tidal cycle takes an average of twelve hours and twenty five minutes, so that two tidal cycles occur for each transit of the moon. Because each tidal cycle occupies roughly half a day, this type of tide is referred to as semidiurnal. Figure 1.1 illustrates the Halifax semidiurnal tide for March 1930. Semidiurnal tides

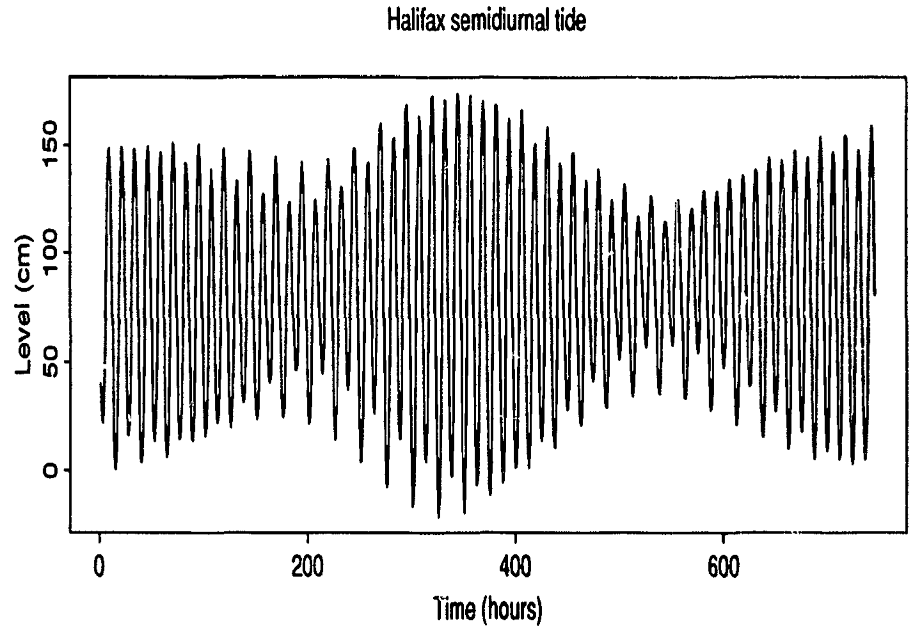

Figure 1.1: Halifax tide in March 1930 showing the semidiurnal component dominating the tidal level. Time (in hours) extends from 1st of March 1930 to 31st of March 1930

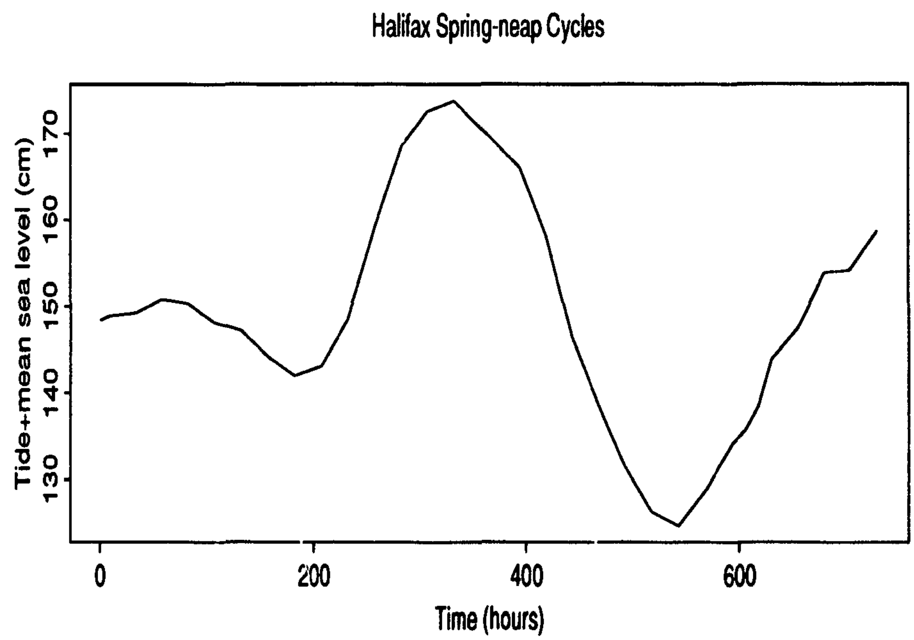

Figure 1.2: Spring neap cycles for Halifax calculated as maximum peak occurring twice a day. (Based on Figure 1.1). Time (in hours) extends from 1st of March 1930 to 31st of March 1930

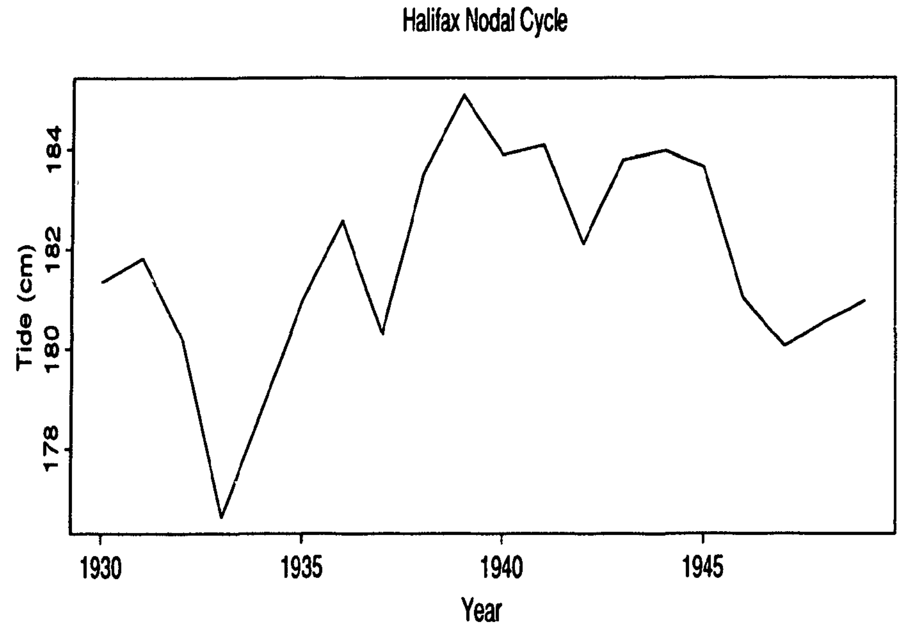

Figure 1.3: Nodal modulation at Halifax. Tide plus mean sea level vs. time (in years) for the period 1930 to 1950.

have a range which typically increases and decreases cyclically over a fourteen-day period. The maximum amplitude of this secondary cycle are called spring tides and occur shortly after both the new moon and full moon. The corresponding minimum amplitude tide is called the neap tide. These spring-neap cycles for Halifax are shown in Figure 1.2. The longest period over which important changes in the tidal cycle occurs is 18.6 years. This is called the nodal modulation and is shown in Figure 1.3 for Halifax for the period of 1930-1940. The maximum level the tide reaches during each of these 18.6 year cycles is known as the nodal tidal peak.

1.1.2 Surge

Surge is considered as a random component whose behavior is governed solely by stochastic laws. The surge can be obtained from a time series by subtracting the pre-determined tidal component and the mean sea level from the observed sea level record. Figure 1.4 shows the time series plot of Halifax hourly surge during the year

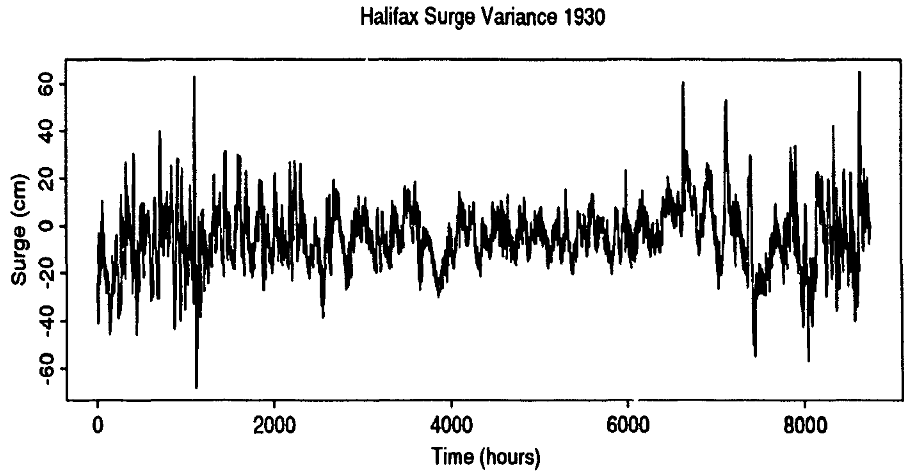

Figure 1.4: Halifax hourly surge time series in the year 1930 during the period 1st January to 31st December 1930.

1930. Note that the variations of the surge in the winter and fall are higher than that in the spring and summer. Middleton and Thompson (1986) fitted a sinusoidal model to the Halifax and Victoria monthly surge variances to explain this seasonality in the surge variance. The possibility that the surge variance has seasonal cycles makes the stochastic surge process nonstationary in the second order.

Another important feature apparent in Figure 1.4 is that the surges in the fall and the winter seasons do not decorrelate as fast as in the spring and summer. This suggests a seasonal autocorrelation structure in the surge series. First order nonstationarity in time series models can easily be handled using the methods described in Box and Jenkins (1976). However, no straightforward methods are available to describe second order nonstationarity in time series models.

1.1.3 Mean sea level

Climatic variability results in a mean sea level that changes slowly with time. For example, since the last ice-age 10,000 years ago the sea level has increased by approximately 40 meters globally (Pugh, 1987). As the rate of increase over time is very low it can be assumed without loss of generality that the mean sea level within a period

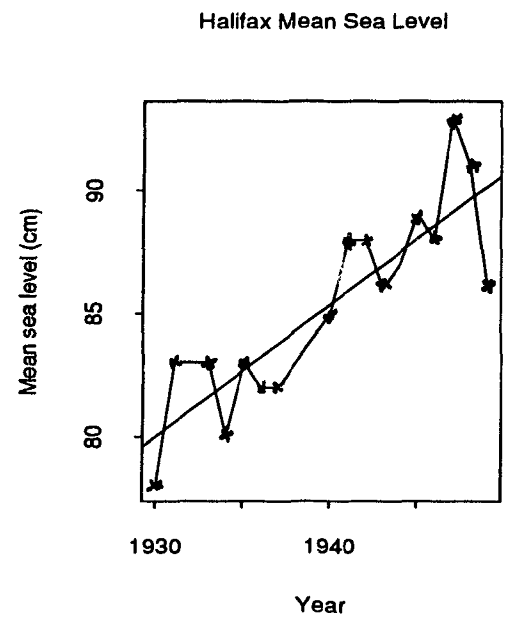

Figure 1.5: Annual mean sea level for Halifax from the year 1930-1949. The calculated means are are marked by *–* and the solid line represents the fitted line.

of one year is roughly constant. The annual mean sea level calculated for Halifax for the years 1930-1949 is plotted in Figure 1.5. Fitting a straight line to this data shows a linear increase of 0.53 centimeters annually.

The effect of the above mentioned three components, tide, surge and the mean sea level, in influencing the overall sea level can be summarized as follows. A comparison of Figures 1.1 and 1.3 or 1.4 reveals that sea level processes are highly dominated by the tide. For instance, in Halifax the tidal variation is about 100 *cm* from the mean sea level, whereas the surge varies within only a 65 *cm* range. Therefore, the tidal variation is larger than the surge variation and it is obvious that the tide has a great impact on the sea level changes. However, the extreme sea levels of interest here usually exceed the maximum level that the tide reaches. Therefore, for the high level exceedances the surge must be included, even for tidally dominated sea levels.

Many authors in the past have considered the surge process as Gaussian, however Middleton and Thompson (1986) modeled the surge using a contaminated normal distribution with a zero mean and time dependent standard deviation. They presented the contaminated normal model as the mixture of two normals. Further examination of the surge process reveals that it possesses a second-order nonstationarity as a result of the seasonally changing variance and autocorrelation structure. High storm surges occur mostly in winter, rather than summer, and have a correspondingly higher variance and stronger autocorrelation during this time. Middleton and Thompson (1986) used the following model to explain the seasonally changing variance for Halifax,

$$\sigma_t^2 = 124.9(1 + 0.8 \cos \omega t)$$

where t is in months running from July to June, σ_t^2 is the variance for a given month in cm^2 and ω is the frequency ($\omega = \frac{2\pi}{12}$).

Based on the above discussion of the stochastic and deterministic behavior of surge and tide, one can describe the sea level process as follows. Sea level is nonstationary in the first-order as well as in the second-order. The first-order nonstationarity is caused by the tidal component and also by the slowly increasing mean sea level. The second-order nonstationarity is due to the seasonally changing variance and autocorrelation structure of the surge. Further complications arise if the tide is also considered to be probabilistic. Sea level then follows the distribution of the surge with the location parameter following the distribution of the tide. This is a case of a doubly stochastic process. As scientists are presently capable of explaining the tide due to planetary motions, in this study the tide is considered as purely deterministic. Hence, the sea level follows a single stochastic model which is governed solely by the surge.

1.2 Extreme events

The discussion of Section 1.1 reveals certain properties of the tide and the surge such as the cyclic behaviour of the tide and the seasonality in the variance and autocorrelation of the surge. It is desirable to know how these properties effect the extreme events.

The maximum sea level in each of the four seasons was extracted from Halifax sea level data for the period 1930-1948 and listed in Table 1.2. According to this table extreme events are more likely to occur in the winter and fall than in the summer and spring. This tendency may be due to the higher seasonal variance of the surge in the winter. In the year 1940 the maximum value in the summer is higher than the other three seasonal maxima contradicting the pattern existing in the other years. This extreme event happened on September the 16th which is at the end of the summer and really into the fall. This anomaly could also be due to sampling variability or possibly a recording or timing error.

Due to the influence of the surge on extreme sea level, it is impossible to estimate return periods from numerical models of tides. Therefore it is necessary to develop an estimation scheme based on statistical techniques to appropriately determine return periods. In the following illustration of various theoretical and practical estimation schemes, particular attention will be paid to the statistical characteristics of the process.

1.3 Return period

The Gumbel definition of the return period T is related to the notion of a series of independent events happening over time, with the same probability of occurrence at each time. In case of sea level exceedances, this leads to a geometric distribution with the parameter p equal to $P[\eta_t \geq l]$. The mean of the distribution, $1/p$, is then defined as the return period. Following Gumbel, many authors (Pugh and Vassie 1980, Smith 1986 and Tawn and Vassie 1989) have used the definition of the return period as the reciprocal of the probability of exceedance, *i.e.* $1/P[\eta_t \geq l]$. However, use of this definition is restricted to independent and identically distributed processes. These methods are problematic in that sense since hourly sea levels are usually autocorrelated and nonstationary. Therefore, either the annual maxima, or peaks over a prespecified threshold have to be considered, this implies the existence of a long series of data. Moreover, the full nodal modulation of the tide is 18.6 years, even annual maxima may not be identically distributed.

Another definition of return period appears in the point process approach of exceedances. The point process of extremes was originally introduced by Pickands (1971). Smith (1989) advocated using a statistical approach, viewing exceedances of peaks over a specific threshold as points in a Poisson process. If $N(T)$ is the number of such points in the interval $[0, T]$ then $N(T)$ follows a Poisson process with the intensity parameter Λ equal to the expected number of exceedances in the unit interval. The return period T was then defined as the time interval $[0, T]$ such that the expected number of exceedances equals to one. This return period is thus obtained as the reciprocal of the intensity parameter Λ. As the intensity depends on an arbitrarily chosen threshold, so does the return period. Smith (1984) has allowed the intensity parameter Λ to vary over time to cope with the seasonality of the process. To estimate the time dependent intensity parameter Λ of a nonhomogeneous Poisson process requires long records. Dependency can also be incorporated into the intensity parameter by using an extremal index (Leadbetter *et. al.* 1983) provided enough data are available for the estimation procedure.

Having recognised these problems in applying the classical definitions of return periods to short records of data, Middleton and Thompson (1986) used a definition of the return period that accounts for both the nonstationarity and the dependence. Their return period was defined as the time interval T such that the integral of the expected number of exceedances in $[t, t+dt]$, $Q_t dt$, equals unity (*i.e.* $\{T : \int_{\tau=t}^{t+T} Q_\tau d\tau = 1\}$).

In all three definitions discussed above, the return period was not explicitly identified as a random variable. However, in practice, p in Gumbel's definition, Λ in Smith's definition and Q_t in Middleton and Thompson's definition have to be replaced by their respective estimates, which are, in fact, random variables. This allows one to make further inferences on the return period estimates.

The return period of the level l, T_{fr}, can also be defined as the first passage time

$$T_{fr} = T \text{ iff } \eta_1 < l, ..., \eta_{T-1} < l, \eta_T \geq l \tag{1.1}$$

where η_t is the sea level at time t, measured every hour. The above definition causes numerous problems in the estimation of return period. For high level exceedances, the probability structure of the return period T_{fr} is quite complicated due to the dependence and nonstationarity. As a result, estimation of the $P[T_{fr} = T]$ for large T is impossible. In Chapter 2, under idealized sea levels, all these definitions will be compared.

The focus of this study is primarily on the estimation of return periods of sea level. However the methods developed here are applicable to any other process which is partly stochastic and partly deterministic, which is the case for many environmental and chronological sets of data. Examples of such cases are current speed at a given time and a specific location, and the wave-tide action on sediment transport where the tidal component is deterministic. Furthermore, the techniques developed are suitable for a complicated stochastic process, even one which is nonstationary in the second-order and highly dependent.

1.4 Outline of the thesis

In this chapter, the problem of accurate estimation of return periods of extreme levels, that has long been studied by statisticians and oceanographers using many different approaches, has been outlined. Estimation methods have been reviewed in the context of the return periods of the sea level process. Finally, problems encountered in applying conventional methods and techniques to nonstationary, dependent and short sea levels records have been addressed.

A description and comparison of previous methods used in return period estimation for sea level are presented in Chapter 2. This comparison is carried out by using idealized processes like iid surge with no tide, and a dependent and stationary surge with a square-top tide. Asymptotic properties based on some classical methods are also included in this chapter.

Chapter 3 describes the nonstationarity in the surge using a parametric model. A description of the parametric model fitting procedure for the surge data, diagnostic tests and model validation techniques are given in Chapter 3. These methods are demonstrated using Halifax surge for the year 1930.

This parametric surge model is then utilized in the estimation of return periods from short sea level records in Chapter 4. The estimation techniques are applied to Halifax sea level data. The validity of the estimates will be judged by comparing them with the empirical annual maxima estimates obtained from 1930-1958 sea levels recorded for Halifax.

Sampling variability of the return period estimates are obtained in Chapter 5. Methods of obtaining the variances of the return period estimates are discussed in this chapter. Ninety-five percent confidence intervals are also derived.

Finally, Chapter 6 contains a brief evaluation of the techniques and methods used in this study. Unresolved issues and some ideas for further investigation are included in this last chapter.

Name	Frequency (Radians per hour)	Amplitude (cm)	Phase lag
Z0	0.00000000	82.6448	0.00
SA	0.00011407	03.8985	346.76
SSA	0.00022816	00.9428	203.03
MSF	0.00282193	00.4925	190.43
MF	0.00305009	00.9971	219.25
2Q1	0.03570635	00.2499	110.40
SIG1	0.03590872	00.2465	69.76
Q1	0.03721850	00.4607	26.05
O1	0.03873065	04.5460	39.00
MSM	0.00130978	00.8278	70.89
NO1	0.04026860	00.2328	76.22
MM	0.00151215	00.9146	38.32
ALP1	0.03439657	00.4185	298.13
P1	0.04155259	03.3219	61.91
RHO1	0.03742087	00.4464	331.47
S1	0.04166667	00.7072	235.58
K1	0.04178075	09.9583	64.23
OO1	0.04483084	00.4149	94.68
PHI1	0.04200891	00.3350	82.92
2N2	0.07748710	01.6232	189.07
EPS2	0.07617731	00.5667	222.33
MU2	0.07768947	01.8288	222.60
N2	0.07899925	14.1370	215.32
NU2	0.07920162	02.7552	216.57
2MN6	0.24002205	00.4196	69.42
H1	0.08039733	00.3678	232.86
M2	0.08051140	63.7716	235.01
L2	0.08202355	01.8174	267.63
LDA2	0.08182118	00.6169	246.83
T2	0.08321926	01.1445	250.09
S2	0.08333334	14.3809	261.12
K2	0.08356149	03.7188	264.31
MN4	0.15951064	01.9555	347.80
M4	0.16102280	03.6744	41.98
MS4	0.16384473	01.7910	168.95

Table 1.1: A sample of tidal constituents for Halifax. The thirty four largest constituents are listed above out of a total of 69 constituents. The phase lag is relative to the time origin January 1st, 1930 1am.

Year	Spring	Summer	Fall	Winter
1930	177	185	206	220
1931	189	186	193	238
1932	188	194	211	205
1933	186	189	229	250
1934	197	177	237	215
1935	188	191	211	214
1936	206	205	205	221
1937	193	183	226	212
1938	186	193	199	208
1939	196	186	205	211
1940	229	244	214	208
1941	205	193	211	214
1942	203	191	214	231
1943	193	221	202	228
1944	205	199	220	223
1944	208	194	238	205
1945	221	191	229	217
1946	196	193	226	234
1947	199	205	226	223
1948	202	202	214	205
Mean	198	196	216	219

Table 1.2: Observed seasonal maxima for Halifax during the period 1930-1948. The winter maxima were extracted from hourly sea levels from (January-March), the spring maxima were extracted from (April-June) hourly sea levels, the summer maxima were obtained from (July-September) hourly sea levels and the the fall maxima were obtained from (October-December) sea levels.

Chapter 2

Outline and Comparison of Existing Methods

The aim of this chapter is to provide a solid basis for the existing approaches to return period estimation. In doing so, we first define the major terms and concepts including exceedances, upcrossings, peaks over thresholds and maxima for a series of data. Important asymptotic results for extreme events are examined. Existing methods of return period estimation are briefly outlined. The performances of these existing methods are judged based on an idealized sea level with no tide and iid surge, and a square top wave tide with dependent surge.

2.1 Definitions of key terms

1. **Extreme or maximum value** - The random variable $M_t(n)$ is defined as the extreme value (or the maximum value) of the set of n random variables $\{\eta_t, \eta_{t+1}, ..., \eta_{t+n-1}\}$ iff

$$M_t(n) = \max\{\eta_t, \eta_{t+1}, ..., \eta_{t+n-1}\}.$$

2. **Peak over a threshold (POT)** - $M_{t,n}^{\text{pot}}(u)$ is called the peak over the threshold u of the t th cluster of size n iff for all positive $\zeta_i = \eta_i - u$,

$i = t, t+1, ...t+n-1,$

$$M_{t,n}^{\text{pot}}(u) = \max\{\zeta_t, \zeta_{t+1}, ..., \zeta_{t+n-1}\}.$$

3. **Exceedance** - There is an exceedance of the level l by the process $\{\eta_t\}$ at time t iff $\eta_t > l$.
4. **Upcrossing** - There is an upcrossing of the level l by the discrete process $\{\eta_t\}$ at time t iff $\{\eta_{t-1} < l \leq \eta_t\}$, or by the continuous process η_t iff $\{\eta_t = l, \frac{d\eta_t}{dt} > 0\}$.

In the definitions (1) and (2) the subscript t can be dropped for iid $\{\eta_t\}$. Note also that extremes and POTs are random variables, whereas exceedances and upcrossings are events. We are interested in these latter two events $\{M_t(n) \geq l\}$ and $\{M_{t,n}^{\text{pot}}(u) \geq l\}$. In the past, all of these events have been used to calculate return periods for different methods.

The difference between an upcrossing and an exceedance is that an upcrossing requires the process to be below the level at $t-1$, *i.e.* $\eta_{t-1} < l$. As far as exceedances are concerned η_{t-1} can be below or above l. Therefore, upcrssings are rare events than exceedances. exceedance.

2.1.1 Asymptotic properties of extreme events

Note that the results stated and derived in this section are restricted to stationary Gaussian processes, so that the subscript t can be dropped from the notations of maxima and POTs. In this section, two basic theorems regarding the asymptotic convergence of extreme events are first stated. These two theorems verify that the distribution of $M(n)$ for an m-dependent process tends to the same limit as for an independence process, for increasing n. First the following definition of m-dependence is stated.

Definition

A stochastic process $\{\eta_t\}$ is said to be m-dependent if $|i-j| > m$ implies that η_i and η_j are independent.

Watson (1954) derived the asymptotic form of $P[\eta_1 \leq l_n, ..., \eta_n \leq l_n]$ for m-dependent processes.

Theorem 1 (Watson 1954) *Let $\{\eta_t\}$ be a strictly stationary stochastic process, unbounded above and m-dependent with the property that,*

$A1: \lim_{l \to \infty} \frac{1}{P[\eta_i > l]} \max_{|i-j| \leq m} P[\eta_i > l, \eta_j > l] = 0$

Then, if $l_n(\alpha)$ is defined such that

$$nP[\eta_i > l_n(\alpha)] = \alpha$$

for α fixed, then

$$\lim_{n \to \infty} P[M(n) \leq l_n(\alpha)] = e^{-\alpha}. \tag{2.1}$$

The results of the above theorem hold true for any stochastic process provided that the conditions stated in the theorem hold true. Watson further showed that the condition A1 always holds for autocorrelated Gaussian processes. Leadbetter (1983) showed that these conditions are statisfied for any strong mixing Gaussian sequence.

The following theorem provides the asymptotic distribution of $M(n)$ in the case of Gaussian white noise. The asymptotic convergence of $M(n)$ to the Type 1 extreme value distribution was first proved by Fisher and Tippet (1928). The extension identifies the normalizing constants a_n and b_n in terms of n for iid standard normal processes, which is stated below. The cumulative distribution function of the Type 1 extreme value distribution is defined as $F(x) = exp(-exp(x))$. The norming constants a_n and b_n have been known for many years probably since Gnedneko (1943).

Theorem 2 *If $\{\eta_t\}$ are standard normal iid sequences of random variables then the asymptotic distribution of $M(n)$ is of Type 1. Specifically,*

$$P[a_n(M(n) - b_n) \leq l] \to exp(-exp(-l))$$

where

$$a_n = \sqrt{2 \log n}$$

and

$$b_n = \sqrt{2 \log n} - (1/2\sqrt{2 \log n})(\log \log n + \log 4\pi).$$

If $\{\eta_t\}$ is iid Gaussian then the conditions for Watson's theorem are satisfied. In that case, $\alpha = exp(-l)$ and $l_n = b_n + l/a_n$. Using both theorems, it can be shown that $M(n)$ has the same limit distribution for dependent and independent processes provided that the conditions stated in Watson's theorem are satisfied.

A more commonly used dependence restriction for stationary process was introduced by Rosenblatt (1956) and is called *strong mixing.* A process is called strong mixing if for any event based on the past up to time t is nearly independent of any event based on the future from time $t+n-1$ when n becomes large. Kolmogrov and Rozanov (1960) showed that Gaussian autoregressive processes are strong mixing. Loynes (1965) argued that the condition $A1$ in Watson's theorem can be relaxed by a strong mixing condition. Watson's result has been used in the past for sea levels and the probability of annual maxima exceeding an extreme level has been approximated by $exp(-\alpha)$ with α estimated from the data. This idea has been used in the joint probability method, which will be discussed in detail later in this chapter.

Another useful result proved by Watson (1954) relates to the asymptotic convergence of upcrossings. Watson showed that, if the process $\{\eta_t\}$ is strictly stationary and Gaussian then for any η_t and η_{t+j},

$$\lim_{l\to\infty} \frac{P[\eta_t > l, \eta_{t+j} > l]}{P[\eta_{t+j} > l]} = 0.$$

Let $j = 1$ and then it follows

$$\lim_{l\to\infty} P[\eta_t > l | \eta_{t+1} > l] = 0.$$

Therefore,

$$\lim_{l\to\infty} \{1 - P[\eta_t < l | \eta_{t+1} > l]\} = 0.$$

From this result it immediately follows that

$$\lim_{l\to\infty} \frac{P[\eta_t < l, \eta_{t+1} > l]}{P[\eta_{t+1} > l]} = 1.$$

In other words as the level increases the probability of an upcrossing tends to the probability of an exceedance.

Leadbetter (1983, Theorem 7.3.2) showed that the expected number of upcrossings in the interval $[t, t+\Delta t]$ tends to $\frac{1}{2\pi}\lambda exp(-\frac{l^2}{2})$, as $\Delta t \to 0$, which is the probability of an upcrossing derived by Rice (1954) for the continuous case, where $\lambda^2 = \lim_{\tau\to 0} r''(\tau)$ and $r''(\tau)$ is the second derivative of the autocovariance function at lag τ.

In summary the discussion of this section reveals that $M(n)$ of a stationary, strong mixing process converge to the same limit as that of an independent and stationary process, *i.e.*

$$P[a_n(M(n) - b_n) \leq l] \to exp(-exp(-l)),$$

where a_n and b_n are normalizing constants. Moreover, as the level increases the probability of upcrossing tends to the same limit as the probability of exceedances for a stationary Gaussian process. The events of upcrossings, exceedances and $(M(n) \geq l)$ have been used in the different methods for estimating return periods and are discussed in the next section. It can be shown that all these events converge in probability to the same limit, for Gaussian process or more generally in the domain of attraction of a Type 1 limit (Leadbetter, 1983).

2.2 Outline of existing methods

Until 1980, return periods of sea levels had been estimated using Gumbel's (1958) annual maxima method which is sometimes known as the extreme value method. This method was discussed briefly in Chapter 1 and is not particularly well suited for obtaining return periods of sea levels.

This section provides a brief outline of the following methods which have been used more recently for return period estimation:

1. Annual maxima method (AMM) - Gumbel (1958)
2. Peak over threshold method (POT) - English Flood Studies Report (NERC, 1975) and Smith, R. L. (1984)
3. Joint probability method (JPM) - Pugh and Vassie (1980)

4. Exceedance probability method (EPM) - Middleton and Thompson (1986)
5. Methods based on extreme value theory of the r-largest annual events - Smith (1986), Tawn (1988)
6. Revised joint probability method (RJPM) - Tawn and Vassie (1989), Tawn (1992)

2.2.1 Annual maxima method

The annual maxima method (AMM) requires a very long sketch of hourly data. The full length of the record is considered as a combination of blocks of length n. For the ith block, the maximum value $M_i(n)$ is chosen such that the sequence of random variables $M_i(n), i = 1, 2, ...$ are asymptotically independent. The existence of such a sequence was discussed in Section 2.1.1. For analysis of sea level data, the block size n is generally chosen as one year ($n = 8766$ hours) hence the name annual maxima method.

The AMM assumes strict stationarity and independence among the annual maxima, hence the subscript i can be dropped. The AMM return period of the level l, T_g, is defined as

$$T_g = \frac{1}{P[M(n) \geq l]}. \tag{2.2}$$

As discussed in Section 2.1.1, the probability of $P\{M(n) \geq l\}$ asymptotically is given by the extremal Type 1 distribution, provided that the process is Gaussian, Leadbetter (1983). In this case,

$$P[a_n(M(n) - b_n) \leq l] \rightarrow exp(-exp(-l))$$

For sufficiently large l, this gives

$$T_g = 1/[1 - exp(-exp(-(l - b_n)a_n))]$$

where a_n and b_n are normalizing constants. The relationship between l and T_g can then be written as

$$l = b_n - log(-\log(1 - 1/T_g))/a_n.$$

According to the above formula a plot of l against $-\log(-\log(1-1/T_g))$ follows a linear relationship and is usually called the Gumbel plot.

The AMM is not readily applicable to this study as it requires many years of data. However, the AMM will be used as a baseline method for comparing the other methods in the estimation of return periods in Chapter 4.

2.2.2 Peak over threshold method

Gumbel's return period definition requires independence among adjacent data points. As a result, several techniques have been introduced to ensure independence among observations including the peak over threshold (POT) method. The POT method has been described in some detail in the English Flood Studies report (NERC 1975) and a comprehensive coverage of it was given by Smith (1984) who applied it to wave heights.

The POT method is based on an independent sequence of peaks over a specific threshold level. A peak is defined as the maximum value above a threshold level achieved during any sequence of consecutive exceedances. A cluster is defined as a consecutive set of data points above the threshold. The threshold level is determined arbitrarily in most of the cases and should be chosen such that it is high enough to ensure approximate independence among clusters, but low enough to leave enough observations in the resulting series of peaks.

Besides the threshold level, a cluster interval must be chosen as well. The cluster interval is necessary in order to determine which observation belongs to which cluster. The cluster interval should be such that all the dependent observations are within the interval and none outside is dependent with them. Within each cluster, the maximum value is selected and the dependent series is reduced to a set of independent peaks above a high threshold. Smith (1984) proposed an empirical rule for identifying clusters and cluster intervals based on the mean number of clusters per unit time.

The occurrence of peaks over a threshold can be considered as a point process of events. Ross (1987) considered peak values as following an exponential (β), with the number of peaks as Poisson (Λ). The peak value is the corresponding excess over the threshold. The parameters β and Λ were determined using maximum likelihood estimates. If the random variable $N(t)$ denotes the number of POTs within an interval of width t, $N(t)$ follows a Poisson distribution with parameter Λt provided that the peaks are independent. Then, the POT return period T_{pot}, as discussed in Chapter 1, is given by $1/\Lambda$. Smith (1984) extended this method to cope with seasonality and serial dependence using nonhomogeneous Poisson processes. This technique requires a long series of data and thus is not of direct concern in this work.

2.2.3 Joint probability method

Pugh and Vassie (1980) recognized the problem of the unavailability of the long records of sea level data required by the existing return period estimation methods. They introduced the joint probability method (JPM) to take into account the nature of the sea level data and the lack of long records of data.

The sea level was considered to have three components: the mean sea level μ_t, a tidal component η_t^T, and the surge η_t^S. The tide was considered as deterministic and a probability distribution was calculated numerically from 18 years of hourly predictions (Section 1.1.1.) The probability of a certain tidal level was calculated by using the number of times that the level appears in 18 years hourly predictions divided by the number of hourly values in 18 years. This idea of the probability of a predictable (or deterministic) component seems unusual. Generally we talk about the probability distribution of random variables (not deterministic functions) where the value of each random variable has an associated uncertainty expressed in terms of a probability distribution. For deterministic functions the magnitude of this uncertainty is zero. Tawn (1992) recognized this problem with the JPM and has appropriately incorporated the deterministic tide so that the probability of exceeding the level l by the sea level at time t η_t was expressed as the probability of the surge exceeding the gap between the tide and l.

In the JPM, the probability density function of the sea level η_t, $f_{\eta_t}(l)$, where l, is measured from the mean sea level, was calculated as follows

$$f_{\eta_t}(x) = \int_{y=-\infty}^{\infty} f_{\eta_t^T}(x-y) f_{\eta_t^S}(y) dy$$

where f_{η_t}, $f_{\eta_t^T}$ and $f_{\eta_t^S}$ are respectively the probability densities of the sea level, tide and surge. The above equation results from the convolution of two independent random variables η_t^T and η_t^S and hence the term joint probability method.

The joint probability method was designed to estimate return periods from short records. Therefore, the sea level probability density function $f_{\eta_t}(l)$ was determined with one year of hourly data. The probability of annual maxima exceeding the level l, $P[M(n) \geq l] = \tilde{Q}_n(l)$, was calculated assuming independence among hourly sea levels η_t as follows. Let $\tilde{Q}_1(l) = P[\eta_t \geq l] = \int_{x=l}^{\infty} f_{\eta_t}(x)dx$. Then if hourly sea levels are independent, $\tilde{Q}_n(l) = 1 - [1 - \tilde{Q}_1(l)]^n$. If the level is large enough to assume $l_n = l$ then

$$[1 - \tilde{Q}_1(l)]^n = [1 - \frac{\alpha}{n}]^n \rightarrow exp(-\alpha)$$

provided that the number of hourly observations per year n is large enough to attain the limit in the above formula, where α is defined as in Watson's theorem,

$$nP[\eta_i > l_n(\alpha)] = \alpha.$$

It follows that

$$\tilde{Q}_n(l) = 1 - exp[-n\tilde{Q}_1(l)]$$

and the return period is calculated using Gumbel's definition as

$$1/\tilde{Q}_n(l) = 1/(1 - exp(-n\tilde{Q}_1(l))) \approx \frac{1}{n\tilde{Q}_1}.$$

To take care of the dependence between hourly sea levels, Cartwright's (1958) correction factor for 1-dependence was used. 1-dependence is a special case of m-dependence as defined in Section 2.1. Cartwright's correction factor for 1-dependence is given by

$$\tilde{Q}_n(l) = 1 - exp\left[-n\tilde{Q}_1(l)(1 - \frac{\tilde{Q}_2(l)}{\tilde{Q}_1(l)})\right]$$

where $\tilde{Q}_2(l) = P[\eta_t \geq l, \eta_{t+1} \geq l]$. The JPM return period T_{jpm} with the correction for the dependence is then given by

$$T_{jpm} = 1/\{1 - exp[-n\tilde{Q}_1(l)(1 - \frac{\tilde{Q}_2(l)}{\tilde{Q}_1(l)})]\}. \qquad (2.3)$$

Cartwright's correction factor was designed for 1-dependent processes. As the sea level process is highly dependent, the assumption of 1-dependence may cause problems for autoregressive processes with a large AR parameter. In the JPM method no allowance is made to take the nonstationarity in the surge into account. These deficiencies may seriously influence the return period estimates of rather small levels. However, as the level becomes larger the high level exceedances occur less frequently thus diminishing the effect of nonstationarity.

The fundamental importance of JPM is the separation of tide and surge so that the predictability of the tide can be incorporated in to the predictability of the sea level by convolving with a surge model. This concept first introduced by Pugh and Vassie was used in the exceedance probability method. The fundamental problem with the JPM is the return period T_{jpm} depends on the sampling frequency n as $T_{jpm} \approx 1/n\tilde{Q}_1$. Recognizing this problem, Middleton and Thompson (1986) produced the exceedance probability method.

2.2.4 Exceedance probability method

Middleton and Thompson (1986) introduced the exceedance probability method (EPM). It takes advantage of the deterministic nature of the tide and the stochastic nature of the surge estimate as originally introduced in the JPM.

For iid processes EPM return period is estimated using the reciprocal of the expected number of upcrossings in the unit interval. This definition does not depend on the sampling frequency and thus eliminates the problem associated with the JPM. As outlined in Chapter 1, Rice's (1954) formula can be used to estimate the instantaneous probability of crossing the level. This can be interpreted as the expected number of upcrossings in the unit interval. Rice derived the probability of a normally distributed process crossing a specific level within $(t, t+dt)$ in order to analyse the noise in electrical currents. It was shown that the probability of upcrossing or the expected number of upcrossings in $[t, t+dt]$, $P[\eta_t < l < \eta_{t+dt}] = Q(t)dt$, is equivalent to $\frac{1}{2\pi\sigma}\lambda \exp(\frac{-l^2}{2\sigma^2})$. Rice's derivation is briefly outlined next.

For continuous η_t instantaneous probability of upcrossings in $[t, t+dt]$ is given by $P[\eta_t < l < \eta_{t+dt}, \dot{\eta}_t > 0]$ where $\dot{\eta}_t = d\eta_t/dt$. If η_t follows normal distribution with zero mean and σ standard deviation, it can be shown that the derivative process $\dot{\eta}_t$ is independent of η_t and follows the same distribution with the same mean and the standard deviation λ, which is equal to $\sqrt{-r''(0)}$, where $r(h)$ is the autocorrelation at lag h. Then $r''(0) = \lim_{h\to 0} d^2r(h)/dh^2$. It follows that the joint density of η_t and $\dot{\eta}_t$ is given by

$$f(\eta_t, \dot{\eta}_t) = \frac{1}{2\pi\sigma\lambda} \exp[-(\eta_t^2/\sigma^2 + (\dot{\eta}_t)^2/\lambda^2)/2].$$

Then the expected number of upcrossings

$$Q_t dt = \int_{\dot{\eta}_t=0}^{\infty} \dot{\eta}_t f(\dot{\eta}_t, \eta_t = l) d\dot{\eta}_t.$$

Evaluation of the integral leads to the final result.

The surge standard deviation σ was modeled as seasonal and was assumed to follow $\sigma^2 = \sigma_0^2[1 + \epsilon\cos(\omega i)]$ where i was given in months and then $\omega = 2\pi/12$. The parameter estimates of σ_0^2 and ϵ were obtained from the least square method. The parameter λ was estimated using the power spectrum of the surge (Middleton and Thompson, 1986).

The EPM return period T_r is obtained using the definition

$$T_r = T \text{ iff } \int_{\tau=t}^{T+t} Q(\tau)d\tau = 1. \tag{2.4}$$

In this definition T_r is referred to a specific time origin which allows for a trend. The noteworthy feature of this method is that the seasonal variations of the tide and surges are taken into account. Middleton and Thompson predicted the tide using the tidal packages of Foreman (1977) for Halifax. The residual or the surge was then tested for a seasonally changing variance. The following model was then fits to Halifax monthly surge variances

$$\sigma^2 = \sigma_0^2(1 + \varepsilon \cos \omega t)$$

where t is in months, $\sigma_0^2 = 124.9 cm^2$, and $\varepsilon = 0.8$. The autocorrelation structure, which is necessary to estimate λ, was found to be autoregressive of order one for Halifax. However, unlike the usual ARMA models, the residual error from the AR surge model was found to follow a contaminated normal distribution due to the asymmetry in the tails of distribution. The estimate for λ was obtained using the estimated spectrum of the surge data. The EPM estimates were compared with AMM and JPM estimates for Halifax and Victoria sea levels and found to be in reasonably good agreement.

2.2.5 Extreme value methods using r-largest annual events

Smith (1986) extended the AMM by using r-largest annual events. The tide was considered to have both a trend and a periodic component. This method was further extended by Tawn (1988) for a more general class of extremal processes using generalized extreme value distributions. The method is explained below. The r largest values in a year were derived from the total sea level. Here a value of r=1 refers to the case of annual maxima.

In the long history of extremal analysis, Type-1 extreme value distributions were used to describe the distribution of annual maxima. However in most applications, deviations from the linear Gumbel plot (see Section 2.1.5) were noted. Smith (1986) suggested using the generalized extreme value (GEV) distribution in place of the Type-1 extreme value distribution. The cumulative GEV distribution function is given by

$$P[\eta_i \leq x | \mu, \sigma, k] = exp[-(1 - k\frac{(x-\mu)}{\sigma})^{\frac{1}{k}}] \tag{2.5}$$

on the set of x for which $1 - k(x-\mu)/\sigma > 0$. Gumbel's Types 1, 2 and 3 are special cases corresponding to $k = 0$, $k < 0$ and $k > 0$, respectively.

The major drawback of the AMM is that only a single observation from a year long record is used which reduces the precision of the final estimate. Smith suggested instead using the r-largest annual values. The distribution of the r-largest iid values was obtained by Weissman (1978). Supposing that N years of data are available, estimates of the parameters like μ and σ can be obtained numerically using the maximum likelihood method.

Suppose that the r-largest for each of the N years of data are $\eta_{1,n} \geq \eta_{2,n} \geq, .. \geq \eta_{r,n}$ for $1 \leq n \leq N$. If the year-to-year data are assumed to be iid then by taking $\mu_n = \mu$, $\sigma_n = \sigma$ and $k_n = k$, the likelihood for the r-largest can be written as

$$\sigma^{-\sum_{n=1}^{N} r(n)} \exp[-\sum_{n=1}^{N}(\{1 - k[\eta_{r,n} - \mu]/\sigma\}^{1/k} + (1/k - 1)\sum_{j=1}^{r(n)} \log[1 - k((\eta_{j,n} - \mu)/\sigma)])],$$

where $r(n)$ is the rth largest in the nth year. In the presence of a trend plus seasonal component of period p, μ_n the location parameter for the nth year was modeled as

$$\mu_n = \alpha + \beta\frac{n}{N} + \zeta\cos(\frac{2\pi n}{p} + \phi).$$

The parameters α, β, ζ, ϕ and σ were then estimated by maximum likelihood methods.

This method was applied to sea levels in Venice. It is reasonable to consider μ_n as representing the tidal variation plus the mean sea level since all deterministic variations are included in the location parameter μ_n. If the component representation of the sea level is given by $\eta_t = \eta_t^T + \eta_t^S$, then η_t follows the same distribution as η_t^S with the mean given by the tidal component η_t^T and the variance given by that of η_t^S.

The standard errors of the estimated parameters were assessed by comparing the observed and expected information matrices. Basically the closer they are to each other, more evidence to confirm that η_t belongs to an exponential family of distributions.

The return period was estimated from the model as follows. For a linear annual trend $\mu_n = \alpha + \beta n/N$, the n year return value l was estimated by

$$l = \hat{\alpha} + \frac{\hat{\beta}n}{N} - \hat{\sigma}\log(-\log(1 - \varepsilon))$$

wher ε is the exceedance probability of annual maxima. In other words, the level l will be exceeded in the year n with probability ε, where

$$[l - \hat{\alpha} + \hat{\sigma}log(-log(1 - \varepsilon))]\frac{N}{\hat{\beta}}.$$

The model and the choice of r were assessed using probability plots. This procedure was considered for $r = 1, 5, 10$ and it was seen that $r = 1, 5$ gave better estimates with closer standard deviations.

This method requires a long record of data. As a result, this method will not be considered further, in this thesis.

2.2.6 Revised joint probability method

Tawn and Vassie (1989) developed a revised joint probability method (RJPM) by including an extremal index to take care of the dependence of the sea level. The RJPM was designed to overcome the difficulties in using Cartwright's correction factor for dependence. The difference is in the use of the extremal index $\theta(l)$ in place of the Cartwright's correction factor.

The extremal index for dependent sequences was first introduced by Loynes (1964). Leadbetter *et al* (1983) further investigated the extremal index in terms of a point process and gave a physical interpretation as the reciprocal of the mean over topping time of the level l. Following Gumbel's return period definition, the RJPM estimate for the return period T_{rjpm} is given by

$$T_{rjpm} = \{N\theta[1 - F(l)]\}^{-1} \tag{2.6}$$

where $F(l) = P[\eta_t \leq l]$ and is obtained by the tide and surge convolution (Section 2.2.3) and $N = 8766$ for one year of hourly data. Given l, θ can be estimated as the limiting value of the reciprocal of the mean over topping time as $l \to \infty$. Note that T_{rjpm} is invariant with sampling frequency.

Tawn (1992) extended the extremal index specifically for sea levels by introducing two extremal indices, one for the surge and the other for the sea level. According to this approach, the distribution of the annual maxima hourly surge levels $G_s(l)$ is given by

$$G_s(l) = F_s^{N\theta_s}(l)$$

where $F_s(l) = P[\eta_t^S \leq l]$ and θ_s is the extremal index for the surge. Now the density,

$$f_S(l) = \frac{d[G_s(l)]^{(N\theta_s)^{-1}}}{dl}$$

is expressed as the derivative of the distribution function. The original JPM method was restricted to the observed largest surge plus the tide. Use of the $G_s(l)$ in the revised method allows the extrapolation to the tail of the surge distribution.

Using the convolution concept of the JPM gives

$$F(l) = \int_{x=l}^{\infty} f_S(\eta_t^S - x) f_T(x) dx$$

where $F(l)$ is the hourly sea level cumulative probability distribution with f_s and $f_T(y)$ are respectively the surge and tide densities. The distribution of annual maxima $G(l)$ was obtained as in RJPM by

$$G(l) = [F(l)]^{N\theta}$$

where θ is the extremal index for the total sea level, $0 < \theta_s < \theta \leq 1$. Once the probability of a level of exceedance was established the return period of that level was calculated using Gumbel's definition $T_{rjpm} = \frac{1}{G(l)}$.

Extremal indices θ and θ_s were estimated for the data as follows. Both indices are defined as limits. The reciprocals of the indices, $\theta^{-1}(x)$ and $\theta_s^{-1}(x)$, can be obtained as the mean overtopping of the level x from the observed sea level and surge data. More details on finding independent clusters and appropriate levels are provided by Tawn (1992). Instead of finding an optimum value for $\theta^{-1}(x)$ and $\theta_s^{-1}(x)$, as $x \to \infty$, the use of the estimate

$$\hat{\theta}^{-1} = \sum_i w_i \hat{\theta}^{-1}(x_i) / \sum_i w_i,$$

was suggested by Tawn, where $w_i = \mathrm{Var}\{\hat{\theta}^{-1}(x_i)\}^{-1}$.

2.3 Comparison of the methods

Five existing techniques for return period estimation were discussed in the previous section. These methods will now be compared keeping in mind the particular case of interest, that is estimation of return periods from short records.

The two historical methods of estimating return periods, POT and AMM methods require long series of data. Smith (1984) introduced a model based approach for selecting the threshold and cluster interval. It was based on a hypothetical doubly-stochastic model for the point process of high level exceedances.

In the AMM, a single data point is chosen within the period of one year, and the remainder are discarded. Even though the AMM requires between 10-25 years of hourly data to estimate return periods, the ultimate estimate is based on only 10-25 data points. Thus the precision of the estimate is reduced. No theoretical basis has been developed which leads to the proper choice of the time interval over which the maximum is defined. The final estimate is in units of the chosen range (*e.g.* years). Therefore, the precision has again been reduced in another sense. However, the AMM will be considered here for both comparisons and validations.

The method based on r-largest annual events also requires a long series of data. This method has the same deficiencies as the annual maxima and POT method when short series are used. The JPM, EPM and RJPM are all specifically designed to obtain return periods of sea levels from short records. These three methods will be investigated further in Chapter 4. Finally, if the length of the record is long enough to identify the stochastic components of the process, a method which emphasizes parametric modeling of the surge might be more appropriate. This is considered in Chapter 3.

2.3.1 No tide and iid surge

The return periods obtained by the methods discussed in the previous section will be compared using an idealized sea level process: no tide and iid surge. If the process $\{\eta_t\}$ is iid then the Gumbel's definition leads to the probability of the return period given as

$$P[\eta_t < l]^{T-1} P[\eta_t \geq l]$$

which is a geometric density whose mean is equal to $\frac{1}{P[\eta_t \geq l]}$. Gumbel's return period estimate T_g is defined as the reciprocal of $P[\eta_t \geq l]$.

Define the point process of the POT as

$$I_t(l,u) = \begin{cases} 1 & \text{if } \eta_t \geq l \text{ given that } \eta_t \geq u \\ 0 & \text{otherwise.} \end{cases}$$

Then, the number of POTs exceeding the level l can be considered to follow a Poisson(Λ) distribution, where the intensity parameter Λ is given by

$$\Lambda = P[\eta_t \geq l | \eta_t \geq u] = \frac{1 - F(l)}{1 - F(u)}$$

with $F(u) = P[\eta_t \leq u]$. The return period T_{pot} is then $\frac{1-F(u)}{1-F(l)}$. The threshold level u is selected such that the conditions for clustering and independence are met. For iid sea levels these conditions are met at any value of u. Choosing a threshold u such that $1 - F(u) = 1$ leads to the case of, $T_{pot} = 1/P[\eta \geq l]$ which is same as T_g.

The EPM return period T_r was originally defined for continuous time. The equivalent version in discrete time is defined as the minimum length of time that ensures the expected number of upcrossings is equal to 1, *i.e.*

$$T_r(l) = \min\{T : \sum_{i=1}^{T} Q_i > 1\}$$

$Q_i = P[\eta_{i-1} < l \leq \eta_i]$. For iid sea levels, the subscript i can be dropped and then $T_r = 1/P[\eta_{i-1} < l \leq \eta_i]$ for any time i. It was shown in Section 2.1.1, that the probability of an upcrossing, $P[\eta_{i-1} < l \leq \eta_i]$, and the probability of exceedance, $P[\eta_i \geq l]$, tend to the same limit in which case T_r is equal to T_g.

The other return period estimates due to the JPM and the RJPM will not be considered because if the process is iid, the extremal index and the Cartwright correction factor will equal unity thus leading to the same return periods as the AMM. In summary for iid processes, all the definitions considered in this chapter leads to the same return period estimate.

2.3.2 Return periods of sea levels with a square-top tide and a dependent surge

Since, in reality, the sea level process is dependent and stationary we would like to relax the iid assumption and investigate the behavior for a non iid process. It is almost guaranteed that the return periods of extreme levels will occur at or around the high tides. Our purpose here is to estimate return periods of extreme levels at least two or three surge standard deviations away from the tidal maxima. An exceedance occurs only when the surge exceeds the gap between the level of concern and the tide. For tidal cycle of length T the probability of the event

$$P[\eta_1 < l, \eta_2 < l, ..., \eta_{T-1} < l, \eta_T < l]$$

can be approximated by

$$P[\eta_{i-j} < l, \eta_{i-j+1} < l, ..., \eta_i < l, ...\eta_{i+j} < l]$$

where i is the time of high tide and j the time either side of high tide that could provide an exceedance of the level l, *i.e.* the probability of exceeding the level l at other times in the tidal cycle are effectively zero.

Let number of points around the ith tidal maximum be 3. The tide is then reduced to 3 equally spaced points. Our concern is with the surge exceeding the gap between the level of interest and the tide. Without loss of generality, the level of the tide can be considered as zero at the ith tidal peak and $-\infty$ elsewhere so that the probability of exceedances at points other than the maxima will be zero. This concept reduces the tide to a square-top of length three hours.

Let P_{000} be the probability of being below the level l (> 0) at the ith tidal square-top, for $i = 1, 2, ...$ Here we assume independence between tides. According to Gumbel's definition of return period

$$T_g = \frac{1}{1 - P_{000}} \tag{2.7}$$

where $P_{000} = P(\eta_i^S < l, \eta_{i+1}^S < l, \eta_{i+2}^S < l)$ and T_g is measured in tidal periods.

The return period of the sea level with a square-top tide will be derived for the AMM, POT method, JPM and EPM. Since some of the methods were derived specifically for extreme levels, the asymptotic behavior of return periods will also be briefly investigated. The return period estimate according to the Gumbel definition given as the reciprocal of the three dimensional probability of not being below the level l is considered as the baseline estimate.

The following notation will be used in the derivations,

1. $P[\eta_t^S \geq l] = P_1$ and $P[\eta_t^S < l] = P_0$
2. $P[\eta_t^S \geq l, \eta_{t+1}^S \geq l] = P_{11}$, $P[\eta_t^S < l, \eta_{t+1}^S < l] = P_{00}$
   $P[\eta_t^S \geq l, \eta_{t+1}^S < l] = P_{10}$, $P[\eta_t^S \geq l, \eta_{t+2}^S \geq l] = P_{1.1}$
3. $P[\eta_t^S \geq l, \eta_{t+1}^S \geq l, \eta_{t+2}^S \geq l] = P_{111}$
   $P[\eta_t^S < l, \eta_{t+1}^S < l, \eta_{t+2}^S < l] = P_{000}$
   $P[\eta_t^S < l, \eta_{t+1}^S < l, \eta_{t+2}^S \geq l] = P_{001}$.
   $P[\eta_t^S \geq l, \eta_{t+1}^S < l, \eta_{t+2}^S \geq l] = P_{101}$.

Ratios of return periods from other methods with respect to the Gumbel baseline method will be calculated in order to see how the estimation proceeds as the level gets large. Each method is now considered below.

AMM return period

Let k be the number of tidal periods in a year. Then,
$P[\text{annual maxima} < l] = P_{000}^k$ and the annual maxima return period in years is

$$T_{amm} = \frac{1}{1 - P_{000}^k}.$$

The same return period in terms of tidal periods is given by

$$T_{amm} = \frac{k}{1 - P_{000}^k}$$

which is an overestimate of (2.7). It can be shown that the difference is always within one year, *i.e.* $|T_{amm} - T_g| \leq 1$. A comparison of T_{amm} and T_g reveals that the factor

k in T_{amm} results in the difference, for as $k \to 1$, $T_{amm} \to T_g$. This difference is due to the fact the maximum is taken over a year rather than over a tidal period.

POT return period

For a square-top tide, the level of the tide at peak times, *i.e.* $\eta_t^T = 0$, can be considered as the threshold level. Let $M(3)$ denote the maximum (or the peak) of three consecutive levels of the surge $\{\eta_t^S, \eta_{t+1}^S, \eta_{t+2}^S\}$. Define the indicator variable as

$$I_t(l) = \begin{cases} 1, & \text{if } M(3) \geq l \\ 0, & \text{otherwise.} \end{cases}$$

Then, the number of peaks exceeding the level l in the interval $[0, t]$, say $N(t)$, follows the Poisson distribution

$$P[N(t) = n] = \frac{e^{-\Lambda t}(\Lambda t)^n}{n!}$$

where the intensity parameter $\Lambda = P[I_t(l) = 1]$. The POT return period is given by

$$T_{POT} = \frac{1}{\Lambda}$$

where

$$\Lambda = P[M(3) \geq l].$$

Then

$$T_{POT} = \frac{1}{1 - P_{000}}.$$

This is equal to the base-line estimate of T_g. Therefore, if the square-top tide is taken as the threshold level then the estimate T_{pot} is the same as T_g.

JPM return period

The tide and surge convolution is used to obtain the probability of exceedance at each hour. The probability of the tide equal to the the level of the square-top tide is given by

$$P[\eta_t^T = 0] = \frac{3}{\nu}$$

at t equal to the peak times (say $t = 1, 2, 3$) and

$$P[\eta_t^T = -\infty] = \frac{\nu - 3}{\nu,} \text{ for some } t = 4, i+1, ..\nu$$

where ν is period of the tide in hours. It follows that $P[\eta_t > l] = \frac{3P_1}{\nu}$. In the JPM annual maxima are usually considered and we have already seen that the return period given by the AMM is different from the baseline estimate T_g. Therefore, hourly sea levels will be used in order to check the compatibility of the JPM estimate with T_g. If hourly sea levels are assumed to be independent, then

$$\begin{aligned} T_{jpm}(ind) &= \frac{\nu}{3P_1} \text{ (in hours).} \\ &= \frac{1}{3P_1} \text{ (in tidal periods).} \end{aligned}$$

If Cartwright's correction factor for 1-dependence is used

$$\begin{aligned} T_{jpm}(1 - dep) &= \frac{1}{3P_1(1 - \frac{P_{11}}{P_1})} \\ &= \frac{1}{3P_{10}}. \end{aligned}$$

The use of Cartwright's correction factor for 2-dependence leads to

$$\begin{aligned} T_{jpm}(2 - dep) &= \frac{1}{3P_1(1 - \frac{P_{11}}{P_1} - \frac{P_{1.1}}{P_1} + \frac{P_{111}}{P_1})} \\ &= \frac{1}{3(P_1 - P_{11} - P_{1.1} + P_{111})} \\ &= \frac{1}{3P_{100}}. \end{aligned}$$

By comparing the estimates given by the JPM with T_g, it can be concluded that the two estimates are different, even after using Cartwright's correction factor. Different return periods are not only due to the independence assumption for surges at the high tide limit, but also as a result of the convolution of the tide and the surge.

EPM return period

This method is based on the expected number of upcrossings in the unit interval, which is equal to $1 - P_{000} + P_{101}$, and the return period T_r is given by $\frac{1}{1 - P_{000} + P_{101}}$. T_r

Method	Symbol	Return Period
Annual maxima method	T_{amm}	$\frac{k}{1-(P_{000})^k}$
Peak over threshold method	T_{POT}	$\frac{1}{1-P_{000}}$
Joint probability method		
Independent case	$T_{jpm}(ind)$	$\frac{1}{3P_1}$
1-dependent	$T_{jpm}(1-dep)$	$\frac{1}{3P_{10}}$
2-dependent	$T_{jpm}(2-dep)$	$\frac{1}{3P_{100}}$
Exceedance probability method	T_r	$\frac{1}{(1-P_{000}+P_{101})}$
Baseline method	T_g	$\frac{1}{1-P_{000}}$

Table 2.1: Return periods (in tidal periods) for various methods for a square-top tide of length three hours.

then differs from the baseline estimate T_g by a P_{101} in the denominator, which tends to zero as the level becomes extreme.

In general, this method provides slight overestimate of T_g for levels with a square-top tide. The rate of overestimation increases with the length of the square-top tide. However, since the contribution of the extra term for extreme levels is negligible, the return period can be estimated as the reciprocal of the expected number of upcrossings in an interval of width 3.

Summary

The results derived in this section for a square-top tide are summarized in Table 1. From the comparisons carried out in this section it was revealed that the return periods T_{pot} and T_g are identical. It can easily be verified as the level gets higher the AMM, JPM and EPM provide similar estimates for T_g. Of these methods the EPM provides the estimate closest to the baseline method. However, if the difference is considerably small compared to the magnitude of the estimated return period then those methods could still be used. The accuracy of return period estimates depends on the precision of the estimate of the probability of exceedance (*e.g.* $1 - P_{000}$).

It can be shown that the ratios listed in Table 2.1 tends to one as the level increases. According to the asymptotic results discussed in Section 2.1.1, all these estimates should converge to the same value with increasing level. However, the rate of convergence may be different from one method to the other. This will be investigated next.

Rate of convergence for a Gaussian AR(1) surge with a square-top tide

The purpose of this section is to investigate the rate of convergence of the return period estimates of each method to the baseline estimate T_g as the level increases. It was seen in Table 2.1 that each return period can be interpreted using $P_0, P_{10}, P_{00}, P_{101}, P_{100}, P_{000}$. Now the problem is to obtain accurate estimates of these probabilities for a parametrically specified model.

Accurate tables are available to estimate the single dimensional probability P_0 for small values of l. For large values of l the approximation

$$P_1 \approx \frac{1}{l\sqrt{2\pi}} exp(-\frac{l^2}{2})$$

(Cramer, 1893) can be used. Two and three dimensional probabilities can be estimated using numerical subroutines such as those found in NAG or IMSL. However, it is observed that the accuracy decreases as l increases and, in fact, irregularities occur for very large values of l. The use of the following expression seems to avoid those irregularities,

$$P_{11} = (P_1)^2 + A(l,\rho) \tag{2.8}$$

where

$$A(l,\rho) = \frac{1}{\pi}\int_{\sqrt{\frac{1-\rho}{1+\rho}}}^{1} \frac{exp(-\frac{1}{2}l^2(1+x^2))}{1+x^2}dx$$

and ρ is the correlation between η_t^S, η_{t+1}^S. Further, it can be shown that

$$A(l,\rho) = P[\eta_t \geq l, \frac{l-\rho\eta_t}{\sqrt{1-\rho^2}} \leq \eta_{t+1} \leq l].$$

The above expression for P_{11} was derived as follows. Since

$$1 - P_{00} = 2P_{10} + P_{11}$$

then

$$P_{11} = 1 - P_{00} - 2P_{10}.$$

Since $P_{10} = P_0 - P_{00}$,

$$P_{11} = 2P_1 + P_{00} - 1.$$

Owen (1956) showed that

$$P_{00} = (P_0)^2 + 2T(l,1) - 2T\left[l, \sqrt{\frac{1-\rho}{1+\rho}}\right]$$

where

$$T(l,a) = \frac{1}{2\pi}\int_0^a \frac{exp(-\frac{1}{2}l^2(1+x^2))}{1+x^2}dx$$

and as a result

$$P_{11} = (P_1)^2 + 2T(l,1) - 2T\left[l, \sqrt{\frac{1-\rho}{1+\rho}}\right].$$

Furthermore since $\sqrt{\frac{1-\rho}{1+\rho}} < 1$ for $\rho > 0$, $T\left[l, \sqrt{\frac{1-\rho}{1+\rho}}\right]$ can be written as follows

$$T\left[l, \sqrt{\frac{1-\rho}{1+\rho}}\right] = T(l,1) - \frac{1}{2\pi}\int_{\sqrt{\frac{1-\rho}{1+\rho}}}^1 \frac{exp(-\frac{1}{2}l^2(1+x^2))}{1+x^2}dx.$$

The integral given by $A(l,\rho)$ can be evaluated using the NAG subroutines subroutines for quadrature D01BCF and D01FBF.

Of the various methods of computing the tri-variate normal integral the method due to Steck (1958) claims that most errors occur after the fourth of fifth decimal place. When using the approximation given by Steck, it was noticed that for extreme levels greater than five standard deviations away from the mean, changes in P_{000} that occur beyond the fifth decimal place are the most important. For example, the Steck approximation gives for $l = 5.5, P_{000} = .9999909$ and for $l = 5.0, P_{000} = .9999992$. Therefore, the estimation schemes were restricted to $l \leq 5$.

An idealized surge of the form

$$\eta_t^S = \rho\eta_{t-1}^S + \varepsilon_t$$

is used, where $\varepsilon_t \sim N(0,1)$ and $\rho = 0.95$. The return times as a ratio of the baseline estimate for different estimation methods, and using the AR(1) surge model, were

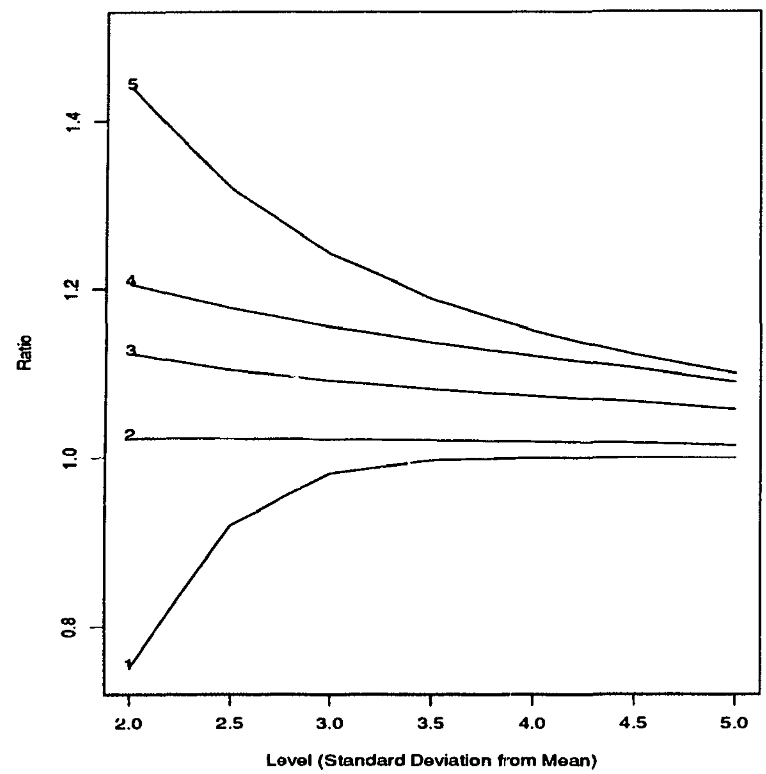

Figure 2.1: The return time ratios with respect to baseline estimate. The return time ratio for the Gumbel estimate is marked 1, the EPM is marked 2, JPM 1-dependent is marked 3, JPM independent is marked 4 and the JPM 2-dependent is marked 5 respectively.

calculated assuming the tidal period is large enough to assume independence between consecutive square-top tides. Two dimensional probabilities were calculated using (2.8) and the expression given by Steck was used to evaluate the three dimensional probabilities. To calculate P_{000} from P_{111} the following equation was used

$$P_{000} = 1 - 3P_1 + 2P_{11} + P_{1.1} - P_{111}.$$

Figure 2.1 shows that all the methods provide similar estimates for the return time as the level becomes large. However the rate of convergence varies greatly between the methods. As seen in Figure 2.1, the exceedance probability method gives closer estimates than the other methods. The use of the EPM reduces the estimation problem to a two dimensional probability of upcrossing. However, note that all the other return period estimates do converge to T_g asymptotically.

2.4 Summary

The discussion carried out in this chapter reveals that the return period has been defined using different events such as upcrossings, exceedances, peaks over a threshold exceeding a level and annual maxima exceedances. Since these events are asymptotically equivalent for iid processes, the resulting return periods are also asymptotically equivalent.

All the different methods were considered for the estimation of return periods for a Gaussian AR(1) surge with a square-top tide. For the purposes of comparison, the Gumbel's definition of return period was used as a baseline. It was found that out of all the methods considered, only the POT method with a square-top tide acting as the threshold level gives the same estimate as the Gumbel method. However, this method causes problems with a seasonally varying tide. As described earlier, the real tide is a curve not a square wave in the high tide limit. In this case the exceedances follow a nonhomogeneous Poisson process with intensity Λ varying seasonally over time.

It would be difficult to use the baseline estimate of T_g with a correlated surge as difficulties arise in calculating the higher dimensional probabilities which are required. The two estimates T_{jpm} and T_r only require the probability of exceedance and the probability of upcrossing. There are numerical methods and computer programs available to calculate these probabilities accurately. The two methods EPM and JPM can be used with short records of data provided that the surge process is parametrically specified. Both of these methods converge to T_g asymptotically. Modifications to the JPM are necessary for use with a deterministic tide and the EPM must be redefined for use with discrete time probabilities of upcrossings.

One point of fundamental importance in using a short record of data is that nonstationarity in the surge be parametrically explained using seasonally varying model parameters. This will be done in Chapter 3.

Chapter 3

A Periodic Autoregressive Surge Model

A description of the model fitting procedure for hourly surges is presented in this chapter. Our objective is to explain the stochastic behavior of the surge by a parametric model. Given that the important stochastic features, like autocorrelation and variance, have annual cycles, a year of data may be sufficient to capture all the necessary features in the data. On that basis, the information in the surge may be condensed into a small number of parameters with a known distribution. This would enable one to estimate the probabilities of exceedance or upcrossings required by the return period estimations by using only a year or so of data. This approach provides a means of dealing with some of the problems resulting from the unavailability of long records of data.

Hourly surges are subject to systematic changes in their variance and autocorrelation structure. Observations for Halifax show that the hourly variations of the surge level in the winter is substantially higher than that in the summer. Further, the autocorrelation of the surge in the winter is stronger than in the summer. This is evidenced by the Halifax surge having high surge values clustering for a longer period in the winter than in the summer.

The features discussed above suggest a seasonally varying autocorrelation and variance structure for the Halifax surge series. Nonstationarity, which usually appears in the mean in conventional autoregressive moving average (ARMA) models, can be eliminated by taking first differences of adjacent values in the series to gain first-order stationarity. Second-order nonstationarity, which exists in the form of seasonally varying autocorrelation and variance, leads to more complicated models than the usual ARMA models.

The level of the surge at any time t, η_t^S, was obtained by removing the level of the tide η_t^T from the observed sea level η_t. The tidal package of Foreman (1977) determines the tidal constituents from data and provides the surge after removing all possible deterministic tidal components. However, there still may be some unidentified components remaining in the surge, leading to a contaminated noise process. Moreover, any distortion in the surge may also be due to measurement errors in the observed sea level. Upon examination of time series plots of Halifax sea level, it was noticed that a nonsystematic change in the surge level appears. These irregularities may be due to recording errors.

A useful class of models, originally designed by engineers to explain the systematic distortion in signals, is that of state space models. In this chapter, state space models with and without noise will be fitted to the surge. A model which describes well the stochastic behavior of the data will then be selected. As we only deal with surge, the superscript s will be dropped and hereafter η_t is the observed surge at time t. In cases where the noise is present, η_t is expressed by a measurement equation (Harvey 1981)

$$\eta_t = x_t + w_t \tag{3.1}$$

where the measurement noise component w_t is assumed to be serially uncorrelated and normally distributed with zero mean and variance θ.

Note that η_t cannot be filtered or standardized in a time invariant manner to achieve second-order stationarity due to the seasonally changing variance and autocorrelation structure. Middleton and Thompson (1986) pointed out that the surge variance is seasonally varying and higher in winter than in summer. In places like

Halifax, where extremely high surges due to storms occur only in the winter time, the autocorrelation and the variance of hourly surges in the winter may be different from that of the summer.

A class of models which describes the second-order seasonal behavior is that of periodic autoregressive moving average (PARMA) models (Jones and Brelsford 1967, Pagano 1978, Troutman 1979, Tiao and Grupe 1980). This particular class of models allow the usual ARMA parameters to change over time. A periodic autoregressive model of order 1, PAR(1), for x_t is given by

$$x_t = \alpha(t)x_{t-1} + \beta(t)\epsilon_t, \tag{3.2}$$

where the innovation ϵ_t is assumed to be a white noise series. The periodic AR parameter at time t, $\alpha(t)$, is given by

$$\alpha(t) = \alpha_0 + \alpha_1 \cos(\omega t) + \alpha_2 \sin(\omega t) \tag{3.3}$$

and $\beta(t)$ is assumed to follow a similar seasonal pattern

$$\beta(t) = \beta_0 + \beta_1 \cos(\omega t) + \beta_2 \sin(\omega t). \tag{3.4}$$

Here the frequency ω is equal to $2\pi/8766$ for hourly data and allows for leap years. The innovation ϵ_t a measurement noise w_t, are assumed to follow normal distributions.

The method of maximum likelihood (ML) is used to estimate the model parameters. ML estimation of PARMA parameters was used by Vechia (1985) for stream flow data. The variance for this data set changed bimonthly and the autocorrelation was constant. It was found by Vechia that the ML method generally reduces the mean squared error of estimates compared to the moment estimation method. Another possible estimation method, generally used in ARMA model fitting, is to use seasonal Yule-Walker equations. In PARMA models, seasonal Yule-Walker equations are complicated as the autocorrelation function of lag varies over time. The estimates obtained by Vechia are not applicable to the surge parameters in PAR(1) model, as in (3.2). The model presentation in (3.2) is also different from the conventional ARMA models presented in Box and Jenkins (1981) in which α and β are constant.

The objective of the estimation procedure is to find a well fitting parametric model for the surge, using a single year of data. In Section 3.2, the estimation techniques and diagnostic checks are demonstrated using the 1930 hourly surge series for Halifax. The year 1930 was free from missing values, however may not be a typical year. Possible timing errors and errors due to horizontal and vertical shifts of the sea level gauge plotter are eliminated using the technique developed by Thompson and Smith (COWLIS report, personal communication).

The ML method of estimating model parameters for different types of postulated models is outlined in Section 3.1. The covariance matrix of the ML estimates of the parameter vector can be approximated by the inverse of the sample information matrix (Bickel and Docksum,1977) and significance tests can be based on the asymptotic normality of ML estimates. Likelihood ratio techniques will be used to test the significance of parameters like the measurement noise variance θ or the AR coefficients. Once a plausible model is identified, significance tests will be carried out for all of its parameters. Model adequacy will be checked by comparing the estimated seasonally varying autocorrelation and variance structure of the model with the same features for the observed surge. The normality assumption of the noise is checked by examining the residuals of the chosen surge model.

The selected model will be utilized to explain the stochastic behavior of the Halifax surge in Section 3.3. Parameters are estimated using a year of data. As it is natural to have year-to-year sampling variability, confidence intervals for the vital statistics, like variance and autocorrelation, will be constructed.

A special type of a surge parametric model is designed and fit in this chapter. One distinguishing feature of the surge parametric model stipulated in this study is the explanation of the second-order nonstationarity, appearing in the form of seasonally changing variance and autocorrelation, by a seasonally varying set of parameters $\alpha(t)$ and $\beta(t)$. The influence of such nonstationarity in the final return period estimation is examined below using Halifax sea level data to motivate construction of a surge parametric model.

The return period estimates discussed in the previous chapter require the estimation of the probability of high level exceedances. As the tide is deterministic, this probability can be expressed as the probability of the surge exceeding the gap between the level of concern and the tide. The most commonly used annual maxima return period of the level η^* is the reciprocal of the probabilities of the annual maxima exceeding η^* minus the level of the tide. For simplicity in examining the seasonal variance, the tide will be assumed to be a delta function of height (δ) every twenty four hours. Then, the return period of the level η^* is stated as the reciprocal of the probability annual maxima exceedance of ℓ, where $\ell = \eta^* - \delta$.

To examine the influence of the seasonality in the variance, the surge will be assumed to be a moving average of order less than twenty four hours, thus allowing for exceedances at the diurnal tides to be independent of one another. If intraseasonal variance change is assumed to be negligible, the surge variance in winter, spring, summer and fall can be assumed to be 289.41, 118.70, 65.82 and 217.72 cm^2 respectively. These values are the seasonal averages from the estimated model in Section 3.3. The average annual variance from the estimated model, for the whole year, is taken to be 173.52 cm^2.

The annual maxima return period was calculated in two ways. The first estimate is based on the different variances for each season and thus allows the variance to change with season. The second estimate is based on the average variance for the whole year and thus assumes that the variance does not change over the year. Table 3.1 provides return period estimates for these two cases for the levels $\ell = 10, 15, 20, 25, ..., 55, 60cm$. Table 3.1 shows that as the level becomes extreme, the difference between estimated return periods with and without seasonal variance increases. Differences begin to appear around the 40 cm level which is about three standard deviations away from the surge mean. The seasonal variance estimate tells us that the level of 40 cm is exceeded in another year or so, but the use of nonseasonal variance forecasts the same to be four years. If the level of exceedance is five standard deviations away from the mean, around 60 cm, the exceedances could occur in another 49 years time according

	Return period in years	
Level (cm)	with seasonal variance	without seasonal variance
25	1.00	1.00
30	1.00	1.04
35	1.00	1.58
40	1.47	4.19
45	2.69	16.02
50	6.16	76.55
55	16.45	435.32
60	48.83	2881.20

Table 3.1: Return periods from annual maxima method

to seasonal variance estimate, whereas the nonseasonal variance estimate is 2881 years. This enormous difference can lead to disastrous consequences in environmental planning. The above noted difference motivated us to look for a seasonally varying parameter structure for the surge model, which is presented below.

3.1 Plausible models and likelihood functions

Four types of models will be fitted using the combination of measurement noise and AR(2) coefficient as set down in the table below.

Noise	AR(2) coefficients	
	Absent	Present
Absent	Model 1	Model 2
Present	Model 3	Model 4

MODEL 1: PAR(1) model without noise

The simplest model that explains the second-order nonstationarity of the surge is PAR(1), where the observed surge at time t, η_t is given in terms of the state, x_t, according to

$$x_t = \alpha(t)x_{t-1} + \beta(t)\epsilon_t$$

$$\eta_t = x_t.$$

Parameter functions $\alpha(t)$ and $\beta(t)$ are given in equations (3.3) and (3.4) respectively.

The likelihood function for a single year of data can be written as

$$L(\vec{\alpha}, \vec{\beta}/\vec{\eta_n}) = \frac{1}{(2\pi)^{n/2}} \frac{\exp(-\sum_{t=1}^{n}(\eta_t - \alpha(t)\eta_{t-1})^2/2\beta^2(t))}{\prod_{t=1}^{n}\beta(t)},$$

where the parameter vectors $\vec{\alpha}$ and $\vec{\beta}$ are given by $\vec{\alpha} = (\alpha_0, \alpha_1, \alpha_2)'$, $\vec{\beta} = (\beta_0, \beta_1, \beta_2)'$ and $n = 8766$ giving $\vec{\eta_n} = (\eta_1, \eta_2, ..., \eta_n)'$. Up to an additive constant the log likelihood is proportional to ℓ_n

$$\ell_n = -\sum_{t=1}^{n}[\frac{\eta_t - \alpha(t)\eta_{t-1}}{\beta(t)}]^2 - \sum_{t=1}^{n}\log(\beta^2(t)). \tag{3.5}$$

Notice that in the above likelihood equation η_0 was considered as zero. As explained by Box and Jenkins (1976) if the sample size n is considerably large an approximation to the conditional likelihood can be obtained by using unconditional likelihood with suitable starting values for parameters. The ML estimates of $\vec{\alpha}$ and $\vec{\beta}$ were obtained by maximizing ℓ_n using a quasi-Newton optimization subroutine from NAG (E04JAF). This particular subroutine is simple to use and returns accurate estimates as long as parameters are unconstrained and unbounded. However, the representation of $\alpha(t)$ and $\beta(t)$ in (3.3) and (3.4) are bounded such that $-1 \leq \alpha(t) \leq 1$ and $\beta(t) > 0$. To aid in numerical optimization all the parameters with a restricted domain were transformed into $\gamma_i \epsilon(-\infty, \infty)$ using the transformations given in Table 3.2. Parameter estimation using this iterative procedure also requires starting values and here, $\gamma_i = 0$ for i=1,2,... were used as such. The variance of the surge at time t, σ_t^2, can be written as

$$\sigma_t^2 = \alpha^2(t)\sigma_{t-1}^2 + \beta^2(t). \tag{3.6}$$

Parameter	Transformation
γ_0	$\log[(a_0^2)/(1-a_0^2)]$
γ_1	$\log[((a_1+2)/4)/(1-(a_1+2)/4)]$
γ_2	$\log[(a_2/2\pi)/(1-a_2/2\pi)]$
γ_3	$\log[b_0]$
γ_4	$\log[(b_1)(1-b_1)]$
γ_5	$\log[(b_2/2\pi)/(1-b_2/2\pi)]$
γ_6	$\log[(c_0^2)/(1-c_0^2)]$
γ_7	$\log[((c_1+2)/4)/(1-(c_1+2)/4)]$
γ_8	$\log[(c_2/2\pi)/(1-c_2/2\pi)]$
γ_9	$\log(\theta)$

Table 3.2: Reparameterization, The parameters, $a_0, a_1, a_2, b_0, b_1, b_2$ and c_0, c_1, c_2 are expressed as $\alpha(t) = a_0(1 + a_1 \cos(\omega t + a_2))$, $\beta(t) = b_0(1 + b_1 \cos(\omega t + b_2))$ and $\lambda(t) = c_0(1 + c_1 \cos(\omega t + c_2))$ with $\omega = 2\pi/8766$.

The lag k autocorrelation at time t, $\rho_t(k)$, is given by

$$\rho_t(k) = \alpha(t)\rho_t(k-1)\frac{\sigma_{t-1}}{\sigma_t} \tag{3.7}$$

where $\rho_t(k)$ is explicitly defined as

$$\rho_t(k) = \frac{\text{cov}(\eta_t, \eta_{t-k})}{\sigma_t \sigma_{t-k}}. \tag{3.8}$$

Consequently, the lag 1 autocorrelation at time t, $\rho_t(1)$, can be written as

$$\rho_t(1) = \alpha(t)\frac{\sigma_{t-1}}{\sigma_t}.$$

Recursive substitution in (3.7) gives

$$\rho_t(k) = \prod_{i=1}^{k} \alpha(t+1-i)\frac{\sigma_{t-k}}{\sigma_t}. \tag{3.9}$$

Under the assumption of slowly varying $\rho_t(k)$ (*i.e.* if $\rho_t(k) = \rho_{t-1}(k)$)

$$\rho_t(k) = \alpha^k(t)(\frac{\sigma_{t-1}}{\sigma_t})^k.$$

This seems like a reasonable assumption for Halifax surge. If the standard deviation of the surge at time t varies slowly (*i.e.* if $\sigma_{t-1} = \sigma_t$), which appears to be a reasonable assumption, then $\rho_t(1) \approx \alpha(t)$. The function $\alpha(t)$ then represents the autocorrelation at lag 1 at time t. $\sigma^2(t)$ in (3.6) shows the variance at time t follows first order difference equation with parameters $\alpha^2(t)$ and $\beta^2(t)$. For a serially uncorrelated surge, $(\alpha(t) = 0)$, $\beta^2(t)$ represents the variance of the surge process. The autocorrelation function (ACF) at time t, $\rho_t(k)$, as a function of lag k, given in (3.9), decays exponentially to zero as one would expect in a stationary AR(1) model. However, the rate of decay depends not only on the PAR parameter $\alpha(t)$, but also on the $\frac{\sigma_{t-1}}{\sigma_t}$.

It was noticed that the ACF function of the observed surge decays slower than that of the PAR(1) model (see Figure 3.3). Since the decay pattern in (3.9) is governed by autoregressive parameters as well as the variance, it was thought that either the surge follows a higher order PARMA model or the observed surge is contaminated by a noise with nonunit variance, or possibly both. Therefore, the following models were also considered.

MODEL 2: PAR(2) model without noise

The observed surge at time t, η_t, can be written as

$$x_t = \alpha(t)x_{t-1} + \lambda(t)x_{t-2} + \beta(t)e_t$$

$$\eta_t = x_t$$

with $\alpha(t)$ and $\beta(t)$ as expressed in equation (3.3) and (3.4). $\lambda(t)$ also can be written in a similar fashion as

$$\lambda(t) = \lambda_0 + \lambda_1 \cos(\omega t) + \lambda_2 \sin(\omega t). \tag{3.10}$$

As before, up to an additive constant the log likelihood is proportional to ℓ_n

$$\ell_n = -\sum_{t=2}^{n}[\frac{\eta_t - \alpha(t)\eta_{t-1} - \lambda(t)\eta_{t-2}}{\beta(t)}]^2 - \sum_{t=1}^{n} \log \beta^2(t).$$

The autocorrelation at lag 1 for time t, $\rho_t(1)$, is given by

$$\rho_t(1) = \frac{\alpha(t)\sigma_{t-1}}{\sigma_t - \lambda(t)\sigma_{t-2}}.$$

If the variance changes slowly over time then $\rho_t(1)$ is approximately equal to $\frac{\alpha(t)}{1-\lambda(t)}$, which is same as the autocorrelation at lag 1 for a stationary AR(2) model. The variance of the surge at time t, σ_t^2 is given by

$$\sigma_t^2 = \alpha^2(t)\sigma_{t-1}^2 + \lambda^2(t)\sigma_{t-2}^2 + \beta^2(t) + 2\lambda(t)\alpha(t)\rho_t(1)\sigma_{t-1}\sigma_{t-2} \tag{3.11}$$

Under the assumption of slowly changing variance, *i.e.* if $\sigma_t^2 = \sigma_{t-1}^2 = \sigma_{t-2}^2$, the variance at any time t can be approximated by

$$\sigma_t^2 \approx \frac{\beta^2(t)}{1 - \alpha^2(t) - \lambda^2(t) - 2\alpha(t)\lambda(t)\rho_t(1)}.$$

If the surge process is serially uncorrelated, the above relationship reduces to $\sigma_t^2 = \beta^2(t)$. The ACF at lag k at time t, $\rho_t(k)$, is given by the recursive relationship

$$\rho_t(k) = \alpha(t)\rho_{t-1}(k-1)\frac{\sigma_{t-1}}{\sigma_t} + \lambda(t)\rho_{t-2}(k-2)\frac{\sigma_{t-2}}{\sigma_t}. \tag{3.12}$$

In the above PAR(2) representation of the surge model, the variance function as well as the ACF are influenced by all three parameter functions $\alpha(t)$, $\lambda(t)$ and $\beta(t)$, in contrast to stationary AR(2) models. Nevertheless, all the features of a stationary AR(2) model can be resolved by imposing the condition that σ_t^2 does not change over time in the PAR(2) model. Therefore, the above model representations are quite compatible with conventional AR models, except for the second-order nonstationarity.

If the surge component is contaminated by a noise, the next two state space models may represent the surge.

MODEL 3: PAR(1) model with noise

In this model, the measurement equation for the observed surge η_t is given by

$$\eta_t = x_t + w_t \tag{3.13}$$

where the measurement noise w_t is assumed to be Gaussian white noise with variance θ. The surge state x_t is modeled by the PAR(1) process

$$x_t = \alpha(t)x_{t-1} + \beta(t)\epsilon_t,$$

where the innovation ϵ_t is assumed to be Gaussian white noise with variance 1.

The Kalman filter (Kalman, 1960) provides a useful device with which the likelihood of a PARMA model can be evaluated. Using the prediction error decomposition (e.g Harvey, 1981) the loglikelihood function is proportional to

$$\ell_n = -\sum_{t=1}^{n}[\frac{v_t^2}{f_t} + \log(f_t)]. \tag{3.14}$$

where v_t and f_t are described below, and are returned by the Kalman filter.

Let $x_{t|t-1}$ denote the one step ahead prediction of the surge state given the observations $\{\eta_1, \eta_2, ..., \eta_{t-1}\}$, and $\hat{x}_t$ be the one step ahead prediction of the state based on information available at $t-1$.

Let $s^2_{t|t-1}$ and s^2_{t-1} be the variance of $x_{t|t-1}$ and $\hat{x}_{t-1}$ respectively and denote the prediction error by $v_t = \eta_t - x_{t|t-1}$. The prediction and updating equations for the Kalman filter are:

<u>Prediction</u>

$$x_{t|t-1} = \alpha(t)\hat{x}_{t-1}. \tag{3.15}$$

This estimator is unbiased for x_t and has variance

$$s^2_{t|t-1} = \alpha^2(t)s^2_{t-1} + \beta^2(t) \tag{3.16}$$

<u>Updating</u>

$$f_t = s^2_{t|t-1} + \theta.$$

$$s^2_t = s^2_{t|t-1} - \frac{s^4_{t|t-1}}{f_t}. \tag{3.17}$$

$$\hat{x}_t = x_{t|t-1} + \frac{s^2_{t|t-1}}{f_t}v_t, \tag{3.18}$$

The term $(s^2_{t|t-1}/f_t)v_t$ is called the Kalman gain and is designed so that $\hat{x}_t$ is the minimum mean square error estimator. Reduction of the variance by the Kalman filter is equal to $s^4_{t|(t-1)}/f_t$ which is the variance of the Kalman gain.

The variance and autocorrelation structures of x_t remains the same as in equations (3.6), (3.7) and (3.8) since the PAR structure of the surge state x_t is preserved.

However, the measurement noise w_t makes the variance and the autocorrelation of the surge measurement η_t different from that of surge state x_t. The variance of the η_t, $\sigma^2_{\eta(t)}$, is the sum of variances of x_t and the noise variance θ, *i.e.*

$$\sigma^2_{\eta(t)} = \sigma^2_t + \theta. \tag{3.19}$$

The autocorrelation at lag k, $\rho_{\eta(t)}(k)$, is given by

$$\rho_{\eta(t)}(k) = \rho_t(k)\frac{\sigma_t\sigma_{t-k}}{\sqrt{\sigma^2_{\eta(t)}\sigma^2_{\eta(t-k)}}}, \tag{3.20}$$

where σ_t is given in (3.6) and $\rho_t(k)$ is given in (3.9).

MODEL 4: PAR(2) with noise

The measurement equation that links the observed surge to the surge state with noise remains the same as in equation (3.13). The transition equation takes the form of a PAR(2) model

$$x_t = \alpha(t)x_{t-1} + \lambda(t)x_{t-2} + \beta(t)\epsilon_t$$

where $\lambda(t)$ is given by (3.10).

The prediction equations are

$$x_{t|t-1} = \alpha(t)\hat{x}_{t-1} + \lambda(t)\hat{x}_{t-2} \tag{3.21}$$

with the corresponding prediction variance $s^2_{t|t-1}$ being

$$s^2_{t|t-1} = \alpha^2(t)s^2_{t-1} + \lambda^2_t s_{t-2} + \beta^2_t + 2\lambda(t)\alpha(t)r_t(1)s_t s_{t-1} \tag{3.22}$$

where $\hat{x}_t$ is the MMSE estimate of x_t based on past values and $r_t(1)$ is given by

$$r_t(1) = \frac{\alpha(t)s_{t-2}}{s_{t-1} - \lambda(t)s_{t-3}},$$

and the updating equations are same as for the PAR(1) representation in Model 3.

3.2 Model selection

The proceding four models were fit to 1930 surge data for Halifax by the method of maximum likelihood. The unknown parameters were obtained by maximizing the log likelihood ℓ_n. A numerical subroutine from NAG, E04JAF, was used to maximize ℓ_n as described at the beginning of the last section.

In order to select a good model to describe the second-order nonstationarity, diagnostic checks are carried out using likelihood ratio tests (Bickel and Docksum, 1977). Parameter estimates are then investigated further in terms of the sample autocorrelation and sample variance.

Likelihood ratio (LR) tests are used to test the significance of coefficients like the measurement noise variance θ and $\vec{\lambda} = (\lambda_0, \lambda_1, \lambda_2)'$. In all four models, it was assumed that $\alpha(t) \neq 0$ and $\beta(t) \neq 0$ as the prior knowledge of the surge suggests that it is serially autocorrelated with a seasonally changing variance. However once a model is selected, the significance of each of its parameters ($\vec{\alpha}$, $\vec{\beta}$, $\vec{\lambda}$ and θ) will be tested.

Consider the LR test of the hypothesis $\theta \neq 0$ when $\vec{\lambda} = 0$ (model 1 vs. 3). The following test criteria will be adopted. The test statistic (TS) of a likelihood ratio test of the null hypothesis $H_0 : \theta = 0$ against the alternative of $H_1 : \theta > 0$, is given by $-2 \log L_r$ where L_r is the likelihood ratio

$$L_r = \frac{\text{Likelihood under } H_0}{\text{Likelihood under } H_1}.$$

This test is nonstandard as H_0 assigns θ to the boundary of the parameter space and the null distribution of the test statistics is 50 : 50 mixture of a χ_0^2 and a χ_1^2 distribution (Self and Liang, 1987). The χ_0^2 density function is given by $f(x) = x^{-1} \exp(-x/2)$ for $x > 0$.

The tests of $H_0 : \vec{\lambda} = 0$ with $\theta = 0$ or $\theta \neq 0$ are standard, and the reference distribution is χ_3^2.

The results of such tests are summarized in Table 3.3.

The likelihoods under H_0 and H_1 were calculated given the Halifax surge data. The parameter estimates of $\vec{\alpha}$ and $\vec{\beta}$ were not fixed for H_0 and H_1. For instance, in

Hypothesis	TS
H_0: $\lambda = 0/\theta = 0$ $H_1 : \lambda \neq 0/\theta = 0$	39.69
H_0: $\lambda = 0/\theta \neq 0$ $H_1 : \lambda \neq 0/\theta \neq 0$	39.22
H_0: $\theta = 0/\lambda = 0$ $H_1 : \theta \neq 0/\lambda = 0$	6034.87
H_0: $\theta = 0/\lambda \neq 0$ $H_1 : \theta \neq 0/\lambda \neq 0$	6034.40

Table 3.3: Likelihood ratio test results

the test of $\theta = 0$ when $\vec{\lambda} = 0$ (model 1 and 3) the parameter estimates of $\vec{\alpha}$ and $\vec{\beta}$ in model 1 are different from that of model 3. No attempt was made to address multiple comparisons issues.

According to the LR test results, the reduction of deviance by θ for one degree of freedom is very large compared to the reduction due to $\vec{\lambda}$, for three degrees of freedom. Approximate p-values were less than 10^{-3}. Reduction of deviance due to θ is not influenced by the fact that λ is in the model and vice-versa. Both parameters appeared to be statistically significant while the parameter θ shows signs of high significance, regardless of whether or not λ is in the model. Therefore, models 3 and 4 are likely to be the best models according to LR criteria, for explaining the variation of Halifax surge.

Our primary objective is to obtain a model that describes well the seasonality in the variance and autocorrelation of the surge. To what extent this objective has been accomplished by each model will be investigated by visual comparisons of observed and estimated ACF and variance. Our second step in the model selection procedure is to compare the sample ACF and variance functions obtained from each model. The model which gives the closest functional behavior to these sample functions is selected.

The sample variance for each month in Figure 3.1 was calculated assuming the change of variance within each month is negligible. For example, the sample variance for January was calculated by, $\sum_{t=1}^{730} \frac{(\eta_t - \text{monthly mean})^2}{729}$, using 730 observations for the month January. In Figure 3.1, models 1 and 3 slightly overestimate the variance, whereas models 2 and 4 underestimate the variance. The degree of overestimation and underestimation is higher in the stormy seasons of winter and fall compared to the summer. The rate of overestimation has been reduced in models 3. However, note that these overestimation and underestimations are much smaller than the year-to-year sampling variability shown in Figure 3.2. Overall then, as far as the change of variance over the months are concerned, model 3 is closer to the sample variance function for the year 1930 than are models 1,2 and 4

For comparison purposes, the sample ACF function for each season as a function of lag was calculated separately for 1930-1934 assuming intraseasonal autocorrelation changes at any lag are negligible. Also the ACF from each model was calculated using the parameter estimates, $\alpha(t), \beta(t)$ and $\lambda(t)$ for a time t equal to the middle of the season. For example, the ACF for winter, $\rho_t(k)$, was calculated at t=1095.

Figures 3.3, 3.4, 3.5 and 3.6 show the ACF functions for the four surge models. Models 1 and 2 clearly underestimate the ACF function. The rate of underestimation varies seasonally and is greater in the winter and fall seasons than in the summer and spring. However, inclusion of the second order autoregressive parameter $\vec{\lambda}$, in Figure 3.4 makes the ACF of model 2 fit slightly better than model 1 in the winter and fall and somewhat worse in the spring and summer seasons.

Remarkable improvement can be seen in Figures 3.5 and 3.6 which shows the ACF function for models 3 and 4. This suggests that the observed surge is accompanied by noise. However, the slight deviation, that can be seen in Figure 3.5 for summer and Figure 3.6 for spring are much smaller than the year-to-year sampling variability. On the basis of these variance and ACF comparisons, models 3 and 4 are chosen for further investigation.

From the above mentioned graphical comparisons, it was revealed that the models 3 and 4 captured much of the second-order nonstationarity in the model. Model 3

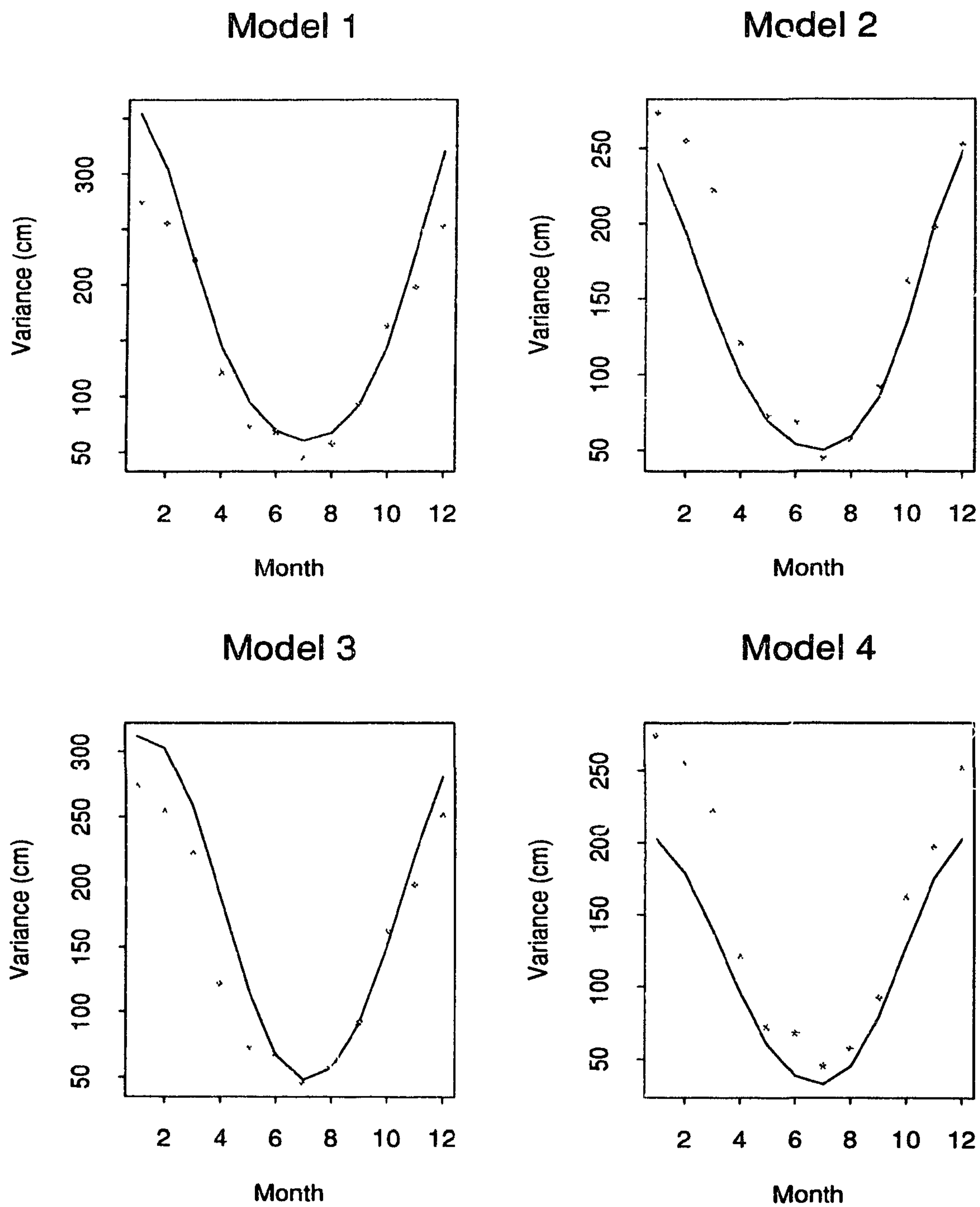

Figure 3.1: Annual changes in variance from the four surge models. The solid line '—' represents the estimated variance from the various models, '*' represents the sample variance from 1930 data. The month is denoted by 1-January, 2-February,....,11-November, 12-December.

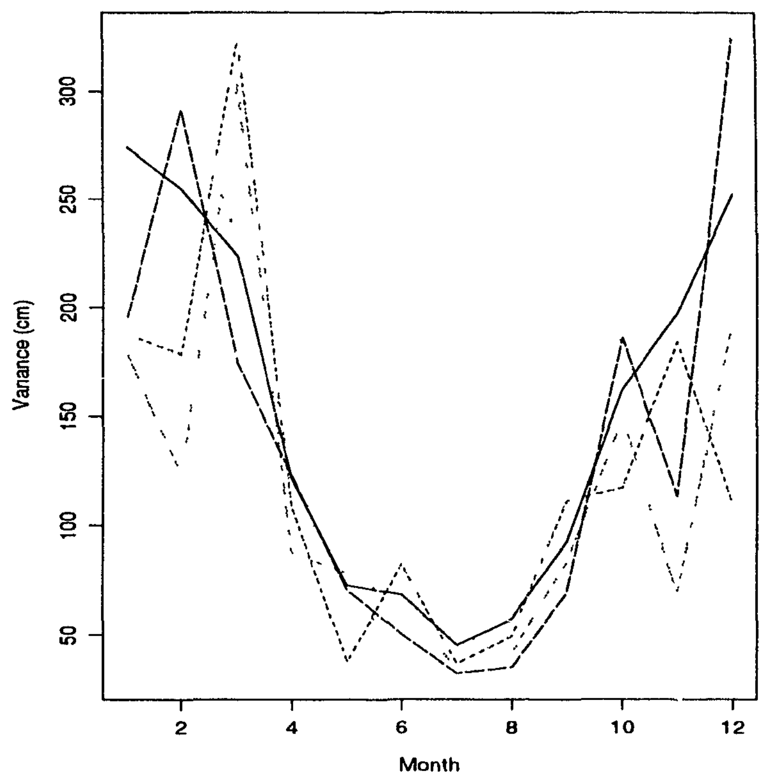

Figure 3.2: Annual variation of sample variance for 1930-1934. Different lines represent different years. The month is denoted by 1-January, 2-February,....., 11-November, 12-December.

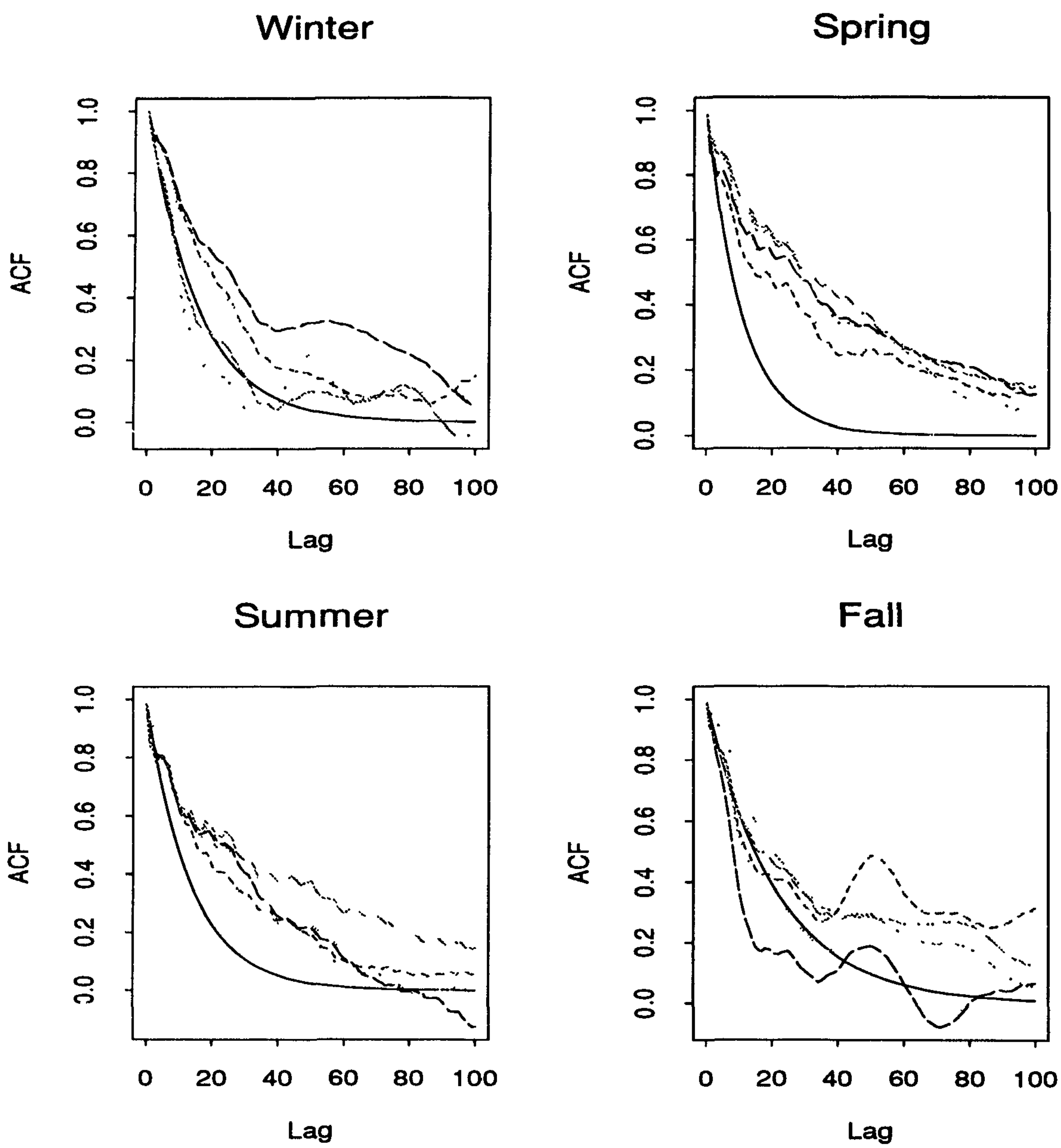

Figure 3.3: The ACF function for four seasons from model 1. Solid line '—' represents the estimated ACF, whereas all five dashed and dotted lines represents sample ACF for the years 1930-1934. Units on the abscissa are hours.

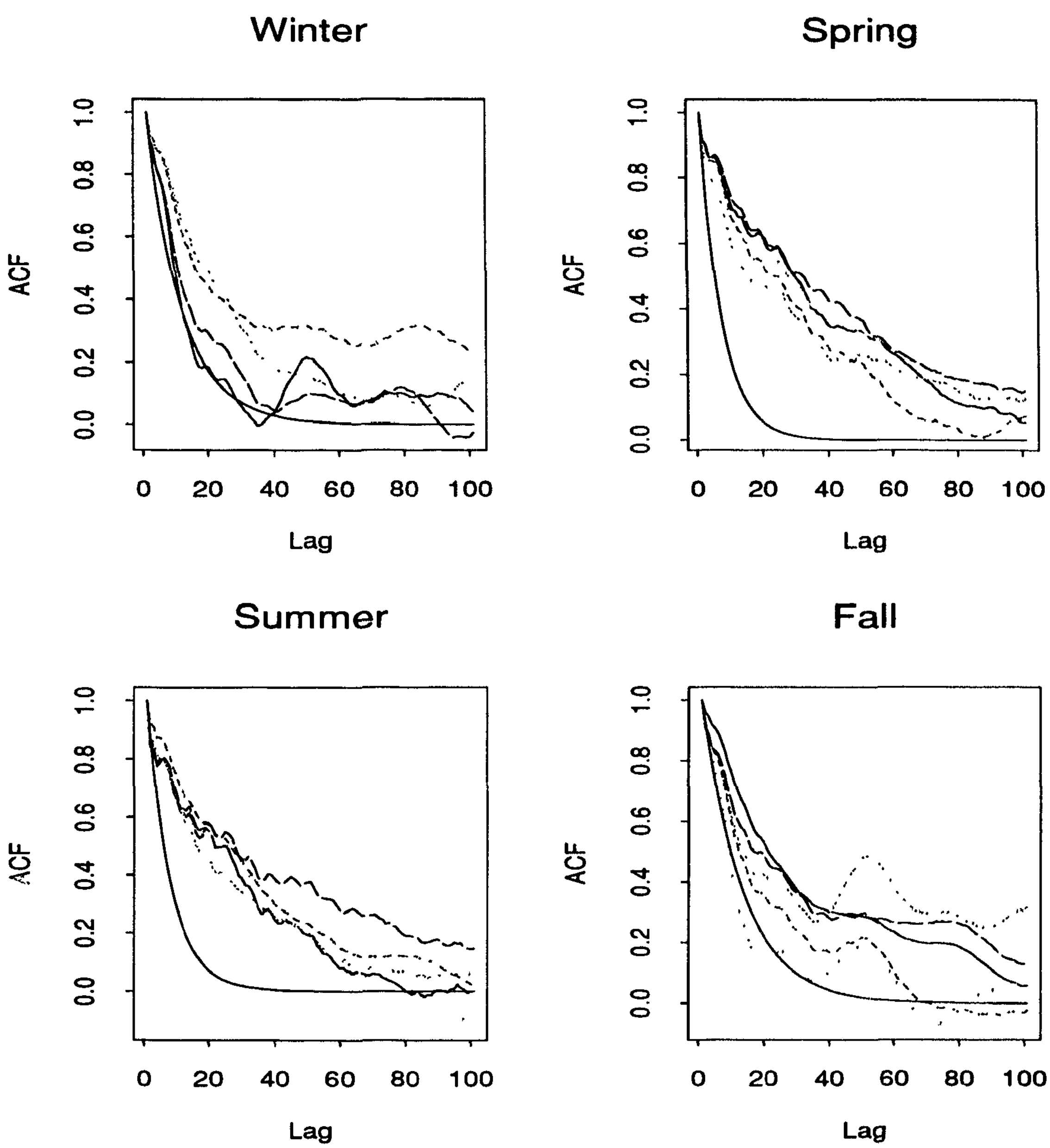

Figure 3.4: The ACF function for four seasons from model 2. Solid line '—' represents the estimates ACF, where as all five dashed and dotted lines represents sample ACF for the years 1930-1934. Units on the abscissa are hours.

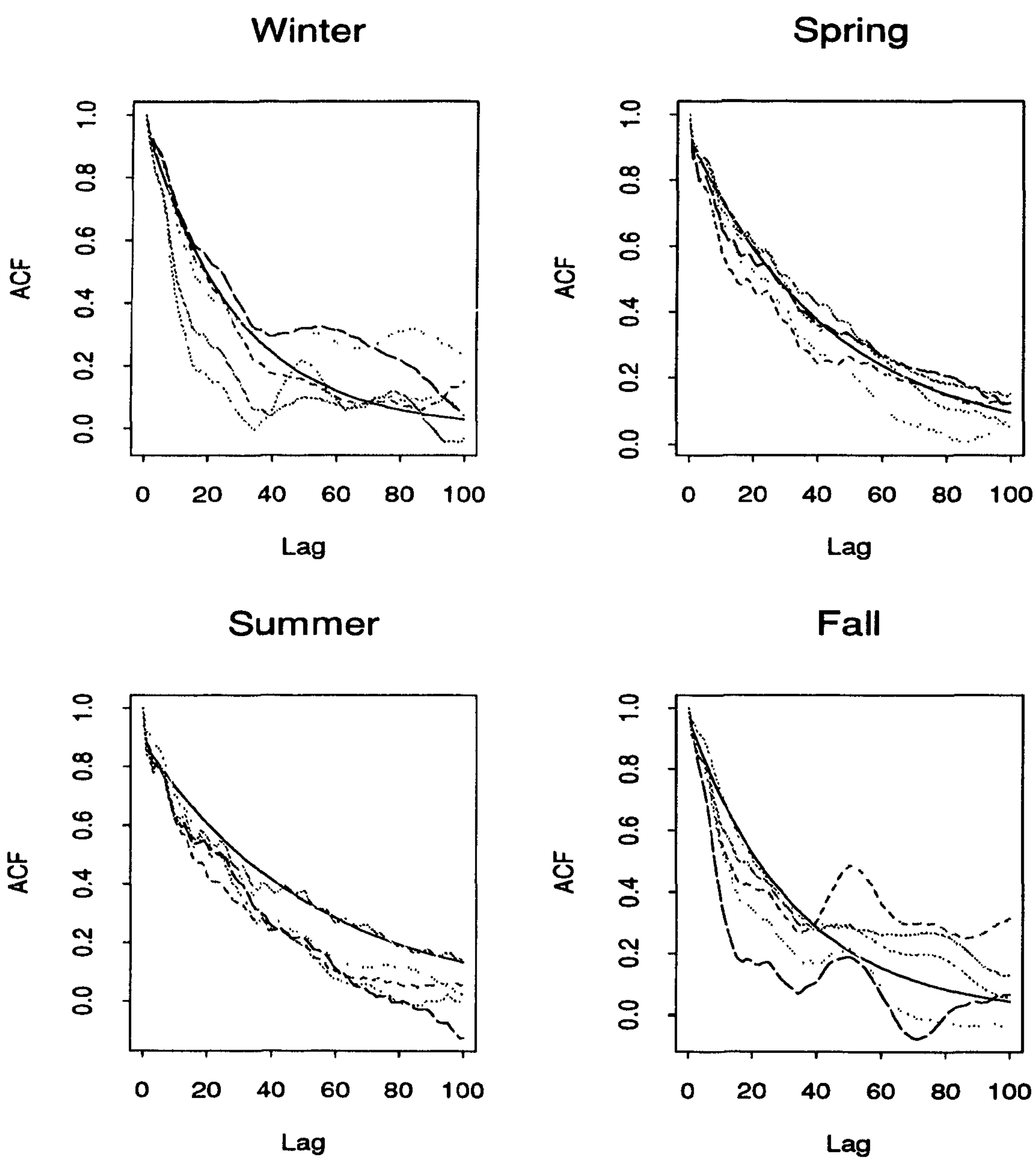

Figure 3.5: The ACF function for four seasons from model 3. Solid line '—' represents the estimates ACF, where as all five dashed and dotted lines represents sample ACF for the years 1930-1934. Units on the abscissa are hours.

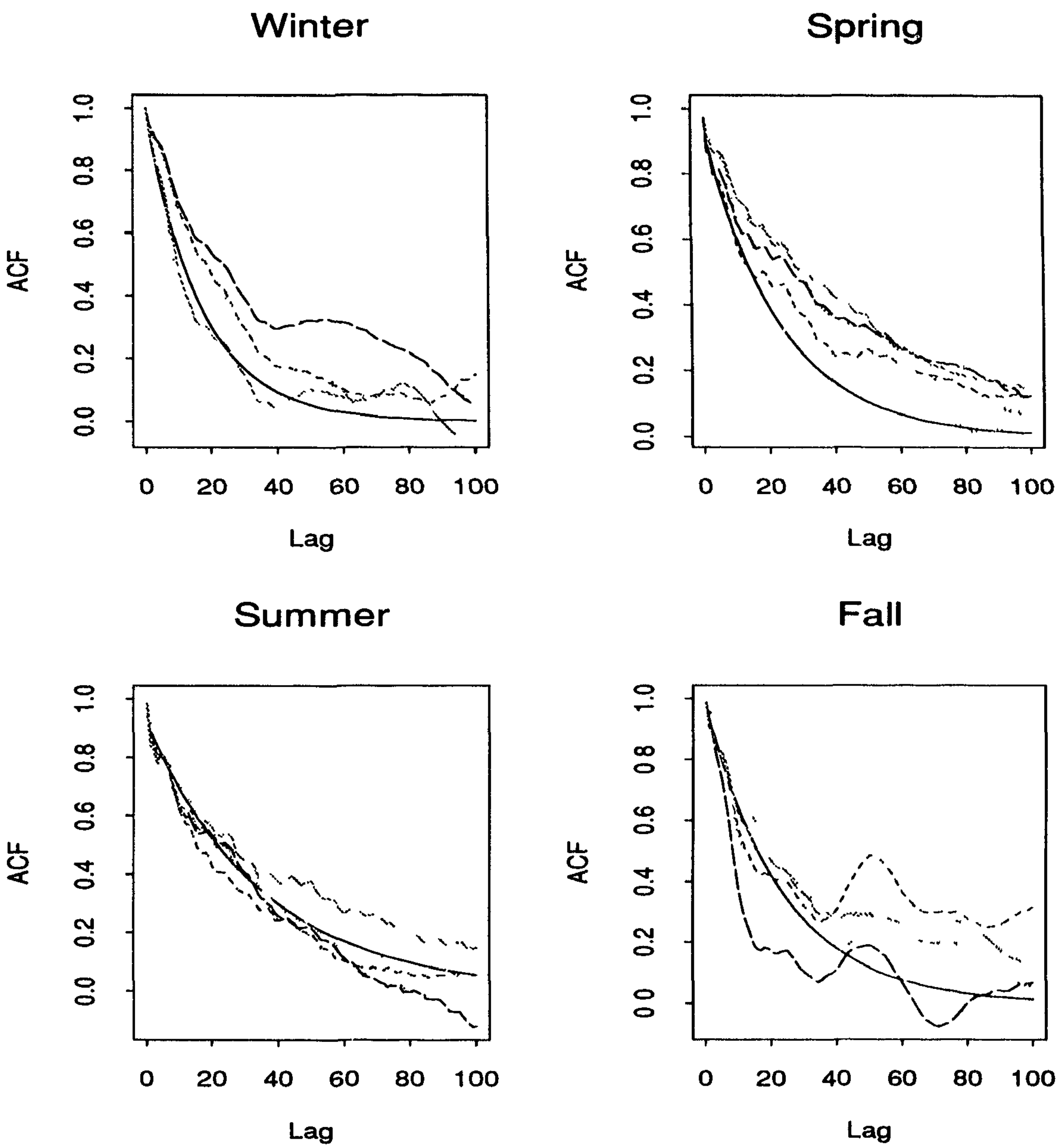

Figure 3.6: The ACF function for four seasons from model 4. Solid line '—' represents the estimates ACF, where as all five dashed and dotted lines represents sample ACF for the years 1930-1934. Units on the abscissa are hours.

consists of seven parameters and model 4 consists of 10 parameters. At this point it is worth examining the significance of each parameter individually.

The parameter vectors of models 3 and 4 are

$$(\alpha_0, \alpha_1, \alpha_2, \beta_0, \beta_1, \beta_2, \theta)'$$

and

$$(\alpha_0, \alpha_1, \alpha_2, \beta_0, \beta_1, \beta_2, \lambda_0, \lambda_1, \lambda_2, \theta)'$$

respectively. Each parameter was estimated using the maximum likelihood method with 8766 data points.

Derivations of the exact expressions for the variance and covariance of parameter estimates are quite complicated as the likelihood contains prediction errors which were calculated using an iterative procedure. Consequently, the terms like partial summation of the products of parameters make the task of obtaining the explicit expressions for second derivatives difficult. Therefore, the covariance matrix of transformed parameters was approximated by the inverse of the sample information matrix. However, since the data set is reasonably large, the sample information matrix provides a reasonably good approximation of its expected value. In other words standard errors estimates are consistent (Bickel and Docksum, 1977). Variances of original parameters $\vec{\alpha}$, $\vec{\lambda}$, $\vec{\beta}$ and θ were then obtained by the delta method.

Table 3.4 provides ML parameter estimates and their standard errors. Significance tests were carried out for the transformed variables. In the table, parameter estimates which are nonsignificant at 5% level are noted. The estimated correlations between parameter estimates were found to be small. The highest correlation observed was 0.003 between β_0 and β_1. For an uncontaminated model, when $\theta = 0$, it can be shown that $\vec{\alpha}$ and $\vec{\beta}$ are orthogonal, in the sense the covariances of the associated estimators are equal to zero.

All three PAR(2) coefficients in model 4, namely λ_0, λ_1 and λ_2, fail the test of significance for the hypothesis that they are significantly different from zero at the 5% level of significance. However, λ_0 is only marginally nonsignificant at the 5% level.

Parameter	Model 3	Model 4
α_0	0.973603 (0.0024)	0.965695 (0.0066)
α_1	-0.008148 (0.0032)	-0.009038 (0.0026)
α_2	-0.003129 (0.0036)	-0.007204 (0.0062)
λ_0		-0.007699** (0.0066)
λ_1		-0.000802** (0.0027)
λ_2		-0.003942** (0.0063)
β_0	2.876584 (0.0491)	2.87479 (0.0313)
β_1	1.606181 (0.0575)	1.605179 (0.01565)
β_2	0.448985 (0.0626)	0.448705 (0.0367)
θ	6.99816 (0.2246)	6.989433 (0.1079)

Table 3.4: Parameter estimates and estimated standard deviations (in brackets) for model 3 and 4. Parameter estimates which are nonsignificant at 5% level of significance are marked by **.

The model with λ_0 did make some improvements in the ACF compared to the other two models 1 and 2. However, as far as the annual changes in variance is concerned, model 3 fits the Halifax surge better than model 4.

Nonsignificance of the second order PAR(2) coefficients reduces the model to PAR(1) with noise, that is model 3. All the parameters in model 3 were found to be significant. The parameter α_2 was only marginally significant. Model 3 has explained the second-order nonstationarity remarkably well. Therefore, model 3 will be selected to represent the stochastic behavior of surge data for Halifax.

Various assumptions were checked for the selected model 3 by examining the

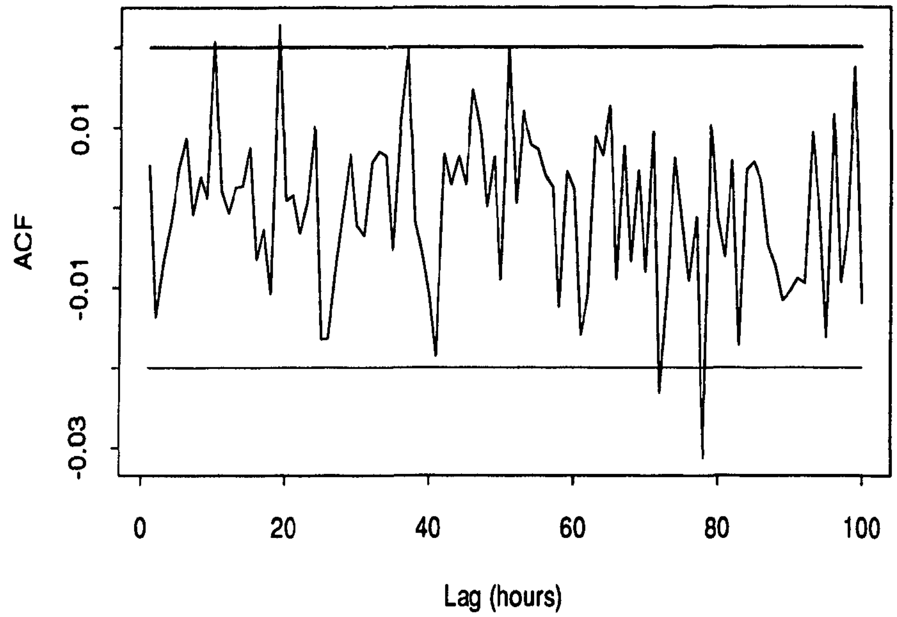

Figure 3.7: The ACF of residuals from MODEL 3. Two horizontal lines enclose the acceptance region for pointwise tests of zero autocorrelation at level 0.05.

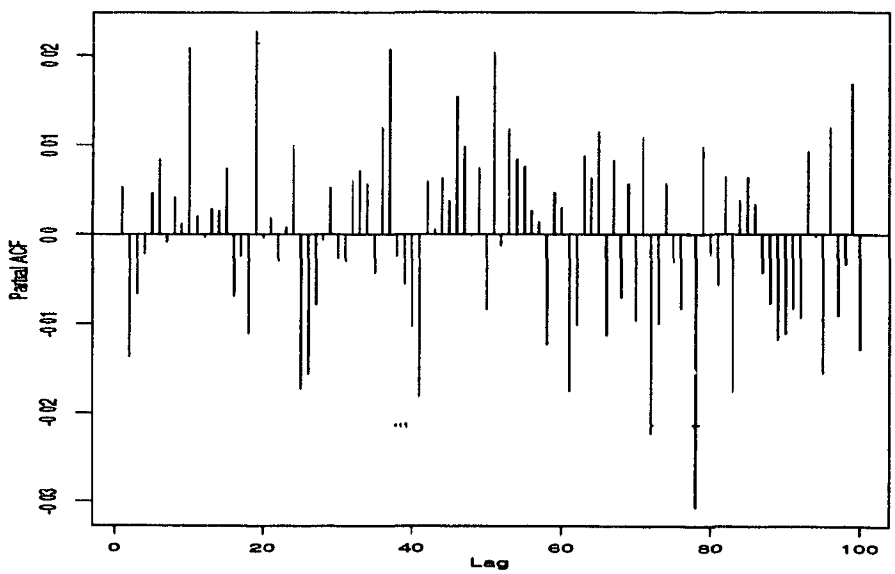

Figure 3.8: The PACF of residuals from MODEL 3. Two horizontal lines enclose the acceptance region for pointwise tests of zero autocorrelation at level 0.05.

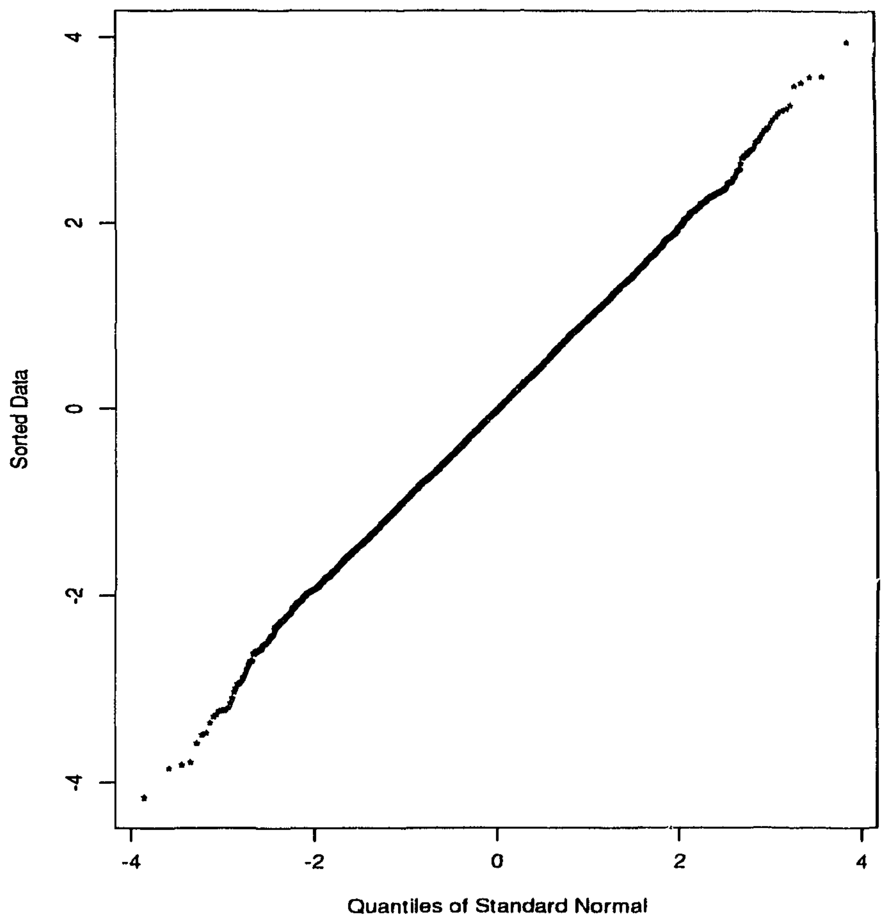

Figure 3.9: The normal q-q plot of residuals from MODEL 3.

residuals. Figures 3.7 3.8 and 3.9 show the autocorrelation as a function of lag (ACF), the partial autocorrelation function (PACF) and the normal probability plot of the prediction errors. The ACF and PACF plots show no sign of serial autocorrelation in the residuals, as 5% of the points would be expected outside the 95% limits due to random sampling alone. The normal quantile plot shows the assumption of normality is plausible.

3.3 Stochastic behavior of surge process for Halifax

In the model fitting and selection procedures carried out in Section 3.1 and 3.2, it was noticed that the observed surge is contaminated by noise. The exact reason for the existence of such a noise is not known. It may be due to physical factors, model or measurement error, or a combination thereof.

It is demonstrated next how the estimated surge model in Section 3.2 is used to explain the stochastic behaviour of surge. The above estimated model 3 can be used to explain the stochasticity of the surge series for Halifax. An important feature of the estimated model is that a successful effort was made to explain the second-order nonstationary behavior through a seasonally changing variance and autocorrelation structure. The efficacy of those estimated model parameters were verified as follows.

The variance of the surge state x_t was calculated using equation (3.6). To obtain the variance of the surge measurement, the estimated noise variance of θ equal to 6.998816 cm^2 was added. The change in surge variance is shown in Figure 3.10.

Figure 3.10 shows that the estimated variance in the winter is substantially higher than in the summer due to the fact that large storms are more likely to occur in the winter. The difference in the winter and summer variances is about 250 cm^2. The sample variance for each month in the year 1930 is extremely close to the estimated surge measurement variance from the model, thus confirming the validity of the model.

The autocorrelation of the surge state and surge measurement were calculated

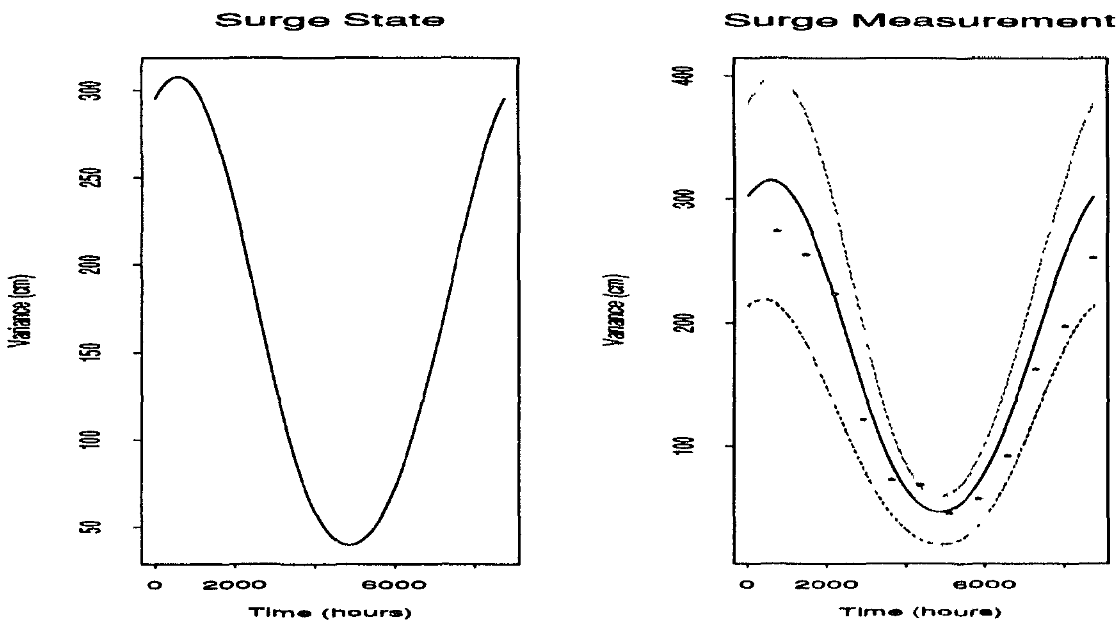

Figure 3.10: Change of surge variance over time for Halifax. Sample variance for each month is marked '*', the solid line represents the estimated model variance, and dotted lines represent the upper and lower bounds of the 95% prediction interval. The time axis is in hours from midnight to January 1.

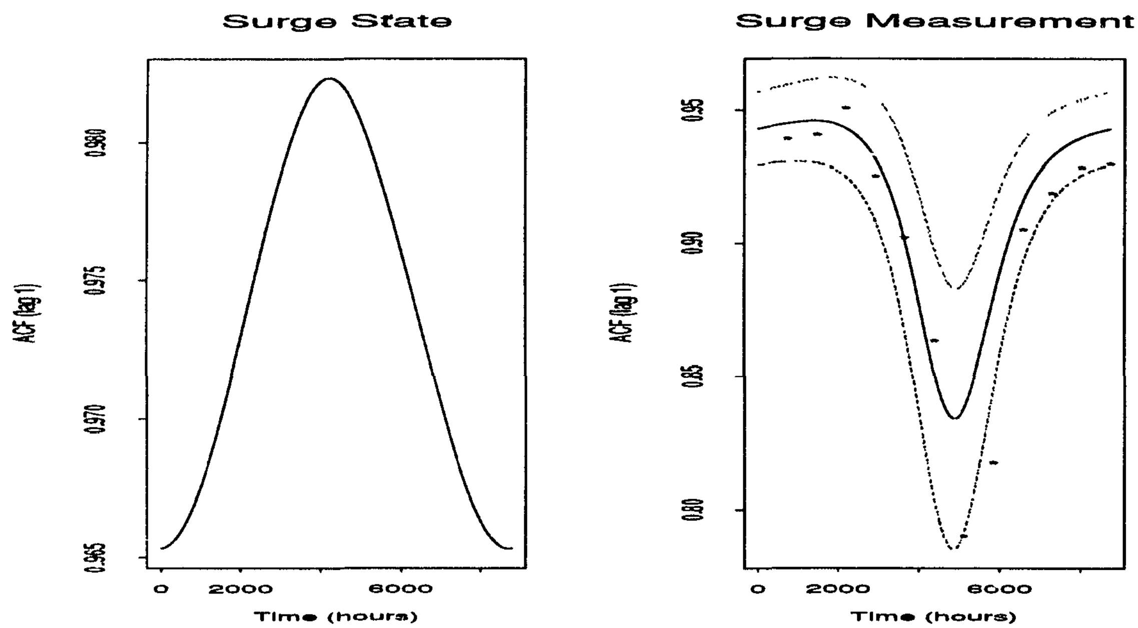

Figure 3.11: Change of surge autocorrelation over time, for Halifax. Sample autocorrelation at lag 1 for each month is marked '*', the solid line represent the estimated model variance, and the dotted lines represents the upper and lower bounds of the 95% prediction interval.

using equations (3.20) and (3.7) for lag 1. Figure 3.11 shows the variation of the autocorrelation at lag 1 over the year for surge state and surge measurement. One noteworthy feature in the autocorrelation plot in Figure 3.11 is that the autocorrelation at lag 1 for the surge state x_t shows the opposite variation over the year, *i.e.* higher autocorrelation in the summer than in the winter. The behavior of the surge state seems contradictory to what the sample autocorrelation structure of the observed surge indicates in Figure 3.11. Nevertheless, the autocorrelation structure of the surge measurement agrees with the sample.

The different patterns shown in the surge measurment autocorrelation and the surge state autocorrelation can be explained as follows. The lag 1 autocorrelation of $\rho_{\eta(t)}(1)$ can be written as

$$\rho_{\eta(t)}(1) = \frac{\beta^2(t) + \alpha(t)}{\beta^2(t) + \theta(1 - \alpha^2(t))}$$

and is equal to

$$\frac{1}{1 + \theta/\sigma_t^2}.$$

Since the ratio of θ/σ_t^2 is higher in the summer than in the winter, $\rho_{\eta(t)}(1)$ is higher in the winter than in the summer.

The autocorrelation at lag 1 is higher in the winter than in the summer for the surge measurement. Estimated surge measurement autocorrelation from the model seems to agree with the sample autocorrelation except on a few occasions in the summer. In particular, the sample estimated $\rho_t(1)$ for the month of July is equal to 0.790173 and does not agree with the model estimate. Such deviations can be avoided by taking into account the year to year sampling variability. In order to make allowances for such deviation, 95% confidence intervals for the surge measurement variance $\sigma^2_{\eta(t)}$ and autocorrelation at lag 1 $\rho_{\eta(t)}(1)$ as function of time, were calculated as follows.

To calculate upper and lower bounds of the 95% confidence interval for the estimated standard deviations, estimates of $\sigma^2_{\eta(t)}$ and $\rho_{\eta(t)}(1)$ must be calculated. In this situation, it is common practice to use the delta method. In order to do so,

$\sigma^2_{\eta(t)}$ and $\rho_{\eta(t)}(1)$ have to be interpreted explicitly as functions of $\alpha(t), \beta_t$ and θ. For simplicity in the calculations, it was assumed that $\sigma_t^2 = \sigma_{t-1}^2$, which seems to be a reasonable assumption for Halifax surge according to the estimated variance function from equation (3.6). In this case, $\sigma^2_{\eta(t)}$ and $\rho_{\eta(t)}(1)$ can be expressed as

$$\sigma^2_{\eta(t)} = \frac{\beta^2(t)}{1-\alpha^2(t)} + \theta$$

and

$$\rho_{\eta(t)}(1) = \frac{\beta^2(t)+\alpha(t)}{\beta^2(t)+\theta(1-\alpha^2(t))}.$$

The surge state variance σ_t^2 and the autocorrelation $\rho_t(1)$ are obtained from equations (3.6) and (3.7).

As the original estimates were calculated using the ML method we find that if the normality assumption holds, at least asymptotically, the covariance matrix of such ML estimates can be approximated by the inverse of the information matrix. Repeated application of the delta method leads to the variances of $\sigma^2_{\eta(t)}$ and $\rho_{\eta(t)}(1)$. When required, log transformations were used to express surge statistics $\sigma^2_{\eta(t)}$ and $\rho_{\eta(t)}(1)$ as linear combinations of parameters α_0, α_1, α_2, β_0, β_1, β_2 and θ, so that the conditions of the delta method are met (Lehmann, 1983).

Figures 3.10 and 3.11 show the pointwise 95% confidence interval for the estimates of σ_t^2 and $\rho_t(1)$ from model 3 . The Halifax monthly sample variances for each month plotted in Figure 3.10 are within 95% confidence bounds. The confidence intervals for the fall and winter are wider than for summer. This is due to the greater sampling variability in the fall and winter seasons noted in Figure 3.2.

Almost all the monthly autocorrelations calculated from the surge data are within 95% confidence bounds in Figure 3.8 except in the month of August. Confidence intervals for the summer are wider than that of the fall and winter. This indicates higher sampling variability in the autocorrelation exists in the summer time than in the fall and winter. Even though the sampling variability (Figure 3.2) is higher in the fall and winter it does not reflect in the autocorrelation, but in the variance.

3.4 Summary

In this chapter four different types of periodic autoregressive models were presented, two of which are state space models. It was seen that the second-order nonstationarity can be explained using a periodic autoregressive part $\alpha(t)$ and a seasonal noise variance part $\beta(t)$. State space representation is able to take the measurement error into account. ML methods of fitting these models using a short record of data were presented. Model selection procedures based on statistical tests and visual comparisons were discussed. Diagnostic checking techniques for the selected model were described. These methods and techniques were demonstrated using Halifax surge data.

It was noticed that the observed Halifax surge data are contaminated by noise. Therefore, the Kalman filter was used to obtain the maximum likelihood estimates of the PAR model. Diagnostic checks and visual comparisons suggest that the PAR(1) representation fits the Halifax surge. Model parameters were estimated using one year of data. It was noticed that year-to-year sampling variability exists in the sample variance and autocorrelation. In order to take such sampling variability into account, 95% confidence intervals were constructed for the estimated variance and autocorrelation at lag 1. It was seen that almost all the sample estimates are within the confidence bounds.

It was found in Chapter 2 that two methods, JPM and EPM, can be used to estimate return periods using a surge parametric model. The estimated model obtained in this chapter will be utilized in return period estimation and inference processes in the following chapters.

Chapter 4

Estimation of Return Periods

The purpose of this chapter is to demonstrate the estimation of return periods using short records and the parametric surge model derived in Chapter 3. Of various return period estimation techniques discussed in Chapter 2, only two methods, EPM and JPM, are specifically designed for use with both a parametric surge model and short records of data. This chapter presents a brief overview of the EPM and JPM. However, in the original design of these methods, the PARMA surge model was not used. Slight modifications to each method are therefore necessary to cope with the seasonally varying model parameters in the PARMA surge model.

The EPM was originally tested on a parametric surge model fit to one year of hourly surge data. The seasonality that exists in the surge variance and autocorrelation were represented by seasonally varying model parameters. These parameters were incorporated into the probability of an upcrossing in continuous time, based on the Rice (1954) formula for a stationary process, with provisions made for the nonstationarity. Thus the parameters used in Rice's formula are different from the surge parameters derived in Chapter 3.

In this chapter, some revisions are made to the original EPM to accommodate the surge parametric model of Chapter 3. In particular, the discrete time probability of an upcrossing is numerically evaluated every hour using surge statistics such as the standard deviation and autocorrelation as estimated in Chapter 3 under the assumption of a Gaussian surge process. In this thesis, we are considering the surge process as discrete. The revised EPM (REPM) return period estimates are then obtained as the minimum time interval such that the expected number of upcrossing exceeds unity. This definition was used in Chapter 2 for an idealized surge of a stationary AR(1) type. This discrete time version of the return period is within one time step (usually one hour) of the original EPM return period defined for continuous time.

The JPM is based on the probability of exceedance obtained by convolving the tide and surge probabilities. In this thesis, the tide is considered as deterministic and exceedances are viewed as the surge exceeding the gap between the predicted tide and the level l. The probability of this happening is then incorporated into the probability of the annual maxima exceeding l. In doing so, hourly surges are assumed to be independent, or Cartwright's correction factor or the extremal indices are used to take care of the dependence. Tawn (1992) extended the extremal index idea to calculate return periods for extreme sea levels following a generalised extreme value (GEV) distribution. The tide and surge levels were combined to obtain the RJPM return period using the two extremal indices for the surge and the total sea level. The RJPM (Tawn, 1992) is used to calculate return periods and estimates are obtained for Halifax sea levels using the surge parametric model in Chapter 3.

The annual maxima return period will be used as a baseline method for comparisons. The AMM return period will be calculated from observed sea levels using 58 years of data. These empirical estimates are restricted to the levels observed in the data. This restriction is lifted by fitting a GEV distribution to annual maxima sea levels. This parametric model is then used to estimate return periods beyond the maximum level observed.

A comprehensive coverage of return period estimates due to the EPM, JPM and AMM was given in Chapter 2. It was seen that the methods produce comparable estimates at high levels for certain stationary processes. Since the surge process is nonstationary, one might not get equivalent estimates from the three methods.

The 1930 sea level data for Halifax was chosen to estimate surge parameters in Chapter 3. They were free from missing values and the tidal package of Foreman (1977) was used to predict the tide for the fifty years beginning January 1, 1930 so that a full nodal modulation of approximately 18.6 years was included.

In Section 4.1, the return periods are estimated using REPM. Necessary revisions for use with the surge parametric model are also given. The techniques are demonstrated for Halifax sea levels using the surge model in Chapter 3. The importance of the seasonally varying model parameters and the tide are also examined. The use of exceedances in place of upcrossings reduces the dimensionality of the probability to one, thus alleviating the burden of obtaining accurate higher dimensional probabilities. In Section 4.2, methods of obtaining return periods due to the RJPM are described and the use of extremal indices to take care of dependence is demonstrated. In Section 4.3, the empirical annual maxima return periods is obtained, based on observed hourly sea levels from 1930-1988. A GEV distribution is fitted to the observed annual maxima to obtain annual maxima return periods. The return period estimates obtained from REPM, RJPM and annual maxima are compared in Section 4.4.

4.1 Revised EPM return period estimation

The revised exceedance probability method (REPM) definition for the return period using discrete data is

$$T_r = \min\{T : \sum_{t=1}^{T} Q_t > 1\} \tag{4.1}$$

where the probability of an upcrossing for discrete η_t^S, Q_t, is given by

$$Q_t = P[\eta_{t-1}^S < l_{t-1}, \eta_t^S \geq l_t] \tag{4.2}$$

with $l_t = l - \eta_t^T$ being the gap between the level l and the tide at time t. The discrete time approximation of T_r is one time step (usually one hour) away from the continuous time return period definition.

The predicted tide η_t^T and the surge model are combined to obtain the probability of upcrossing Q_t

$$Q_t = \int_{\eta_{t-1}^S=-\infty}^{l_{t-1}} \int_{\eta_t^S=l_t}^{\infty} \phi(\eta_{t-1}^S, \eta_t^S, \sigma_t, \sigma_{t-1}, \rho_t) d\eta_{t-1}^S d\eta_t^S \tag{4.3}$$

where ρ_t is the autocorrelation at lag 1 and $\phi(\eta_{t-1}^S, \eta_t^S, \sigma_t, \sigma_{t-1}, \rho_t)$ is the bivariate normal density of η_{t-1}^S, η_t^S. Note that Q_t is a function of the level l and surge parameters σ_t, σ_{t-1} and ρ_t.

For a given level l, the estimated probability of an upcrossing $\hat{Q}_t$ can be approximated by substituting the estimates $\hat{\sigma}_t$ and $\hat{\rho}_t$ into equation (4.3) and evaluating the integral using the NAG subroutines for quadrature D01BCF and D01FBF. Then the revised return period estimate $\hat{T}_r(l)$ can be estimated from (4.1) by summing the probabilities.

We are interested in decadal long return periods associated with extremely high levels. The above estimation scheme requires the evaluation of the integral Q_t at each hour for say, 40 to 50 years. In order to avoid the computational burden of evaluating the two dimensional integral many times, a three dimensional lookup table was created as follows.

The time dependent variables associated with Q_t are l_t, l_{t-1}, σ_t, σ_{t-1} and ρ_t. A simpler expression for Q_t can be written using standardized limits $\tilde{l}_t = l_t/\sigma_t$ and $\tilde{\eta}_t = \eta_t^S/\sigma_t$, as

$$Q_t = \int_{\tilde{\eta}_{t-1}=-\infty}^{\tilde{l}_{t-1}} \int_{\tilde{\eta}_t=\tilde{l}_t}^{\infty} \frac{1}{2\pi\sqrt{1-\rho_t^2}} \exp[-(\tilde{\eta}_t^2 - 2\rho_t\tilde{\eta}_t\tilde{\eta}_{t-1} + \tilde{\eta}_{t-1}^2)/2(1-\rho_t^2)] d\tilde{\eta}_t d\tilde{\eta}_{t-1}. \tag{4.4}$$

Given l, the above form reduces the time dependent variables in Q_t to $\tilde{l}_t$, $\tilde{l}_{t-1}$ and ρ_t. A three dimensional lookup table has been made for Q_t with $\tilde{l}_t, \tilde{l}_{t-1}$, varying from 0 to 5 in steps of 0.2 and ρ_t varying from 0.8 to 0.99 in steps of 0.01. Accuracy of Q_t for high l was achieved by using the results in Section 2.3.2. This produced a 26x26x20 table for Q_t. This table has been used to obtain $\hat{Q}_t$ for any given values of $\tilde{l}_t$, $\tilde{l}_{t-1}$ equal to the scaled gap between the level and the tide at time t, $t-1$ respectively, and for any $\hat{\rho}_t$ equal to the estimated autocorrelation of the surge at time t. The probability

Level (cm)	Return period (years)
185	0.04
190	0.05
195	0.12
200	0.19
205	1.09
210	2.22
215	6.14
220	11.96
225	27.66
230	71.05
235	206.77

Table 4.1: REPM return period estimated in years from January 1, 1930 for Halifax sea levels.

of an upcrossing for $\tilde{l}_t$, $\tilde{l}_{t-1}$ and $\hat{\rho}_t$ falling inside the grid of the lookup table was found using cubic spline interpolation (NAG subroutines E01DAF, E02DFF and E01BAF). Any estimate of $\hat{Q}_t(l)$ for l beyond the level of 5 standard deviations from the tidal level was approximated by the well known asymptotic form $\phi(l)/l$ for the probability of exceedance (Leadbetter *et. al.* 1983) where $\phi(l)$ is the standard normal density. It was shown in Chapter 2 that the probability of upcrossing tends to the probability of exceedance, $P[\eta_t^S \geq l]$, asymptotically under the assumption of normally distributed η_t^S.

The values produced by the interpolation schemes were compared with the values obtained by direct numerical evaluation using NAG and were found to be accurate to the eighth decimal place at higher levels, such as two standard deviation or more away from the tide. The use of a lookup table made the computation of decadal long return periods extremely efficient. For instance, for Halifax sea level the estimated return period of the level 230 cm is 71 years and the time taken to compute it was 4 seconds on a Sun 4 workstation.

An example of the results obtained from this approach for Halifax sea level is shown in Table 4.1. It is instructive to interpret the level in terms of surge standard deviations away from the tide, $\tilde{l}_t$, to get an idea of the location of the level in the normal distribution. At each tidal height the gap between l and the tide changes. Therefore, the location of the level in the normal distribution also changes with the tidal height. For Halifax the maximum level the tide reaches in 30 years is 101 cm at the peak of a spring-neap cycle. The es mated mean sea level using 1930 hourly sea levels is 78 cm. In Table 4.1 high level exceedances mostly occur in the winter time and the average standard deviation during that time is 17cm. Therefore, the level 225 cm is beyond 2.7 standard deviation away from the maximum tide plus mean sea level, whereas the level 235 cm is more than 3.6 standard deviations away from the same.

The asymptotic behaviour of Q_t as $l \rightarrow \infty$, and the relationship with the Type 1 extreme value distribution leading to the Gumbel plot, was discussed in Chapter 2. A Gumbel plot of the return period estimates given in Table 4.1 is presented in Figure 4.1. The empirical annual maxima return periods are also plotted for comparison purposes. On this Gumbel plot, REPM estimates are close to the annual maxima return period estimates based on 58 years of observed sea level. It was noted in Chapter 2 that the EPM and AMM use different definitions for the return period. Slight deviations of the REPM from the AMM appearing at low levels in Figure 4.1 may be a result of these differences. However, it was seen in Section 2.3 that the differences disappear as the level gets higher. This is evident in Figure 4.1 by having transformed return periods close to each other for levels greater than 215 *cm*. Note that the REPM estimates are based on the parametric surge model in Chapter 3 fitted to only one year of data.

Middleton and Thompson (1986) obtained EPM estimates for Halifax using 1970 sea level data. Figure 4.2 shows the original EPM estimates with annual maxima. It is noted that the revised estimates (Figure 4.1) fit better than the original EPM estimates. The problem of overestimation noted by Middleton and Thompson (1986) seems to have disappeared with the revised method. This may be an indication of the

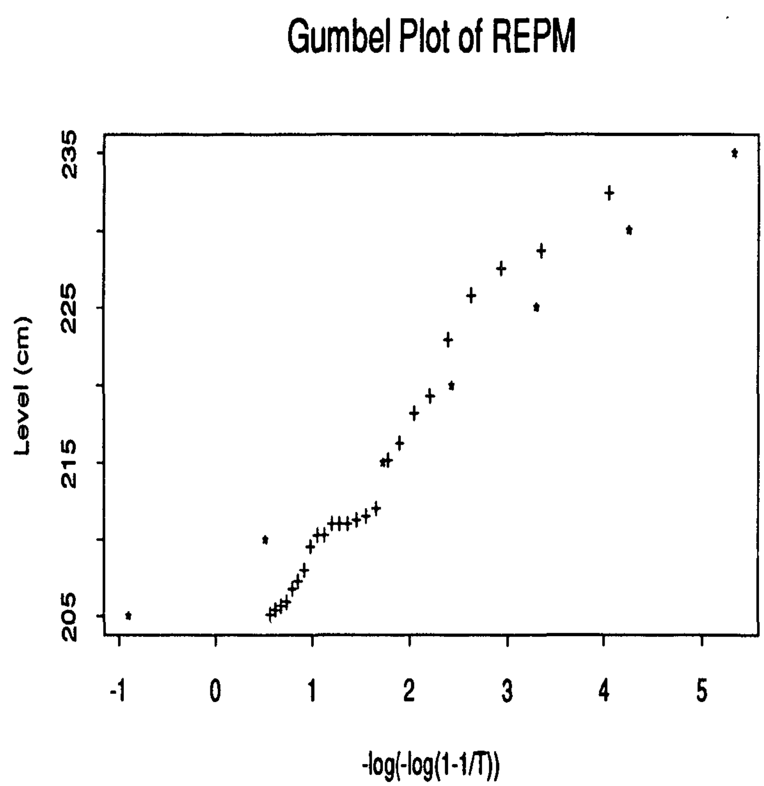

Figure 4.1: Gumbel plot of REPM estimates for Halifax. REPM is marked by '*' and the empirical annual maxima is marked by '+'. Here the annual maxima were obtained as described in Section 4.3.

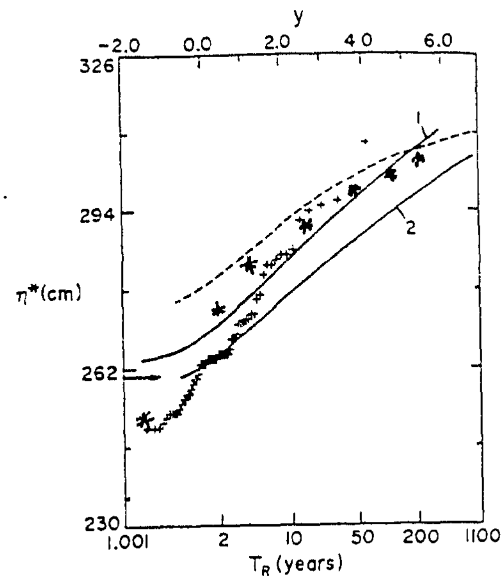

Figure 4.2: Gumbel plot of EPM estimates for Halifax, (Middleton and Thompson, 1986). Curves marked 1 and 2 were based on EPM estimates with observed surge variance and adjusted surge variance. Annual maxima are marked by '+", η^* is the level. The dashed curve shows predictions from JPM. REPM estimates are denoted by '*'.

better fit of the surge parametric model and also the use of discrete time probability (with the Taylor micro-time scale replaced by the seasonally varying autocorrelation at lag 1). Note that the annual maxima in Figure 4.2 have been extracted from a year beginning in July, whereas the annual maxima in Figure 4.1 are based on a calendar year starting the year 1970. This accounts for the slight differences in the plotted annual maxima. It was noticed that the observed sea levels noted in Figure 4.2 by Middleton and Thompson (1986) were up by 45cm compared to the sea level record used for REPM estimates and this was corrected by adding 45cm to the corresponing level in REPM.

In order to determine whether the seasonality in the variance and the autocorrelation have a major influence on the return period estimate, REPM estimates were computed using the average annual surge variance and autocorrelation. The results are presented in Table 4.2. Seasonality of the variance, but not the autocorrelation, seems to be an important feature in return period estimation for Halifax. This suggest that for computational ease one could assume that the autocorrelation is constant throughout the year for Halifax sea levels.

REPM estimates based on one year of tide are given in Table 4.2. The use of one year of predicted tide influences the return periods of extreme levels as the nodal modulation of 18.6 years is ignored. In this case, return period estimates depends strongly on the location of the predicted year in the nodal modulation. If the predicted year is at or near the peak of the nodal cycle the return period will be underestimated. It is clear from Table 4.2 that the tidal prediction cannot be restricted to only one year for Halifax. At extreme levels, beyond 220 cm, the use of the 1930 tide alone clearly overestimates the return period.

It was shown in Section 2.1, that Q_l tends to the probability of exceedance, asymptotically. Accordingly, Q_l can be approximated by the single dimensional probability of exceedance for extreme values of l. REPM estimates for Halifax based on exceedances are also given in Table 4.2. Estimates based on exceedances are almost the same as estimates based on upcrossings at extreme levels. Minor discrepancies are likely due to the error in the numerical integration when calculating Q_l. At lower levels, where the influence of the tide is greater, return periods from upcrossings and exceedances are identical.

Therefore, some simplifications can be made for calculating return periods using Halifax sea levels so that autocorrelation is constant and Q_l is approximated by the probability of exceedances. This may not be the case for other ports. Note, however that the general techniques developed in this study are applicable to any port.

Level(cm)	Return period (years)				
l	$\hat{T}_r$	Constant σ_t	Constant ρ_t	One year tide	Exceedances
185	0.04	0.05	0.04	0.04	0.04
190	0.05	0.12	0.05	0.05	0.04
195	0.12	0.29	0.12	0.12	0.12
200	0.19	1.09	0.19	0.19	0.16
205	1.09	2.31	1.02	1.04	1.09
210	2.22	7.28	2.22	1.12	2.22
215	6.14	15.96	6.15	5.73	5.78
220	11.96	65.38	11.96	13.11	10.87
225	27.66	269.85	27.67	31.10	27.93

Table 4.2: REPM return period for Halifax. The $\hat{T}_r$ is based on PAR(1) model with 18.6 years of predicted tide, the REPM with constant σ_t is calculated with the average annual variance, the REPM with constant ρ_t is calculated using the average annual autocorrelation, REPM estimated using only one year of tide is listed under one year tide and the REPM based on exceedances are listed under exceedances.

4.2 RJPM return period estimates

The RJPM presented here is identical to that of Tawn (1992) except for the use of the surge parametric model of Chapter 3 in place of the generalised extreme value distribution. The generalised extreme value distribution was fitted to extreme surge data for Halifax and there was very little evidence in favor of it describing the distribution for the extreme surges of Halifax.

The RJPM return period is estimated as the reciprocal of the estimated probability of the annual maxima exceeding the level. This annual maxima exceedance probability is estimated using extremal indices for the surge and the sea level. The extremal index for the surge θ_s is defined as the reciprocal of the limit of the mean overtopping time for the surge in each independent excursion above the level, l as $l \to \infty$. For a given extreme level l, the mean overtopping time $\theta_s^{-1}(l)$ and the variance w can be calculated using one year of surge data. The limiting extremal index

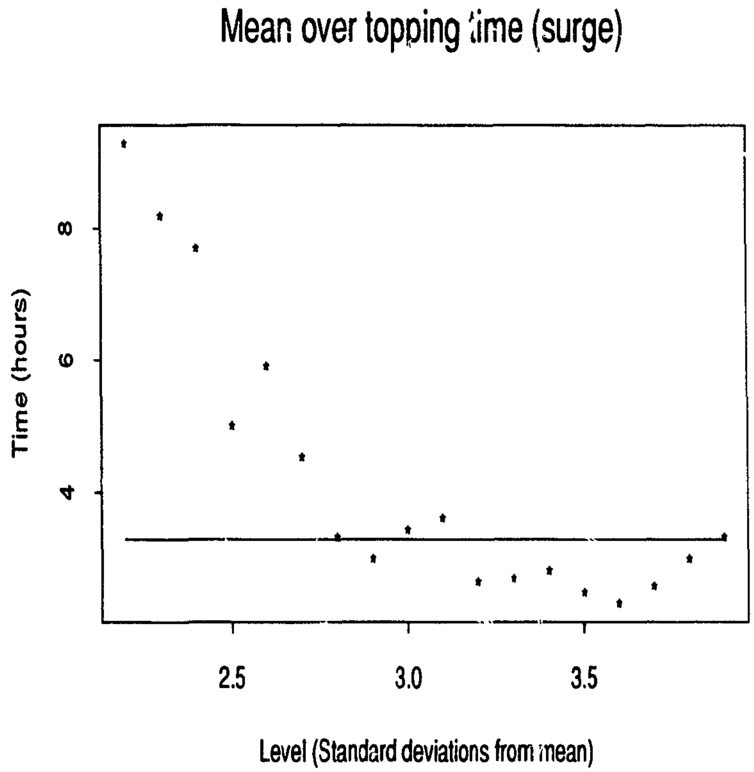

Figure 4.3: Estimates of mean over topping time for Halifax surge estimated using the method by Tawn (1992) and applied to 1930 Halifax surge data.

θ_s^{-1} can be obtained using the formula of Tawn (1992)

$$\hat{\theta}_s^{-1} = \sum_i w_i \hat{\theta}_s^{-1}(l_i) / \sum_i w_i.$$

The $\theta_s^{-1}(l_i)$ estimates for various l_i Halifax are plotted in Figure 4.3 and were obtained using 1930 Halifax surge data. As the level increases the mean overtopping time decreases. However, for extremely high levels, such as 3 or more standard deviations away from the mean surge (typically zero), the mean overtopping time for Halifax converges to a value of three. This may be a result of the high autocorrelation existing in the rare Halifax surges exceeding such high levels in 1930.

The extremal index for the sea level θ was calculated similarly using 1930 sea level data for Halifax. This is shown in Figure 4.4. As the sea level gets higher, the mean overtopping time for the total level converges to a value of one hour.

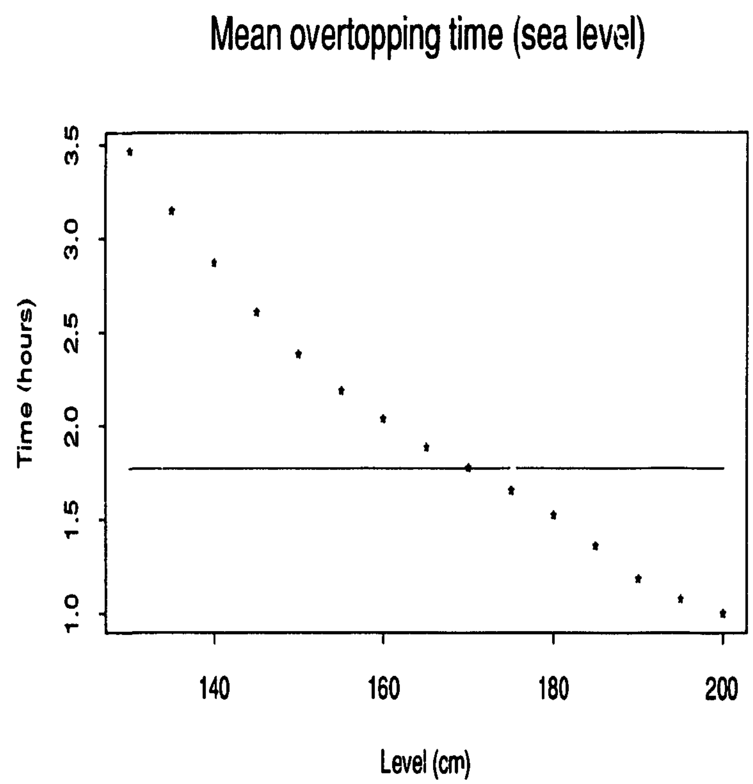

Figure 4.4: Estimates of mean over topping time for Halifax sea level estimated using the method by Tawn (1992) and applied to 1930 Halifax sea level data.

The estimated extremal index of θ_s^{-1} and θ^{-1} for Halifax surge and sea level are 3.03 and 1.772, respectively. These estimates are incorporated into the probability of exceedance as follows. By the definition of the extremal index (Leadbetter *et. al.* 1983), the probability of the annual maximum hourly surge being below the extreme level l can be written as

$$P[\text{annual maxima surge} \leq l] = [P(\eta_i^s \leq l)]^{N\theta_s} \tag{4.5}$$

where N=8766 hours per year. However, due to the nonstationarity of the surge $P(\eta_i^s \leq l)$ changes every hour. No allowance is made in the JPM for seasonality in the variance and autocorrelation of the surge. Therefore, some modifications to the JPM are introduced in order to account for the seasonality in the surge variance.

Following Watson (1954) in Section 2.1.1 (Theorem 1), the probability of an annual maximum of a strictly stationary sequence of N observations being below an extreme level l_N can be approximated by $exp[-NP(\eta_i \geq l_N)]$. Combining this result with (4.5), an approximation for a nonstationary surge can be obtained as

$$P(\eta_i^s \leq l_i) \approx exp(-\sum_{i=1}^{N} P(\eta_i^s \geq l_i)/N\theta_s) \text{ for } i = 1, 2, ..., N \tag{4.6}$$

This generalisation of extremal index for nonstationary sequences was also used by Tawn (1992). The extension of extremal index to nonstationary sequences were shown by Husler (1986).

Now, the probability of annual maximum sea level exceeding the level l can be written as

$$\begin{aligned} P[\text{annual maximum sea level} \geq l] &= 1 - P[\eta_1^s \leq l - \eta_1^T, ..., \eta_N^s \leq l - \eta_N^T] \quad (4.7) \\ &= 1 - \prod_{i=1}^{N} P[\eta_i^s \leq l - \eta_i^T]^{\theta}. \end{aligned}$$

Substituting the approximation (4.6) where $l_i = l - \eta_i^T$ in (4.7) gives the annual maxima hourly sea level exceedance probability as $1 - exp[-\frac{\theta}{\theta_s}\sum_{i=1}^{N} P(\eta_i^s \geq l - \eta_i^T)]$, the reciprocal of which is defined as the RJPM return period.

The surge parametric model of Chapter 3 can be used to estimate $\sum_{i=1}^{N} P(\eta_i^s \geq l - \eta_i^T)$ for $N = 8766$. An example of the modified RJPM return period estimates obtained for Halifax is given in Table 4.3. The Gumbel plot of return periods from Table 4.3 is shown in Figure 4.5. The empirical annual maxima return periods are also included for comparison. RJPM estimates at higher levels are very close to annual maxima plotted on the Gumbel plot. The annual maxima estimated for Halifax are closer to RJPM estimates than EPM estimates. The return period definition used in the RJPM is the same as that of the annual maxima. Therefore, by definition, RJPM estimates should be closer to annual maxima than any other estimates. An important point however is that the estimates are based on one year of data. The estimates were shown to be close to empirical annual maxima return periods. This confirms the validity and the strength of the return period estimation scheme introduced in this thesis work.

In order to investigate whether the seasonality in the variance has a major influence on the RJPM estimates, return periods were computed using the average annual surge variance. The Gumbel plot of RJPM with and without seasonal variance are shown in Figure 4.5. Seasonality in the variance seems to be an important feature in the RJPM return period estimation for Halifax. The estimates without seasonal variance are much larger than both annual maxima and RJPM estimates with seasonal variance for higher levels. For example at $l = 235$ the RJPM estimate with seasonal variance is 99.6 years whereas the estimate without seasonal variance is 348 years. At lower levels the RJPM without seasonal variance underestimates the return period, compared to RJPM with seasonal variance and annual maxima. This trend was also noticed by Middleton and Thompson (1986) in Figure 4.2. Seasonally varying ρ_t would have impact on the overtopping time. This would be an interesting feature in future work of extreme sea level analysis.

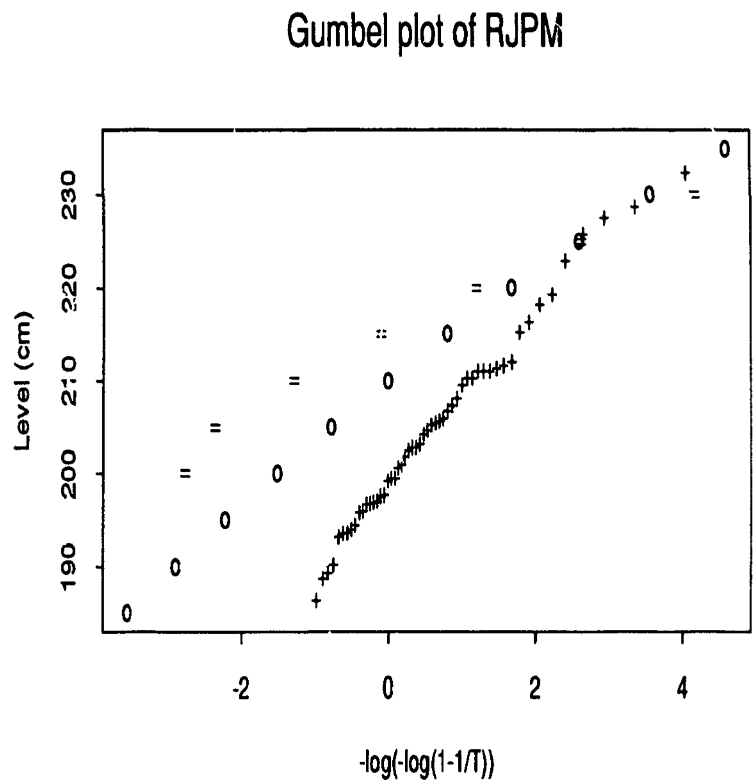

Figure 4.5: Gumbel plot of RJPM estimates for Halifax based on the surge model in Chapter 3. The RJPM is marked by 'o' and annual maxima is marked by '+'. The RJPM without seasonal variance is marked by '='.

Level (cm)	Return period (years)
200	1.01
205	1.12
210	1.57
215	2.75
220	5.78
225	13.71
230	35.46
235	99.60

Table 4.3: The modified RJPM return periods from January 1, 1930 for Halifax sea levels.

4.3 AMM return periods

Annual maxima return periods were calculated empirically based on the 1930-1987 Halifax sea level data obtained from the Marine Environmental Data Service (Ottawa). The annual maximum for each year for the period 1930-1987 was obtained ignoring the missing values. A time series plot of the annual maxima showed an upward linear trend of 0.375 *cm* per year. This trend may be due to global warming or subsidence of the tide gauge, neither of which are included in the predicted tide. In order to make comparisons feasible, the time trend of 0.375 *cm* per year was removed from the observed annual maxima so that the 58 observed annual maxima sea levels are identically distributed around the mean.

The probability of exceedance for an observed level l was calculated using $1 - [\text{number of annual maxima} \leq l]/58$. The empirical annual maximum return period, calculated as the reciprocal of the probability of exceeding the level l, is also plotted on the Gumbel plots in Figures 4.1, 4.5 and 4.6. The empirical annual maxima return periods for Halifax are listed in Table 4.4. Note that the level 235*cm* was not observed during the 58 year period from 1930-1987. In order to obtain return periods of levels beyond the observed annual maxima a parametric model was fitted to the annual maxima sea levels.

Level(cm)	Return period (years)	
l	Empirical	GEV
185	1.05	1.05
190	1.13	1.10
195	1.26	1.19
200	1.71	1.35
205	2.32	1.63
210	3.41	2.11
215	6.44	3.04
220	9.66	5.52
225	14.50	10.18
230	58.00	29.81
235	NA	226.16

Table 4.4: AMM return period for Halifax. The annual maxima estimates based on the fitted GEV distribution are listed under GEV and the empirical annual maxima are listed under empirical.

Tawn (1992) showed that the GEV distribution fits the tail of the sea level distribution better than the extremal Type 1 distribution. The GEV distribution function is given by

$$P[M_i \leq x|\mu, \sigma, k) = exp[-(1 - k\frac{(x-\mu)}{\sigma})^{\frac{1}{k}}]$$

on the set of x for which $1 - k(x - \mu)/\sigma > 0$. The annual maximum for the ith year is M_i, and μ, σ are location and dispersion parameters.

The GEV extreme value distribution was fitted to 58 annual maxima sea levels for Halifax. The parameter estimates, μ, σ and k were found to be $204.4cm$, $13.8cm$ and 0.4, respectively. The return period estimates based on the estimated GEV distribution are also given in Table 4.4. The return periods from the GEV distribution are plotted in Figure 4.6 and are very close to the empirical annual maxima return periods. It is again emphasized that the advantage of using a parametric model for the annual maxima sea levels is the possibility of obtaining return periods for the unobserved levels like $235cm$.

4.4 Summary

The REPM estimates based on one year of data are in good agreement with the empirical annual maxima return periods obtained from Halifax sea level over the period 1930-1987. The Halifax semidiurnal tidal cycle reaches a maximum over in a 15 day spring-neap cycle. At high l, the Q_t at other than the peak times of the spring-neap cycles are negligible. However, at low l, the Q_t at other than the peak times of the spring-neap cycles are not negligible. Thus the influence of the tide at low levels of l is greater than at high levels l.

The return period scales with the dominant tide. As a result, the low level return periods fail to satisfy the requirements of the Gumbel plot. The differences noted in the REPM estimates at lower levels could be due to this factor. In theory, the AMM and the REPM give identical estimates when the process is independent and identically distributed (see Chapter 2). At higher levels the possible exceedances occur further apart fulfilling the requirements of an iid process.

The return period estimates from the RJPM are greater than one year by definition. Therefore, the return periods of lower levels are overestimated by the RJPM compared to the REPM. For higher levels, RJPM estimates are lower than REPM estimates. The difference between REPM estimates and RJPM estimates increases as the level becomes extreme. However, if the level is very high, so that the possible exceedances occur only at the peak of the nodal cycle, it is reasonable to consider return periods of extremely high levels in terms of the nodal cycles of 18.6 years. In this case the estimates of extreme levels, like $235cm$ for Halifax, from two approaches are within one nodal cycle, thus confirming the asymptotic arguments given in Chapter 2. Slight underestimation noticed in RJPM could be due to the exclusion of the full nodal cycle in the estimation.

At lower levels, the RJPM estimates are closer to AMM return periods than REPM estimates. However, at the extreme level $l = 235cm$ the RJPM underestimates the return period compared to the REPM and the annual maxima based on the GEV distribution. At higher levels such as $235cm$, annual maxima estimates based on the

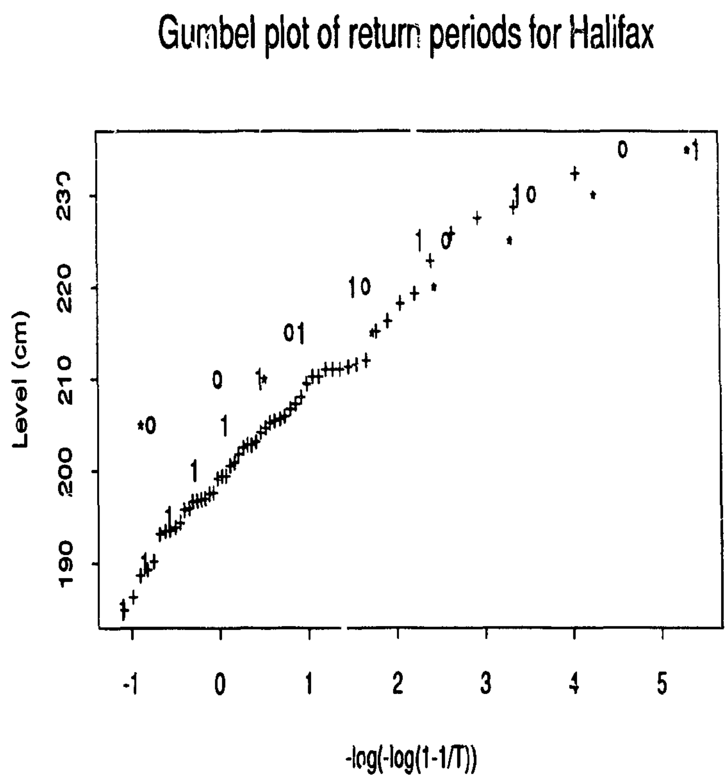

Figure 4.6: Gumbel plot of return period estimates for Halifax. The RJPM is marked by 'o', the REPM is marked by '*' and the empirical annual maxima is marked by '+'. Annual maxima estimates based on the GEV distribution is marked by '1'.

GEV distribution are within one nodal cycle of the REPM. Use of extremal indices at these levels where the independence is achieved, causes this underestimation. The RJPM estimate for the level $l = 235cm$ assuming independence, was 170 years, which is within two nodal cycles of the other estimates. A summary of the return period estimates from all three methods is shown in the Gumbel plot of Figure 4.6.

Overall, the parametric model determined in Chapter 3 seems to perform well in all of the return period estimation schemes considered in this chapter. Middleton and Thompson (1986) noted some discrepancies in Halifax EPM estimates possibly due to inadequate representation of the surge. These discrepancies seem to have been resolved by proper modeling of the surge. Revised estimates seem to be closer to the empirical annual maxima estimates than the original EPM estimates. At lower levels the RJPM estimates are closer to annual maxima estimates than the REPM due to the fact that the same definition of return period is used in the RJPM and AMM and is different from the REPM. At higher levels such as $l = 235cm$ the REPM and AMM estimates are within one nodal cycle of each other. Underestimation noted by RJPM at the level $235cm$ is caused by the extremal index. When the level is extremely high the mean over topping times θ_s and θ both tend to one. Use of values greater than one have resulted in serious underestimation in the RJPM at $l = 235cm$. If the return period estimates at extreme levels are measured in periods of 18.6 years then the estimates from all three methods are close, thus confirming the asymptotic results discussed in Chapter 2. Estimation schemes presented in this chapter are extremely fast.

Chapter 5

Sampling Variability

The purpose of this chapter is to develop statistical techniques to assess the sampling variability of the return period estimates obtained in Chapter 4. The return periods obtained in Chapter 4 were based on one year of surge data. In this thesis work, the question arises regarding the magnitude of the standard errors of the surge statistics (σ_t and ρ_t) and how these deviations affect the return period estimates. It was evident in Chapter 3 (Figures 3.1 and 3.2) that year to year sampling variability exists. The aim of this chapter is to estimate the standard errors and confidence intervals of the return period estimates so that year to year sampling variability in the sea levels is taken into account.

The standard errors of the REPM return period is related to the variability of the surge parameter estimates obtained using one year of surge data. The standard errors of surge parameters represent the year to year sampling variability in the surge process. In the presence of a nonstationary surge and time dependent tide, the EPM return period cannot be explicitly defined as a function of surge parameter estimates. Hence, it is impossible to find explicit expressions for the standard errors based on conventional statistics like the mean square error. In such a situation, it is common practice to use methods such as the delta method (Lehmann 1983) and the bootstrap technique (Efron and Tibshirani 1977, Kunsch 1989).

The delta method will be used in Section 5.1 to obtain an approximate expression for the variance of the return period estimate. Resampling techniques will be used to validate the delta method. Parametric bootstrap estimates of return time variability will be obtained and the efficiency and accuracy of both methods will be discussed. The RJPM return period was explicitly defined as the reciprocal of the probability of the annual maxima exceeding the level l and is a function of the surge parameters. The delta method will again be used to obtain an approximation of the variance of the RJPM return period estimate.

Confidence intervals are of obvious practical significance as they assess the chance (or risk) involved in using short records of surge data. For instance, a 95% confidence interval provides a range for the return periods such that out of 100 independent year long surge records, 95 of them will have parameter estimates leading to return periods within the interval. Estimated REPM and RJPM return periods and standard errors will be used to obtain confidence intervals in Section 5.1 and 5.2. Confidence intervals with an approximate coverage probability of 0.95 will be derived for various exceedance levels. Estimated confidence intervals will be validated by examining the empirical annual maxima return periods based on 1930-1988 Halifax sea level data and the observed return periods obtained using the sea level data provided by Marine Environmental Data Service (Ottawa) for Halifax.

5.1 Confidence intervals for the REPM

The REPM return period T_r is a function of Q_t, which is itself a function of the gap between l and the tide, and the surge parameter vector

$$\vec{\Gamma} = (\alpha_0, \alpha_1, \alpha_2, \beta_0, \beta_1, \beta_2, \theta)'.$$

As Q_t varies with the tide, there is no explicit expression for T_r in terms of the surge parameters. This prevents us from using standard techniques to obtain the variance of the estimated return period $\hat{T}_r$. Approximations to the REPM return time variance are based on the delta method and the parametric bootstrap technique. The model parameters were transformed as in Chapter 3, and in what follows, Γ denotes the reparameterized vector.

In this section we discuss one approach, based on standard asymptotic distribution theory, to the problem of finding interval estimates for $\hat{T}_r$.

A difficulty arises due to the fact that $\hat{T}_r$ is integer valued and therefore not differentiable with respect to time. We define a continuous version of T_r which we denote by T_c, as

$$T_c = \min\{t : \int_{s=0}^{t} Q_s(\Gamma)ds = 1\}$$

where $Q_s(\Gamma) = Q_t(\Gamma),\ t \leq s < t+1$ for any integer t. In this case

$$\int_{s=0}^{t^*} Q_s(\Gamma)ds = \sum_{t=0}^{t^*-1} Q_t(\Gamma), \text{ for all integer } t^*$$

and for any real t'

$$\int_{s=0}^{t'} Q_s(\Gamma)ds = \sum_{t=0}^{[t'+1]} Q_t(\Gamma) - \int_{t'}^{[t'+1]} Q_s(\Gamma)ds \tag{5.1}$$

where $[t'+1]$ denotes the integral part of $t'+1$. Note that $\int_{s=0}^{t'} Q_s(\Gamma)ds$ is a continuous function of t' which is differentiable for (almost) all t' and that T_c is within one time unit of T_r.

We show below how a confidence interval can be constructed for T_c, and this leads to a slightly conservative interval for $\hat{T}_r$.

5.1.1 Sampling variability of $\hat{T}_r$

As discussed in Chapter 3, the maximum likelihood estimator $\hat{\Gamma}$ converges in distribution to Γ. *i.e.*

$$\sqrt{n}(\hat{\Gamma} - \Gamma) \to^L N(0, \Im)$$

where $\Im$ is the approximate covariance matrix of $\hat{\Gamma}$. It follows that if f is a real valued function defined in a neighborhood of Γ and $(\partial f(\Gamma)/\partial\Gamma) \neq 0$, then

$$\sqrt{n}[f(\hat{\Gamma}) - f(\Gamma)] \to^L N\left[0, \left(\frac{\partial f(\Gamma)}{\partial\Gamma}\right)' \Im \left(\frac{\partial f(\Gamma)}{\partial\Gamma}\right)\right].$$

For example see Theorem 5.1.9 of Lehmann (1983). In the above equation $\rightarrow^{L}$ denotes the convergence in law.

Consider the function of Γ given by

$$f[T_c(\Gamma),\Gamma] = \int_{s=0}^{T_c(\Gamma)} Q_s(\Gamma)dt - 1 = 0.$$

An application of Leibnitz' Rule gives

$$\frac{\partial f}{\partial \Gamma} = Q_{T_c}(\Gamma)\frac{\partial T_c(\Gamma)}{\partial \Gamma} + \int_{s=0}^{T_c(\Gamma)} \frac{\partial Q_s(\Gamma)}{\partial \Gamma} ds.$$

Leibnitz' rule follows by the conditions that the functions $Q_s(\Gamma)$ and $T_c(\Gamma)$ are both continuous functions of Γ. As $\partial f/\partial \Gamma = 0$ it follows that

$$\frac{\partial T_c(\Gamma)}{\partial \Gamma} = -\int_{s=0}^{T_c(\Gamma)} \frac{\partial Q_s(\Gamma)}{\partial \Gamma} ds / Q_{T_c}(\Gamma). \tag{5.2}$$

Defining $\hat{T}_c$ as $T_c(\hat{\Gamma})$ this implies that

$$V(\hat{T}_c) = \frac{P_0' \Im P_0}{Q_{T_c}^2(\Gamma)}$$

where

$$P_0 = \int_{s=0}^{T_c(\Gamma)} \frac{\partial Q_s(\Gamma)}{\partial \Gamma} ds.$$

It follows that

$$P_0 = \int_{s=0}^{T_c(\Gamma)} [F_1(s)\frac{\partial \tilde{l}_s}{\partial \Gamma} + F_2(s)]ds$$

with

$$F_1(s) = \phi(\tilde{l}_s)\bar{\Phi}(\tilde{y}_s)$$

and

$$F_2(s) = -\int_{y_s=-\infty}^{\tilde{l}_s} \phi(y_s)\phi(\tilde{y}_s)\frac{\partial \tilde{y}_s}{\partial \Gamma} dy_s.$$

Note $\partial/\partial\Gamma$ is the derivative with respect to the vector Γ. The standardized limits are $\tilde{l}_s = l_{s-1}/\sigma_{s-1}$, $\tilde{y}_s = (\tilde{l}_s - \rho_s y_s/\sigma_s)/\sqrt{1-\rho_s^2}$. The notation $\phi(.)$ and $\bar{\Phi}(.)$ denote the standard normal probability density function and the complementary distribution function respectively. ρ_s and σ_s are as in Chapter 3.

The above discussion implies that in large samples the distribution of $\hat{T}_c$ can be approximated by a Gaussian distribution with mean T_c and variance

$$V(\hat{T}_c) = \frac{P_0' \Im P_0}{\hat{Q}^2_{T_c}}. \tag{5.3}$$

This is estimated by replacing the unknown Γ with the consistent estimate $\hat{\Gamma}$. This procedure leads to confidence intervals for T_c and slightly conservative intervals for T_r.

In order to calculate the variance approximation given in (5.3), one has to calculate P_o which requires an integration over time. This will cause practical difficulties. We show below how P_0 can be approximated by

$$\sum_{t=1}^{\hat{T}_r}[F_1(t)\frac{\partial \tilde{l}_{t-1}}{\partial \Gamma} + F_2(t)]$$

which is easy to compute.

We define the continuous function

$$G^c_s(\Gamma) = \frac{\partial Q_s(\Gamma)}{\partial \Gamma}$$

and the discrete function $G^d_t(\Gamma)$ as

$$G^d_t(\Gamma) = G^c_s(\Gamma) \text{ for all integer } t.$$

Then

$$\int_{s=0}^{T_c} G^c_s(\Gamma) ds = \sum_{t=0}^{[T_c]} G^d_t(\Gamma) + R(T_c)$$

and $[T_c]$ denotes the integral part of T_c. The function $G^d_t(\Gamma)$ represents the derivative of the probability of an upcrossing with respect to Γ, which is bounded and it varies slowly with t. In which case, if $G^d_{t+1}(\Gamma) \approx G^d_t(\Gamma)$ then $R(T_c) \approx 0$. This results in

$$\sum_{t=0}^{[T_c]} G^d_t(\Gamma) = \sum_{t=1}^{\hat{T}_r}[F_1(t)\frac{\partial \tilde{l}_{t-1}}{\partial \Gamma} + F_2(t)]$$

providing an approximation to

$$\int_{s=0}^{T_c} G^c_s(\Gamma) ds = \sum_{t=0}^{[T_c]} G^d_t(\Gamma),$$

where

$$\sum_{t=0}^{[T_c]} G_t^d(\Gamma) = \sum_{t=1}^{\hat{T}_r}[F_1(t)\frac{\partial \tilde{l}_{t-1}}{\partial \Gamma} + F_2(t)].$$

One drawback of the delta method variance approximation is the dependence on the denominator Q_{T_r}, which is the probability of an upcrossing at T_r. This dependence causes serious problems as the tidal process contains significant periodic cycles (spring-neap cycles). If the return period T_r happens to be at the peak of a spring-neap cycle, Q_{T_r} is large and the variance estimate tends to be smaller than when T_r is at the trough of the spring-neap cycle. For high levels having large return periods, the resulting variances may be smaller if T_r happens to be at the peak of the spring-neap cycle. We expect, as the level increases, that both the return period and the corresponding variance will increase, irrespective of where in the tidal cycle T_r falls.

It is thus reasonable to define a smoothed estimator, which for discrete time may be written as

$$T_s = \min\{y : \sum_{u=1}^{y} \bar{Q}_u(\Gamma) > 1\} \tag{5.4}$$

where $\bar{Q}_u(\Gamma)$ is the average exceedance probability for year u. T_s defined as (5.4) is integer valued and not differentiable. We define a continuous version of T_s as

$$T_s^c = \min\{w : \int_{\nu=0}^{w} \bar{Q}_\nu(\Gamma)d\nu = 1\}$$

with

$$\bar{Q}_\nu(\Gamma) = \frac{1}{n}\int_{s=0}^{n-1} Q_{\nu,s}(\Gamma)ds,$$

where $n = 8766$. Note that this $\bar{Q}_\nu(\Gamma)$ is within one hour of $\bar{Q}_u(\Gamma)$. A similar argument as in (5.1) will lead to the result that T_s^c is within one year of T_s. Moreover, T_s^c is differentiable and suggests that the distribution of $\sqrt{n}[T_s(\hat{\Gamma}) - T_s(\Gamma)]$ can be approximated by

$$N\left[0, \left(\frac{\partial T_s^c(\Gamma)}{\partial \Gamma}\right)' \Im \left(\frac{\partial T_s^c(\Gamma)}{\partial \Gamma}\right)\right].$$

According to the discussion above, in large samples the distribution of $\hat{T}_s^c$ can be approximated by a Gaussian distribution with mean T_s^c and variance

$$V(\hat{T}_s^c) = \frac{\bar{P}_0' \Im \bar{P}_0'}{(\bar{Q}_{T_s^c})^2} \tag{5.5}$$

where

$$\bar{P}_0 = \int_{\nu=0}^{T_s^c} \partial \bar{Q}_\nu(\Gamma)/\partial\Gamma.$$

This will lead to confidence intervals for T_s^c which provide approximate confidence intervals for T_s.

In T_s, taking the average over a year seems reasonable as the tide-surge variability has annual cycles (Middleton and Thompson, 1986). In places where the tide-surge variability has cycles longer (or shorter) than a year the average can be taken over a longer (or shorter) period. For an idealized process with iid $\{\eta_t\}$, iid surge and no tide it can be verified that $V(\hat{T}_r) = V(\hat{T}_s)$.

At high levels of l, Q_t approaches the probability of exceedance. The use of exceedances for Q_t in the REPM estimate reduces the variance approximation of T_c to a much simpler form for $V(\hat{T}_c)$ with

$$P_0 = \int_{t=1}^{T_r} l_t/\sigma_t^2 \phi(l_t/\sigma_t) \frac{\partial \sigma_t}{\partial \Gamma},$$

which immediately follows from $P_0 = \int_{t=1}^{T_r} \partial Q_t(\Gamma)/\partial\Gamma$ and

$$\partial Q_t/\partial\Gamma = \partial \int_{x=\bar{l}}^{\infty} \phi(x)dx/\partial\Gamma.$$

The variance approximations given by $V(\hat{T}_r)$ in equation (5.3) and for the smoothed estimator were determined for the levels $l = 185, ..., 235$ cm as obtained for Halifax in Chapter 4. The results are summarized in Table (5.1). The standard error approximation (5.3) gives small values compared to the smoothed estimator and does not steadily increase with the increasing level. For example, when the level increases from 220cm to 225cm the standard error decreases from 1.54cm to 1.38cm. However, the standard error estimates in (5.5) increase consistently with increasing levels as one would expect. The standard error approximations in (5.5) are quite large as one would expect for return periods of several decades (*e.g.* 71 years) and especially for the return periods of two centuries (*e.g.* 206 years). The accuracy of these standard error estimates is not yet clear and we turn to the bootstrap method for verification.

5.1.2 A parametric bootstrap variance estimate

A parametric bootstrap simulation (Efron and Tibishirani 1986) has been developed whereby simulation batches of REPM return times were generated. Samples of $\hat{\Gamma}$ were generated from the multivariate normal distribution with mean vector $\hat{\Gamma}$ and covariance matrix $\Im$ as obtained in Chapter 3. These parameters were then used to obtain realizations of σ_t and ρ_t used for the estimation of Q_t. These were used to generate m sets of REPM estimates for each level $l(\hat{T}_{i,l}, i = 1, 2, ...m)$. The bootstrap REPM return periods $\hat{T}_{i,l}$ were combined to form their bootstrapped mean $\bar{T}$ and the sample variance, $\sum_{i=1}^{m} \frac{(T_{i,l}-\bar{T})^2}{m-1}$.

It was noted that the sample mean and the variance are also quite sensitive to the number of bootstrap samples of m. If m is small, the bootstrap return periods tend to be around the same spring-neap cycle thus underestimating the return period variance. If m is too large, it takes substantial computing time to calculate return times, and so the technique is not particularly efficient.

Table 5.1 illustrates the REPM return period estimates discussed in Section 5.1 and the standard errors obtained for $V(\hat{T}_r)$, $V(\hat{T}_s)$ and the bootstrap method. Note that the bootstrap estimates in Table 5.1 are based on $m = 500$ bootstrap replicates. Up to a level of 215 *cm*, the bootstrap standard errors are within one year of the approximation given by (5.5). Beyond the level of 220 *cm* the delta method variance is within two years of the bootstrap estimate. This suggests that the asymptotic theory leading to (5.5) may be reasonable.

The slight discrepancies that exist at extremely high levels may be due to variability in the bootstrap samples. Sampling variability can be decreased by increasing the number of bootstrap samples. To generate many bootstrap samples for higher levels with longer return periods such as 10 years or greater takes much more computing time than is taken when using (5.5). In this sense, the delta method variance approximation is more efficient than the bootstrap method.

The theory of the previous section is now utilized to obtain confidence intervals. Confidence intervals are often associated with year to year sampling variability in the

Level	Estimate (years)	Standard error (yrs)		
$\ell(cm)$	$\hat{T}_r$	$\sqrt{V(\hat{T}_r)}$	$\sqrt{V(\hat{T}_s)}$	Bootstrap
185	0.04	0.0023	0.0206	0.0008
190	0.05	0.0039	0.0251	0.0023
195	0.12	0.0083	0.1092	0.0690
200	0.19	0.0806	0.2136	0.1033
205	1.09	0.0601	1.6452	0.3084
210	2.22	0.3644	3.2875	2.4694
215	6.14	0.4926	5.9915	4.3668
220	11.96	1.5430	11.4617	8.9302
225	27.66	1.3864	12.1194	10.74
230	71.05	19.042	22.1723	20.16
235	206.77	37.569	72.9347	71.18

Table 5.1: The standard errors of REPM return period estimates, the bootstrap standard errors are based on 500 REPM bootstrap replicates.

data. For instance, a 95% confidence interval for a given level means that, on average, 95 out of 100 year long surge records will lead to estimates within the confidence bounds. Unlike the point estimate, the interval estimate accounts for the sampling variability in the surge, and will give a clearer picture of the effect of using short data records.

Figure 5.1 shows that almost all the REPM estimates for lower levels like $l = 215, 220cm$ are within the 95% confidence intervals. This is not the case at higher levels. At $l = 225cm$ 1 estimate out of 28 estimates is out of confidence bounds whereas for $l = 230cm$ and for $l = 235cm$ 3 and 5 out of 28 are out of the bounds. In theory 2 out of 28 estimates are expected to be outside the confidence intervals. However, without analysing many years of data a definite conclusion can not be reached as to whether the REPM overestimate the standard error at lower levels. Due to the missing values in the observed data set it was not possible to analyse more than 28 years of data for Halifax.

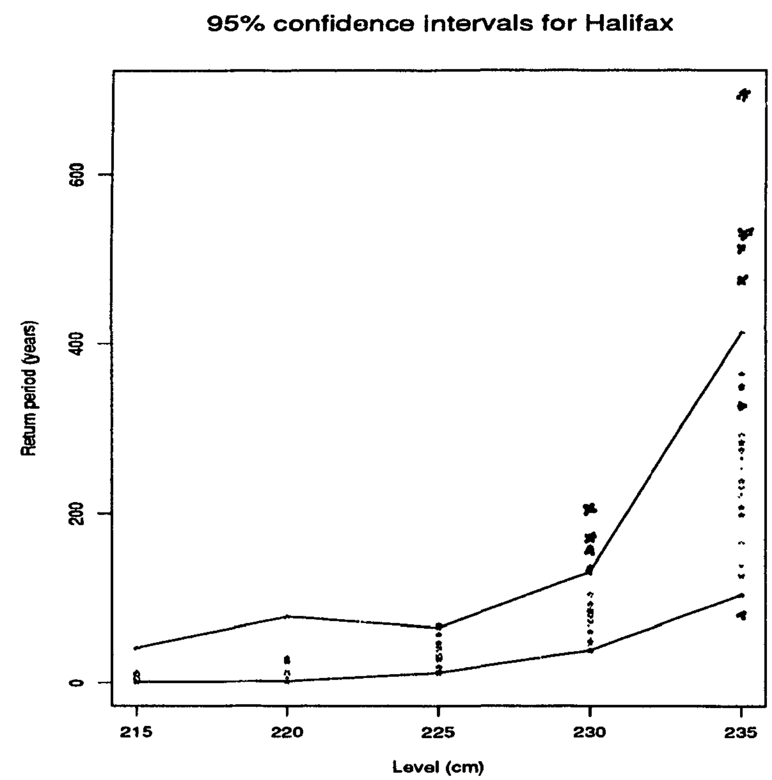

Figure 5.1: 95% confidence intervals of REPM for Halifax. The REPM estimates for 28 years, 1930-1955, 1959-1960 are marked by '*'. Two lines represent the upper and lower bounds of the 95% confidence intervals for REPM.

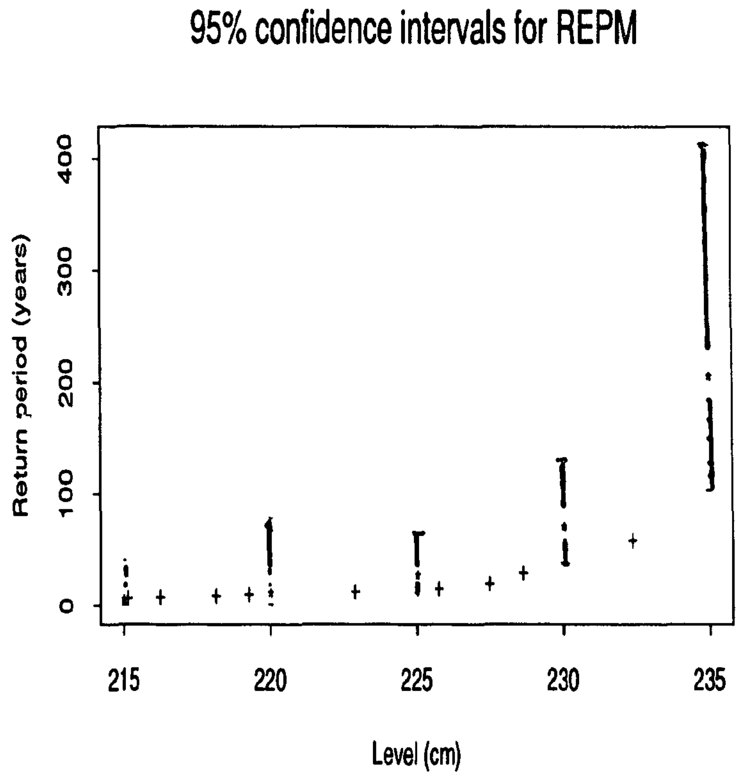

Figure 5.2: 95% confidence intervals of REPM for Halifax. The REPM estimates from Chapter 4 are marked by '*', empirical annual maxima estimates are marked by '+'. The vertical bars are 95% confidence intervals for REPM.

In general, the confidence intervals become wider as the level gets higher. Note that at $l = 225cm$ the confidence interval is narrower than the same at $l = 220cm$. The return period estimate at $l = 225cm$ is 27.66 years from the year 1930. According to the Figure 1.3, since the nodal modulation occurs every 18.6 years, the year 1958 falls on the peak of the nodal cycle, giving a higher value for $\bar{Q}_{T_s^c}$. This will make the standard error estimate (5.5) relatively small, resulting narrower confidence intervals.

The 95% confidence intervals for REPM estimates in Table 5.1 are plotted in Figure 5.2. For comparison purposes, annual maxima return periods are also included. Figure 5.2 shows that the empirical annual maxima return periods are mostly within the 95% confidence limits. The empirical AMM return periods for higher levels are on the lower bound of the 95% confidence interval. This may be due to error in the estimation of the empirical annual maxima, as very few annual maxima exceedances of levels beyond 220 *cm* were observed in the 59 year period from 1930-1958. Almost all the observed return periods for Halifax are within the confidence interval. This could also be an indication of the year 1930 is not a typical year to obtain surge parameter estimates.

5.2 Confidence intervals for RJPM estimates

The RJPM return period estimates obtained in Chapter 4 are also a function of the surge parameters in Γ. Therefore, the variance estimate of RJPM reflects the sampling variability in Γ. A similar approach based on the standard asymptotic theory can be applied to approximate the variance of the RJPM defined as

$$\hat{T}_{rjpm} = \frac{1}{\tilde{Q}_n(\hat{\Gamma})}.$$

where

$$\tilde{Q}_n = 1 - exp[\frac{\theta}{\theta_s}\sum_{i=1}^{N} P(\eta_i^s \geq l - \eta_i^T)]$$

is the estimated annual maxima probability of exceedance described in Chapter 4. Accordingly, in large samples the distribution of $\hat{T}_{rjpm}$ can be approximated by a normal distribution with mean T_{rjpm} and variance $V(\hat{T}_{rjpm})$ equal to

$$(\theta/\theta_s)^2[1 - Q_n(\Gamma)]^2 \frac{\tilde{P}_0' \Im \tilde{P}_0}{Q_n^4(\Gamma)}.$$

where θ and θ_s are extremal indices defined in Chapter 4 with $\tilde{P}_0 = \sum_{i=1}^{n} \partial\tilde{Q}_i(\Gamma)/\partial\Gamma$, for $\tilde{Q}_i(\Gamma)$ being the probability of exceedance at the ith hour.

According to the asymptotic theory stated in Chapter 2, for iid $\{\eta_t\}$ both the REPM and RJPM lead to the same estimate for the return period. It can be verified that, as the level becomes extreme the standard errors of REPM and RJPM based on asymptotic arguments get closer to each other.

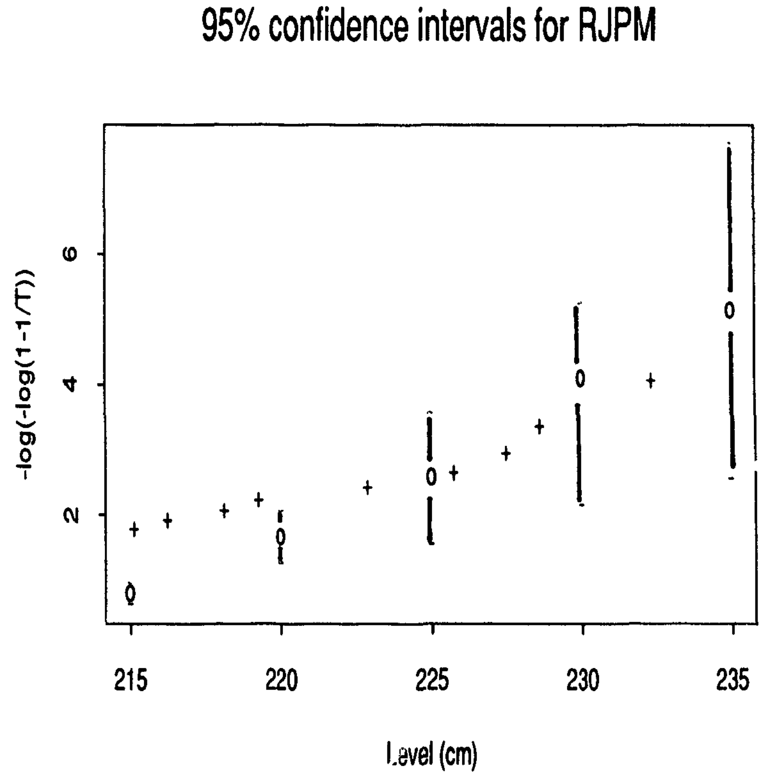

Figure 5.3: The 95% confidence intervals of RJPM for Halifax. The RJPM estimates from Chapter 4 are marked by 'o', empirical annual maxima estimates are marked by '+'. The vertical bar represents the 95% confidence interval for RJPM. For linearization the return periods are transformed using $-log(-log(1-1/T))$.

Confidence intervals can be derived based on the asymptotic normality of return periods using the standard errors calculated as above. The 95% confidence intervals for the RJPM return period estimates are shown in Figure 5.3. Almost all the empirical annual maxima return periods are within the 95% confidence bounds.

5.3 Summary

In this chapter, the return period estimation schemes discussed in Chapter 4 were further extended to account for the sampling variability that exists in the surge data. Techniques were developed to obtain standard errors based on the standard asymptotic distribution theory. Validation techniques were also discussed. It was found that the standard error is comparable with the bootstrap standard deviation confirming the asymptotic theory. However, the asymptotic theory based standard errors are much easier to calculate than that of bootstrap. The techniques developed in this chapter provided the upper and lower bounds such that 95 out of 100 year long surge records will lead to estimates within these bounds. In the derivation of the surge parameters only a year of data was used. The influence of the year to year sampling variability in the surge data is accounted for by the interval estimates. It was found that almost all the empirical annual maxima return periods are within the 95% confidence bounds.

Tawn (1992) had extended the RJPM method to estimate the return level for a given period of time. The estimation techniques presented in this chapter can easily be extended to obtain the return level. The delta method can also be extended to obtain the standard error of the estimated return level.

Chapter 6

Summary and Conclusions

This thesis has presented a set of techniques for obtaining return periods of extreme events from short records. In particular its focus is on situations where the process is partly deterministic and partly stochastic. The stochastic part may be complicated with such features as second-order nonstationarity in the form of a seasonally varying autocorrelation and variance structure. The physical context of the problem arose in the estimation of return periods from short sea level records. Here, the surge process is stochastic and nonstationary in the second-order whereas the tidal process is purely deterministic.

In Chapter 2 existing methods such as AMM, POT, JPM, EPM, RJPM and also the method based on r-largest annual events of estimating return periods were described and then compared for a Gaussian surge process. It was found that all the return period estimation schemes give similar results for iid processes, equal to the mean of the first passage time T_{fr}. The first passage time T_{fr} was defined as

$$T_{fr} = T \text{ iff } \eta_1 < l, ..., \eta_{T-1} < l, \eta_T \geq l.$$

All the return period estimates were then compared to a baseline estimate of $\hat{T}_{fr}$ for additional idealized sea level processes. For an idealized sea level process with an AR(1) surge and a square-top tide, the EPM method gave the closest estimate to the baseline value. However, the methods like the Gumbel annual maxima and the POT method require a long series of data and were thus considered beyond the scope of this thesis. As a result, the EPM and JPM were considered for the estimation and inference of return periods. These methods require the estimation of the single dimensional probability of exceedance and the two dimensional probability of upcrossing to be calculated using a parametric surge model. Briefly, in Chapter 2, it was proved that the various return period estimates converges to the same value as the level becomes extreme. This seems to be an important derivation from a practical point of view since users want to know the accurate return period estimate of high levels, regardless of what definitions and events are being used in the estimation procedure. The results proved in Chapter 2 should convince users of the stochastic equivalence. Another interesting result found in Chapter 2 was that the deterministic component of the tide can be considered as a threshold in POT analysis, thus eliminating the problem of the arbitrary chosen threshold level on POT return period estimates. Since the tide changes over time, modifications to the conventional POT method have to be introduced to cope with the time variant threshold in POT analysis. Numerical schemes of approximating higher dimensional probabilities, also discussed in Chapter 2, are correct to the 8th decimal place for extremely high levels and are useful in the numerical evaluation of these probabilities.

In Chapter 3, several different parametric models were fit to surge data using maximum likelihood techniques. Two special cases of state space models were also included to account for the measurement errors that are usually present in the data. Diagnostic checking techniques were presented and applied to Halifax surge data. Estimates were extended to obtain confidence intervals for the seasonally varying autocorrelation and variance structure. The point and interval estimates are in good agreement with actual values for Halifax.

The PAR state space surge modeling approach used in thesis is original. The notable feature of the PAR surge model produced in this thesis is the representation of the seasonally changing autoregressive and variance components using a functional forms like $\alpha(t)$ and $\beta(t)$ so that seasonal behaviour of the process is captured by relatively few parameters. This form allows fitting a complex surge model to a short record of data. The form of the model presented in this thesis, can be extended to include seasonally varying moving average parameters if necessary. The state space representation can allow the measurement error variance to change seasonally (or functionally) over time to account for seasonally varying error structure. The techniques developed in this thesis also allow the year-to-year sampling variability in the data to be included in the estimated model statistics like σ_t and ρ_t. These estimates can even be extended to other types of sea level data analysis.

The parametric model was successfully utilized in the estimation of return periods in Chapter 4. The two methods, REPM and RJPM, were slightly modified to use the parametric surge model. Estimates from the revised EPM and JPM using one year of data were compared with annual maxima return periods obtained using several decades of data. The surge model worked well and the estimates were compatible with the empirical annual maxima return periods obtained using 59 years of data for Halifax.

The noteworthy feature of the numerical techniques introduced in this chapter is that particular attention was paid to reducing computer time taken for the estimation of the decadal long return periods without sacrificing accuracy in the final result. For example, ideas like the construction of the three dimensional lookup table and interpolation schemes were designed for computational convenience. The techniques presented in this chapter were also found to be extremely fast and accurate.

In Chapter 5, the return period estimation schemes were further extended to include the year to year sampling variability in the surge data. The variance estimates were obtained for REPM and RJPM estimates based on the standard asymptotic results. It was found that the standard deviation estimates were comparable with the bootstrap estimate thus confirming the asymptotic results. The 95% confidence interval estimates were also obtained based on these asymptotic results.

Another important issue in this work is that a great deal of attention was paid to incorporating the effect of sampling variability into the return period estimates.

This has often been ignored in previous estimation studies. The variance formulae presented in this thesis for the REPM and RJPM estimates perform well and can be extended to any form of parametric presentation of the surge.

A final comment is that the estimation and inference methods were restricted to Gaussian models. If the Gaussian assumption is relaxed, return period estimation schemes can still be carried out provided that the explicit functional form of the distribution is known. These can then be incorporated into the numerical integration schemes. It should be pointed out however, that the asymptotic convergence of different return period estimates may no longer be valid.

6.1 Future work

Throughout this thesis work, we relied on the tidal prediction program of Foreman (1977). However, if statistical based regression techniques are used then the estimated tide is given by

$$\eta_t^T = \mu_t + \sum_{i=1}^{M} H_i \cos(\omega_i t - g_i),$$

The mean sea level is denoted by μ_t and the tidal components were explained in Chapter 1. In this case the estimated tide

$$\hat{\eta}_t^T = \sum_{i=1}^{M} \hat{H}_i \cos(\hat{\omega}_i t - \hat{g}_i)$$

is random and described by the random variables $\hat{H}_i, \hat{\omega}_i$ and $\hat{g}_i$. The surge process also follows a state space model representation as discussed in Chapter 3 with a stochastic mean $\hat{\eta}_t^T$. This leads to the problem of return period estimation of a double stochastic process.

It was noted in Chapter 2 that the POT return periods can be obtained by considering the square-top tide as the threshold level. In general, the return periods of the peak over the tide are of interest. In the case of a tide with seasonal cycles, the intensity parameter is a function of time, $\Lambda = \Lambda_t$, leading to a nonhomogeneous Poisson process. This intensity parameter will also influence of the nonstationarity of the surge. Methods of estimating Λ_t would be of interest. The revised POT return period for a nonstationary process could then be defined as the the time T such that $\sum_{t=1}^{T} \Lambda_t = 1$.

One last question that arose in this work is how to extend the return period estimation schemes for short records to a multivariate problem such that the surge and tidal components are vectors of dimension greater than one. An example of a two dimensional problem of estimating return periods would be for current having components in two directions.

Extreme value analysis has been widely used in air quality analysis (Singpurwalla 1972, Horowitz 1980, Smith 1989) for studying air pollution problems. In these type of problems people are primarily interested in the frequency of exceedances which is expressed as the reciprocal of the return period. Most environmental time series are short and serially correlated with seasonal variances and long term trends. The state space model presentation in Chapter 3 can be extended to include the many different physical models. The diagnostic checking techniques and validation methods are also directly extendable.

The additional complications which arise due to missing values in the short series of data were completely ignored. Smith (1989) proposes a broader approach to deal with missing values emphasizing the point-process viewpoint of high level exceedances.

Bibliography

[1] Bickel, P. J. and Doksum, K. A. (1976). Mathematical Statistics, Holden-Day, Inc. San Francisco.

[2] Box, G.E.P. and Jenkins, G.M. (1976). Time Series Analysis: Forecasting and Control. Holden-Day, San Francisco.

[3] Cartwright, D. E., (1958). On estimating the mean energy of sea waves from the highest waves in a record. *Proc. R. Soc., Series A.*, **247** 22-48

[4] Cramer, H (1893), *Mathematical Methods of Statistics*, Princeton U. P.

[5] Efron, B. and Tibshirani, R. J., (1986) Bootstrap methods for standard errors, confidence intervals and other measures of statistical accuracy (with discussion). *Statist. Sci.*, **1** 54-77.

[6] Foreman, M. G. G., (1977). Manual for tidal heights, analysis and prediction, *Pac. Mar. Serv. Rep. 77-10.*, Inst. of Ocean Sci., Patricia Bay, B. C.

[7] Gumbel E. J. (1958). Statistics of extremes, Colombia University Press, New York.

[8] Harvey, A. C., (1981). Time series models, Philip Allan Publishers, Oxford.

[9] Horowitz, J., (1980). Extreme values from a nonstationary stochastic process. *Technometrics,* **22**, 469-482.

[10] Husler, J., (1986). Extreme values for nonstationary random sequences. *J. Appl. Prob.*, **23** 937-950.

[11] Jones, R. H., and Brelsford, W. M., (1967). Time series with periodic structure. *Biometrika*, **54**, 403-408.

[12] Kalman, R. E., (1960). A new approach to linear filtering and prediction problems. *Transactions ASME Journal of Basic Engineering,* **82**, 35-45.

[13] Kunsc!., H. R., (1989). The jackknife and the bootstrap for general stationary observations. *The Annals of Statist.*, **17**, No.3, 1217-1241.

[14] Leadbetter, M. R., Lindgren, G. and Rootzen, H., (1983). Extremes and related properties of random sequences and series, Springer, New York.

[15] Lehmann, E. L., (1983). Theory of point estimation, John Wiley & Sons, New York.

[16] Loynes, R. M., (1965). Extreme values in uniformly mixing stationary stochastic processes. *Ann. Math. Statist.,* **36**, 993-999.

[17] Middleton J. F. and Thompson K. R., (1986). Return periods of extreme sea levels from short records. *J. Geophys. Res.*, **91**, 11701-11716.

[18] NERC (1975). *The flood studies report.* The natural Environment Research Council, London.

[19] Owen, D. B., (1956). Tables for computing bivariate normal probabilities. *Ann. Math. Stat.,* **27**, 1075-1090.

[20] Pagano, M., (1978). On periodic and multiple autoregressions. *The Annals of Statist.,* **6**, 1310-1317.

[21] Pickands, J., (1971). The two-dimensional Poisson process and extremal processes. *J. Appl. Probab.,* **8**, 745-756.

[22] Pugh D. T. and Vassie J. M., (1980). Applications of the joint probability method for extreme sea levels from short records. *Proc. Instn Civ. Engrs, Part 2,* **69**, 959-975.

[23] Pugh, D. T., (1987). Tides, Surges and Mean Sea Level, John Wiley & Sons, New York.

[24] Rice, S.O., (1954). The mathematical analysis of random noise, in *Noise and Stochastic processes,* edited by N. Wax, 133-294, Dover, New York.

[25] Rosenblatt, M., (1956). A central limit theorem and a strong mixing condition. *Proc. Nat. Acad. Sci. U.S.A.,* **42**, 43-47.

[26] Ross, W. H., (1987). A Peak-over threshold analysis of extreme wind speeds. *Canad. J. Statist.,* **15**, No.4, 328-337.

[27] Singpurwalla, N. D., (1972). Extreme values from a lognormal law with application to air pollution problems. *Technometrics*, **14**, 703-711.

[28] Smith, R. L., (1984). Threshold methods forsample extremes. In Statistical Extremes and Applications (J. Tiago de Oliveira, ed.), 621-638, Reidel, Dordrecht.

[29] Smith, R.L., (1986). Extreme value theory based on the r-largest annual events. *J. Hydrology,* **86**, 27-43.

[30] Smith, R. L., (1989). Extreme value analysis of environmental time series: An application to trend detection in ground-level ozone *Ststistical Science*, **4**, 367-393.

[31] Steck, G. P., (1958). A table for computing trivariate normal probabilities. *Ann. Math. Stat.*, **41** 780-800.

[32] Tawn, J. A., (1988). An extreme value theory model for dependent observations. *J. Hydrol.,* **101**, 227-250.

[33] Tawn, J. A. and Vassie, J. M., (1989). Extreme sea levels: the joint probability method revisited and revised. *Proc. Instn Civ Engrs., Part 2,* **87**, 429-442.

[34] Tawn, J. A., (1992). Estimating probabilities of extreme sea levels. *J. Appl. Statist.,* **41**, No. 1, 77-93.

[35] Tiao, G. C., and Grupe, M. R., (1980) Hidden periodic autoregressive-moving average models in time series data. *Biometrika,* **67** 365-373.

[36] Troutman, B.M., (1979). Some results in periodic autoregression. *Biometrika,* **6**, 219-228.

[37] Vecchia, A. V., (1985). Maximum likelihood estimation for periodic autoregressive moving average models. *Technometrics,* **27** No. 4, 375-384.

[38] Walden, A. T. and Prescott, P., (1980). Approximate confidence intervals for port diagram curves *Proc. Instn. Civ. Engrs, Part 2.,* **69** 1015-1023.

[39] Watson, G. S., (1954). Extreme values in samples from m-dependent stationary stochastic processes. *Ann. Math. Statist,* **25**. 798-800.

[40] Weissman, I., (1978). Estimation of parameters and large quantiles based on the k-largest observations. *J. Am. Stat. Assoc.,* **73**, 812-815.